

# NAVAL POSTGRADUATE SCHOOL MONTEREY, CALIFORNIA



## THESIS

BILATERAL FORCE FEEDBACK FOR  
HYDRAULICALLY ACTUATED SYSTEMS

by

Gregory S. Johnson

December, 1994

Thesis Advisor:

Morris Driels

Approved for public release; distribution is unlimited.

19950303 099

DTIC QUANTITY EDITIONED

# REPORT DOCUMENTATION PAGE

Form Approved OMB No. 0704-0188

Public reporting burden for this collection of information is estimated to average 1 hour per response, including the time for reviewing instruction, searching existing data sources, gathering and maintaining the data needed, and completing and reviewing the collection of information. Send comments regarding this burden estimate or any other aspect of this collection of information, including suggestions for reducing this burden, to Washington Headquarters Services, Directorate for Information Operations and Reports, 1215 Jefferson Davis Highway, Suite 1204, Arlington, VA 22202-4302, and to the Office of Management and Budget, Paperwork Reduction Project (0704-0188) Washington DC 20503.

1. AGENCY USE ONLY	2. REPORT DATE December 1994.	3. REPORT TYPE AND DATES COVERED Master's Thesis
4. TITLE AND SUBTITLE BILATERAL FORCE FEEDBACK FOR HYDRAULICALLY ACTUATED SYSTEMS		5. FUNDING NUMBERS
6. AUTHOR(S) JOHNSON, GREGORY S.		
7. PERFORMING ORGANIZATION NAME(S) AND ADDRESS(ES) Naval Postgraduate School Monterey CA 93943-5000		8. PERFORMING ORGANIZATION REPORT NUMBER
9. SPONSORING/MONITORING AGENCY NAME(S) AND ADDRESS(ES)		10. SPONSORING/MONITORING AGENCY REPORT NUMBER
11. SUPPLEMENTARY NOTES The views expressed in this thesis are those of the author and do not reflect the official policy or position of the Department of Defense or the U.S. Government.		
12a. DISTRIBUTION/AVAILABILITY STATEMENT Approved for public release; distribution is unlimited.		12b. DISTRIBUTION CODE

## 13. ABSTRACT

This thesis report discusses the design, construction, and experimentation of force feedback in one and two degrees of freedom, hydraulically actuated systems. A master hydraulic unit is used to positionally control a remotely located slave hydraulic unit. An obstruction in the path of the slave unit is used as a force control to the master unit, reducing the power assist to the operator. An analysis was conducted to predict the performance and stability of the system for various amplifier gain settings. One and two degrees of freedom models were constructed to verify the analysis and to physically observe the force feedback.

14. SUBJECT TERMS Teleoperation, Force Reflection, Robotics			15. NUMBER OF PAGES 120
			16. PRICE CODE
17. SECURITY CLASSIFICATION OF REPORT Unclassified	18. SECURITY CLASSIFICATION OF THIS PAGE Unclassified	19. SECURITY CLASSIFICATION OF ABSTRACT Unclassified	20. LIMITATION OF ABSTRACT UL

NSN 7540-01-280-5500

Standard Form 298 (Rev. 2-89)  
Prescribed by ANSI Std. Z39-18 298-102



Approved for public release; distribution is unlimited.

BILATERAL FORCE FEEDBACK FOR  
HYDRAULICALLY ACTUATED SYSTEMS

by

Gregory S. Johnson  
Lieutenant, United States Navy  
B.S.B., University of Minnesota, Minneapolis, 1988

Submitted in partial fulfillment  
of the requirements for the degree of

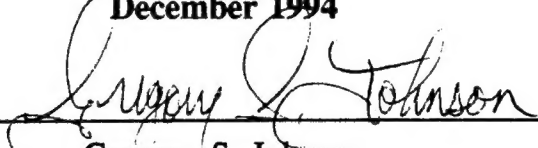
MASTER OF SCIENCE IN MECHANICAL ENGINEERING

from the

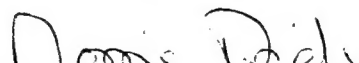
NAVAL POSTGRADUATE SCHOOL

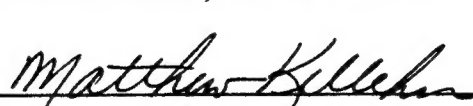
December 1994

Author:

  
\_\_\_\_\_  
Gregory S. Johnson

Approved by:

  
\_\_\_\_\_  
Morris Driels, Thesis Advisor

  
\_\_\_\_\_  
Matthew D. Kelleher, Chairman

Department of Mechanical Engineering

Accession For	
NTIS	CRA&I
DTIC	TAB
Unannounced	
Justification _____	
By _____	
Distribution / _____	
Availability Codes	
Dist	Avail and / or Special
A-1	



## **ABSTRACT**

This thesis report discusses the design, construction, and experimentation of force feedback in one and two degrees of freedom, hydraulically actuated systems. A master hydraulic unit is used to positionally control a remotely located slave hydraulic unit. An obstruction in the path of the slave unit is used as a force control to the master unit, reducing the power assist to the operator. An analysis was conducted to predict the performance and stability of the system for various amplifier gain settings. One and two degrees of freedom models were constructed to verify the analysis and to physically observe the force feedback.



## TABLE OF CONTENTS

I.	INTRODUCTION.....	1
II.	ONE DEGREE OF FREEDOM FORCE FEEDBACK.....	3
A.	OBJECTIVE.....	3
B.	DESIGN AND CONSTRUCTION.....	3
1.	System Overview.....	3
2.	Operation.....	5
a.	Master Unit.....	5
b.	Slave Unit.....	5
c.	Wiring Diagram.....	6
C.	OBTAINING SYSTEM PARAMETERS.....	8
1.	Gain Estimation.....	9
a.	Master Strain Gauge Gain ( $K_{OM}$ ).....	11
b.	Master Servo Valve Gain ( $K_1$ ).....	14
c.	Master Potentiometer Gain ( $K_4$ ).....	15
d.	Slave Servo Valve Gain ( $K_2$ ).....	19
e.	Slave Potentiometer Gain ( $K_3$ ).....	21
f.	Slave Strain Gauge Gain ( $K_{OS}$ ) and Obstruction Spring Gain ( $K_{sp}$ ).....	25
D.	THEORETICAL ANALYSIS.....	28
1.	Gain Values for Theoretical Analysis.....	28
2.	Manual Analysis.....	28
3.	SIMULAB Analysis.....	39
E.	EXPERIMENTATION.....	44
1.	Sensing Force Feedback.....	44
2.	Dynamic Response.....	45

III. TWO DEGREES OF FREEDOM FORCE FEEDBACK.....	49
A. OBJECTIVE.....	49
B. THEORETICAL ANALYSIS USING SYSTEM PARAMETERS FROM SINGLE DEGREE OF FREEDOM MODEL.....	49
1. System Overview.....	49
2. SIMULAB Analysis Using Expected Gains.....	51
a. Expected Gains.....	51
b. Analysis.....	54
C. DESIGN AND CONSTRUCTION.....	55
1. Operation.....	55
a. Master and Slave Unit.....	55
b. Wiring Diagram And Electrical Components.....	58
2. Design Considerations and Constraints.....	58
a. Link Geometry.....	58
b. Variable Position Link Joint.....	60
c. Linear Actuator Placement.....	60
d. Strain Gauge Web.....	63
e. Joint Friction.....	68
f. Link #1 and Rotary Actuator Interface...	69
g. Rotary Potentiometers.....	72
h. Servo Valve Locations.....	73
D. EXPERIMENTATION.....	74
1. System Equilibrium.....	74
2. Sensing Force Feedback.....	75
3. Dynamic Response.....	75
4. System Reversibility.....	76
5. Bending Stress Fluctuations in Links.....	80

IV. DISCUSSION.....	81
A. ONE DEGREE OF FREEDOM SYSTEM.....	81
1. Results.....	81
2. Assumption Errors.....	81
3. Obstruction Stiffness.....	83
B. TWO DEGREES OF FREEDOM SYSTEM.....	85
1. Results.....	85
a. Bilateral Force Feedback.....	85
b. Dynamic Response.....	86
c. System Sensitivity.....	90
V. CONCLUSIONS AND RECOMMENDATIONS.....	93
A. CONCLUSIONS.....	93
B. RECOMMENDATIONS.....	93
APPENDIX A. MASTER STRAIN GAUGE GAIN ( $K_{Om}$ ) EXPERIMENTAL DATA.....	95
APPENDIX B. MASTER SERVO VALVE GAIN ( $K_1$ ) EXPERIMENTAL DATA.....	96
APPENDIX C. MASTER POTENTIOMETER GAIN ( $K_4$ ) EXPERIMENTAL DATA.....	97
APPENDIX D. SLAVE SERVO VALVE GAIN ( $K_2$ ) EXPERIMENTAL DATA.....	97
APPENDIX E. SLAVE POTENTIOMETER GAIN ( $K_3$ ) EXPERIMENTAL DATA.....	98

APPENDIX F. SLAVE STRAIN GAUGE GAIN ( $K_{OS}$ ) AND OBSTRUCTION SPRING GAIN ( $K_{sp}$ ) EXPERIMENTAL DATA.....	98
APPENDIX G. MATLAB CODE FOR A TYPICAL UNIT STEP RESPONSE FOR SINGLE DEGREE OF FREEDOM MODEL.....	99
APPENDIX H. AUTOCAD DRAWING OF LINK SLIDING JOINT.....	100
APPENDIX I. MATLAB CODE FOR ANGULAR ROTATIONS VS. ACTUATOR POSITION FOR TWO DEGREES OF FREEDOM SYSTEM.....	101
APPENDIX J. MATLAB CODE FOR LINEARITY OF LINK ROTATION VS. ACTUATOR RAM DISPLACEMENT.....	102
APPENDIX K. MATLAB CODE FOR WEB THICKNESS VS. APPLIED FORCE.....	103
APPENDIX L. AUTOCAD DRAWING OF MASTER ACTUATOR MOUNTING BRACKET AND LINK MOUNTING PAD.....	104
APPENDIX M. AUTOCAD DRAWING OF SLAVE ACTUATOR MOUNTING PAD.....	105
LIST OF REFERENCES.....	107
INITIAL DISTRIBUTION LIST.....	109

## I. INTRODUCTION

Teleoperators are remotely operated systems that have human or computer control and supervision over its motion. There are many applications for these systems. Space teleoperators are designed for use on the space shuttle by controlling movement of a remote manipulator system (RMS) by a human operator viewing through a window or over video. They can provide for simple, redundant tasks such as routine inspections, maintenance, and scientific experimentation. Telerobotic roving vehicles and manipulators are desired to be controlled from earth for surface exploration of the moon and Mars. Undersea manipulators are used for deep sea salvage and exploration and in the oil industry to withstand the high forces and rugged conditions. Many other applications include toxic waste cleanup, construction, mining, warehouse and mail delivery, firefighting, policing, telesurgery, and in entertainment [Ref.1, pgs 108-121].

Unilateral operation allows a hydraulically actuated system to be positionally driven by a remotely located master hydraulically actuated system. An external force created by an operator generates an input voltage from a strain gauge or potentiometer. The signal goes through a summing junction with an offsetting voltage created by an obstruction force in the path of the slave unit, but the operator senses no effect from the obstruction. This system's limitation occurs when the slave unit encounters a resistive obstruction that the master unit does not know exists. This can lead to equipment damage and the failure to achieve designed tasks. It is therefore desirable to construct a bilateral force feedback loop such that the obstruction in the slave unit's motion will generate a force that can be sent back to the master unit to oppose the input force and provide a resistive force to the operator. The commanded motion should have to

overcome this feedback force just as if the obstruction was actually in the path of the master unit. This provides the operator with the ability to feel a remote environment.

## **II. ONE DEGREE OF FREEDOM FORCE FEEDBACK**

### **A. OBJECTIVE**

The primary objective in designing, building, and testing a single degree of freedom force feedback system is to verify that an operator who physically inputs a force to a master hydraulic system, will feel a resistive hydraulic force proportional to the obstruction force encountered by the slave hydraulic system. A theoretical analysis is conducted to predict system response and stability, and the results will be verified by an experimental comparison.

### **B. DESIGN AND CONSTRUCTION**

#### **1. System Overview**

To simplify the theoretical and experimental analysis, a single degree of freedom system is used with linear hydraulic actuators. The force feedback concept is analyzed by designing the system such that an input force from the operator positionally drives the master unit which positionally drives the slave unit until it comes into contact with an obstruction. A resistive force is generated by this obstruction, and a proportional voltage is fed back to the master servo valve to give a hydraulic resistance to the operator, thus resulting in a resistive force proportional to the obstruction resistive force.

Figure 1 is a top view of the entire system which operates in the horizontal plane. The master and slave units are constructed with geometric similarity, but with different dimensions. The master unit was built by a previous thesis student, and the slave unit was built to match it.

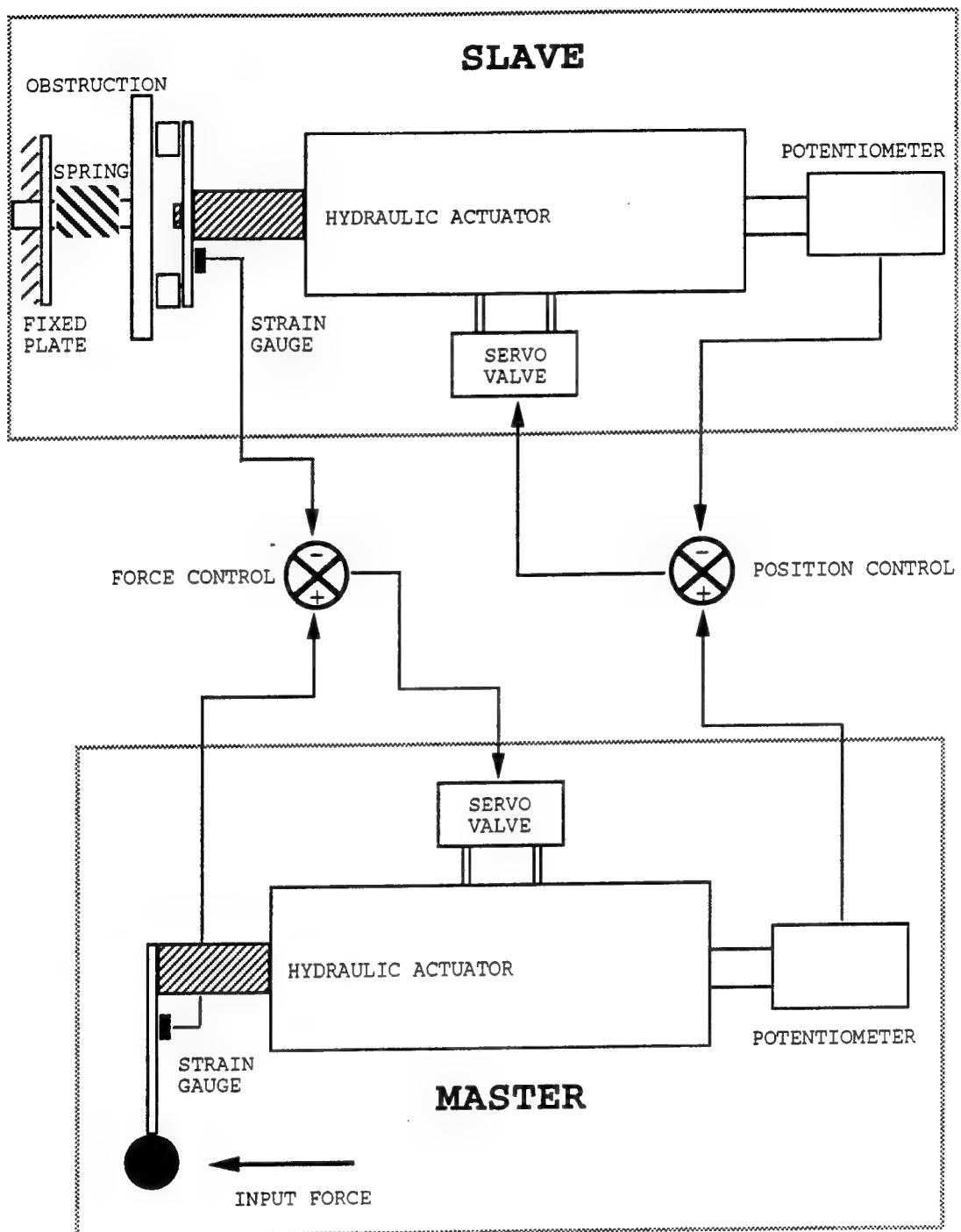


Figure 1. Top view of single degree of freedom force feedback system.

The system operates at a low hydraulic pressure, approximately 450 psi, to minimize equipment size and cost and to have a slower response time.

## **2. Operation**

### **a. Master Unit**

The operator applies an input force to the joystick which causes a proportional bending stress on the master strain gauge. A voltage is produced which is used as a force driver for the master unit by going through a summation junction with an offsetting obstructive force voltage from the slave unit. The combined voltage is used by the master electro-hydraulic servo valve to provide a power assist to the operator. Before the slave unit contacts the obstruction, an input force to the left will generate a tensile bending stress and a positive voltage. Since the initial obstructive force voltage is zero, the resulting summation voltage is positive and extends the hydraulic ram to the left. If the force is reversed to the right a compressive bending stress and negative voltage are generated, resulting in the hydraulic ram retracting to the right. A linear potentiometer on the master generates a voltage corresponding to ram displacement, and it is not used as a positional feedback to the master unit since its position is force driven by the operator. The master potentiometer is used to positionally drive the slave unit.

### **b. Slave Unit**

Before the slave unit comes into contact with the obstruction, the system is operating in a position control mode. The master potentiometer voltage is passed through a summation junction with an offsetting slave potentiometer voltage. The combined voltage is used to drive the slave

electro-hydraulic servo valve until the master and slave positions are proportionally equal.

After contact is made with the obstruction, the system is operating in a force control mode. The obstruction is placed in the path of the slave hydraulic ram. The obstruction consists of a flat plate mounted onto a shaft that passes through a spring before passing through another plate that is fixed to the work bench. This arrangement will give some compliance to the obstruction so that it will not be rigid. At the end of the slave unit's hydraulic ram is a plate and strain gauge to convert the obstructive force resistance into a voltage. When contact is made with the obstruction, a force is generated that is proportional to compressive displacement of the spring. This force will act at both ends of the plate connected to the ram, and it will create a bending stress measured by the strain gauge. The strain gauge converts the stress into a voltage which is used to offset the applied force voltage on the master unit. This offset will decrease the power assist provided by the master servo valve to the operator, thus resulting in an increased input force to maintain a constant velocity for the master ram.

#### **c. Wiring Diagram**

Figure 2 shows the electrical configuration for the single degree of freedom system. The master and slave strain gauges pass through the strain gauge amplifier that has a gain and offset control for each signal. The gain control will adjust the magnitude of amplification of the strain gauge voltage. The offset control alters the strain gauge voltage by adding or subtracting from the preamplified input voltage which is used to bring the entire system into equilibrium before input and obstructive forces are applied to the system. The individual amplified voltages are split

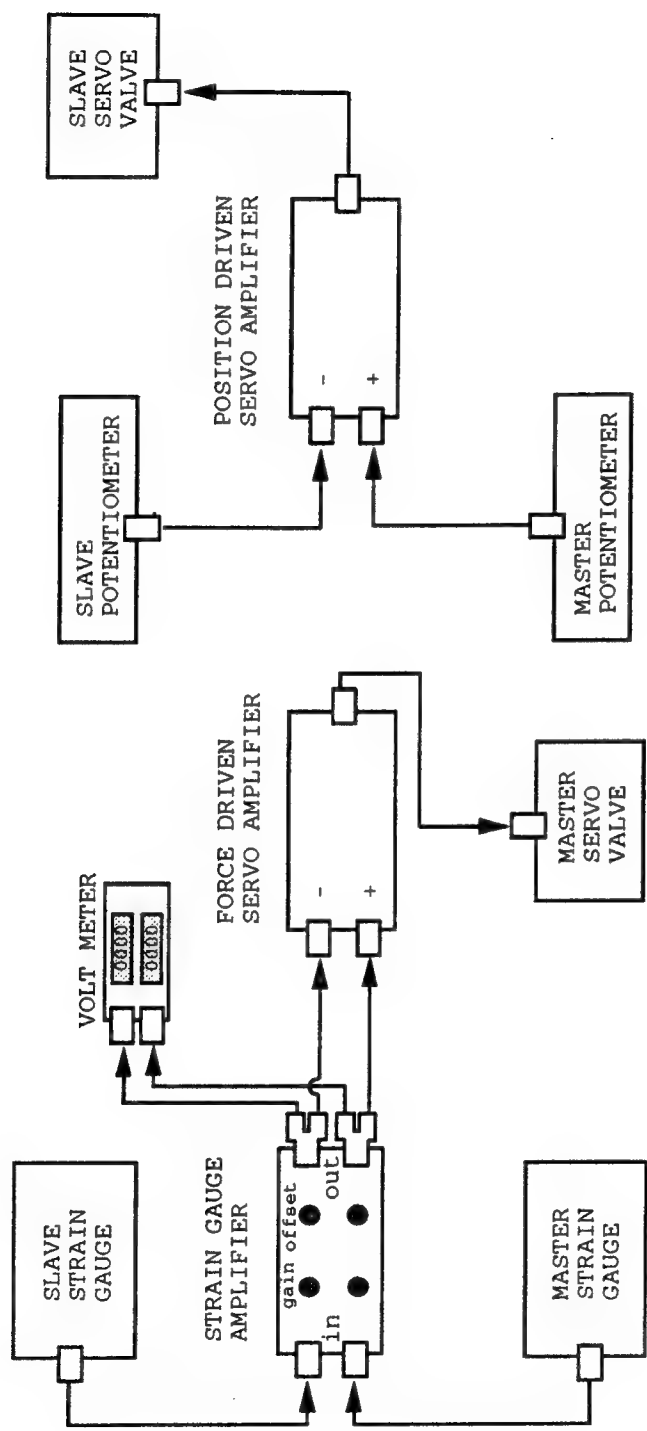


Figure 2. Wiring diagram for single degree of freedom force feedback system.

to pass through a voltmeter and a force driven servo amplifier. The force driven servo amplifier is used to sum the offsetting voltages and to drive the master servo valve.

In a separate electrical relationship, the slave and master potentiometer voltages are passed through the position driven servo amplifier to sum the offsetting voltages and to drive the slave servo valve.

### C. OBTAINING SYSTEM PARAMETERS

In order to predict system stability and performance, a complete block diagram of the master and slave unit must first be constructed with all component parameters identified. Before attempting to take data on the system, it must be allowed to settle into its equilibrium position without drifting. During start up, the oil temperature change affects the performance of the system, and equilibrium will continue to change until the temperature reaches its operating value. The air temperature range from morning to afternoon in the laboratory affects the oil temperature so a different equilibrium occurs during each start up. The hydraulic pump is started and brought to approximately 450 psi. The cutout valve is closed to the system so that the oil will recirculate until the operating temperature is met. Once it is reached, the cutout valve is opened. The system is brought into static equilibrium by moving the joystick of the master unit to the fully retracted position. When the applied force is removed, the slave strain gauge offset is set to zero, and the master strain gauge offset is adjusted to eliminate any drift by the master hydraulic actuator. The slave hydraulic actuator will find its initial equilibrium position when the master and slave potentiometer voltages are equal in magnitude, and this slave actuator position is not

necessarily fully retracted. Once these conditions are obtained, the system is in its equilibrium position.

### 1. Gain Estimation

Figure 3 is the block diagram for the single degree of freedom force feedback system after contact between the slave ram and an obstruction. The performance of the system is assumed to be linear for simplicity, and the servo control valve gains are assumed to be constant since the system operating frequency is lower than that of the servo valve. A theoretical analysis was conducted prior to building the system for experimentation, but the results were quite limited since the gain value assumptions were not based on any known quantities. A more detailed, manual theoretical analysis was conducted after the gain approximations were obtained from the actual system.

A similar approach was used to obtain each gain throughout the system. Each gain was isolated such that the input and output were measured, and the gain was calculated from the input and output by:

$$K(\text{gain}) = \frac{\text{output}}{\text{input}} \quad (1)$$

Figure 4 is the block diagram relating input, output, and gain.

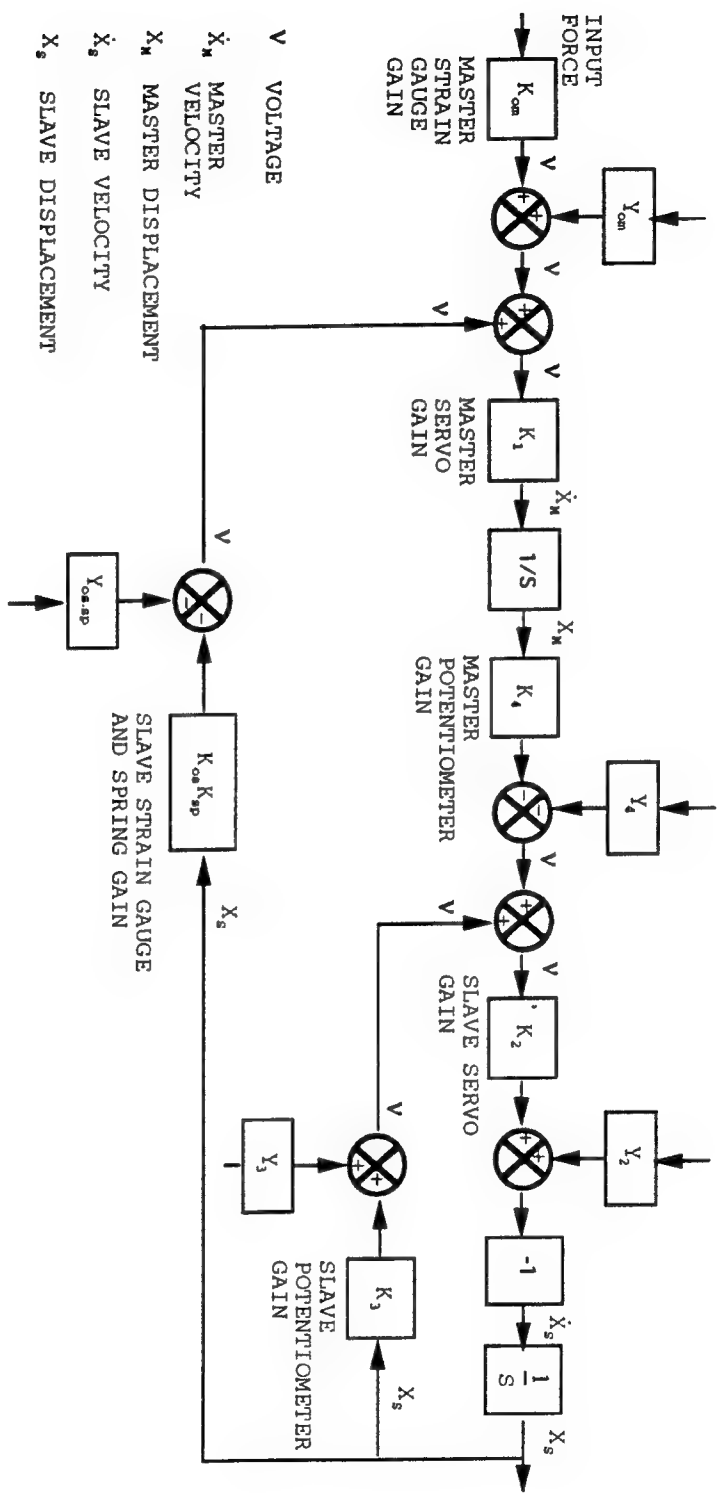


Figure 3. Block diagram for single degree of freedom force feedback system after contact with an obstruction.

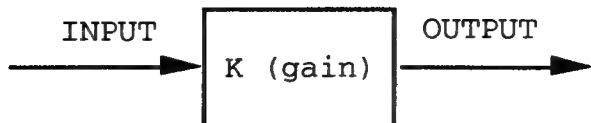


Figure 4. Input, output, and gain relationship.

**a. Master Strain Gauge Gain ( $K_{om}$ )**

Figure 5 is the block diagram relationship for  $K_{om}$ .

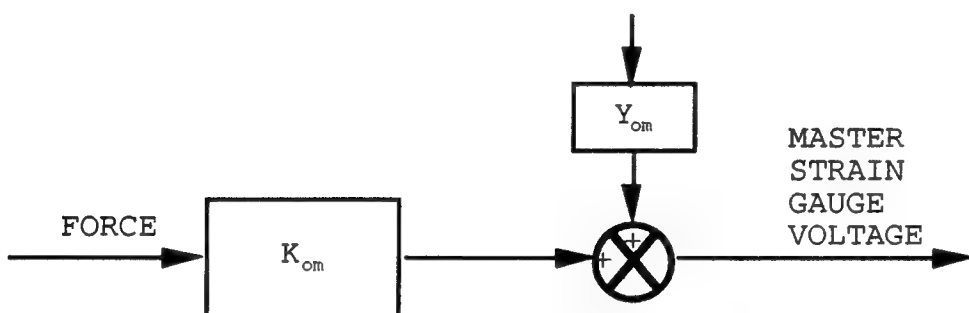


Figure 5. Master strain gauge gain ( $K_{om}$ ) block diagram.

The hydraulic supply was closed off at the cutout valve to the system so that the system would not respond to a force input. The joystick was rotated 90 degrees so that the strain gauge was facing upward. Four individual weights (input) were hung from the end of the joystick so that a tensile bending stress was created on the strain gauge. For each weight, the strain gauge voltage (output) was recorded from the voltmeter for eight incremental values of the master strain gauge amplifier gain control setting from 1.0 to 8.0. See Appendix A for data obtained.

Figure 6 shows the relationship between input force and output voltage for the eight different master strain gauge amplifier gain control settings (G1). The slope of these linear relationships (voltage divided by force) was obtained by using a least squares curve fit, and it is the

gain for the master strain gauge. The curve fit equations for the lines are in the form:

$$\text{VOLTAGE} = (\text{Y-intercept}) + [(\text{GAIN}) \times (\text{FORCE})] \quad (2)$$

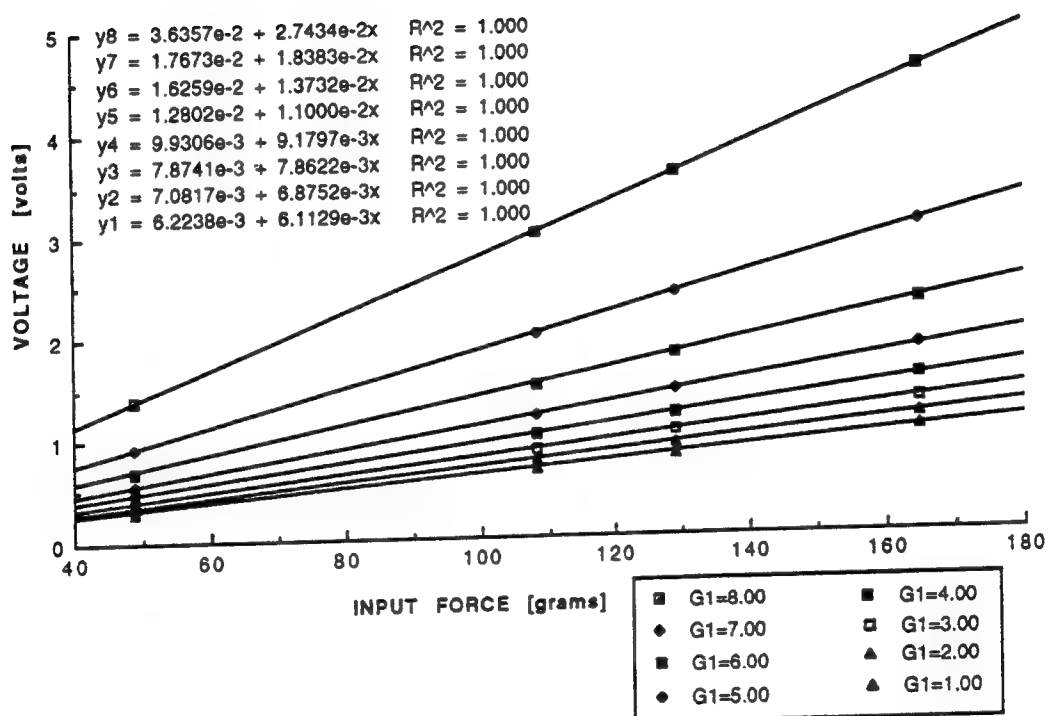


Figure 6. Input force and output voltage relationship for master strain gauge gain ( $K_{om}$ ).

The Y-intercept ( $y_{0m}$ ) for each curve fit represents a constant value that must be added when converting from input force to output voltage. A coefficient of multiple determination,  $r^2$ , is used to illustrate the accuracy of a fitted regression, [Ref.2, p.434], by:

$$r^2 = \frac{\sum_{i=1}^n (\hat{y}_i - \bar{y})^2}{\sum_{i=1}^n (y_i - \bar{y})^2} \quad (3)$$

where  $\hat{y}_i$  is the value of  $y$  as a function of the data abscissa ( $x$ ) using the curve fit equation,  $y_i$  is the data ordinate ( $y$ ), and  $\bar{y}$  is the sample mean of the ordinate ( $y$ ). A perfect fit between the data and curve fit equation results in a value of one. Since the value of  $K_{0m}$  varies with gain control setting, Figure 7 displays the relationship between the master strain gauge gain,  $K_{0m}$ , and master strain gauge amplifier gain control setting,  $G_1$ .

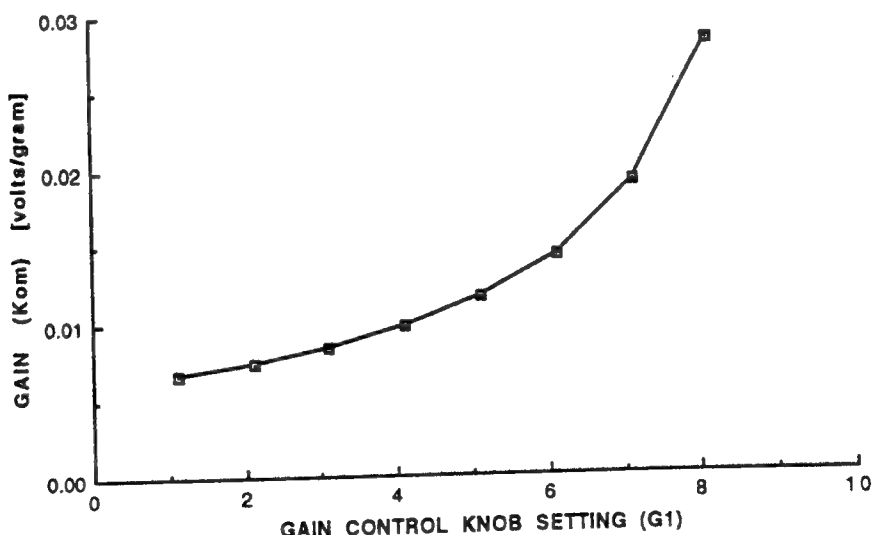


Figure 7. Master servo valve gain for various strain gauge amplifier gain control settings ( $G_1$ ).

This shows how the gain amplification increases for a constant increase in strain gauge amplifier gain control setting.

**b. Master Servo Valve Gain ( $K_1$ )**

Figure 8 is the block diagram relationship for  $K_1$ .

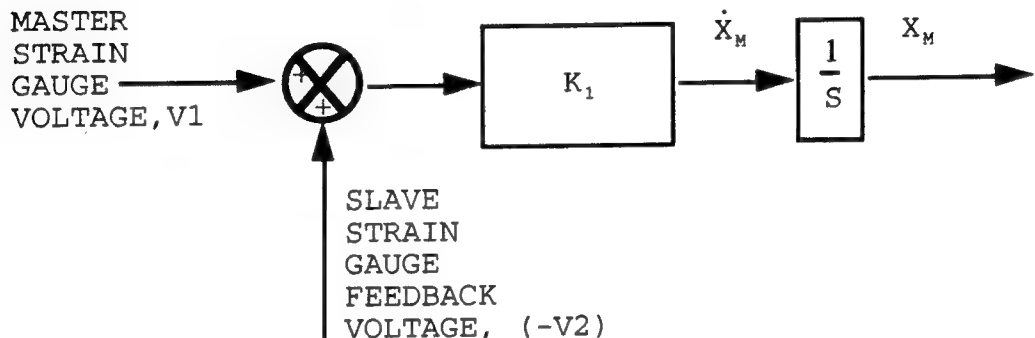


Figure 8. Master servo valve gain ( $K_1$ ) block diagram.

The hydraulic supply cutout valve was opened for the remaining gain estimations. No contact was made between the slave hydraulic ram and the obstruction during this gain calculation. A ruler was set up to measure one inch of travel distance by the master hydraulic ram. The distance measurement begins approximately one-half inch from the fully retracted position. The slave strain gauge feedback voltage was constant, but it was negative to offset the master slave strain gauge feedback voltage. Since no force input is applied, the gain offset for the master strain gauge was set to a positive voltage so that the system would not be in static equilibrium. The master strain gauge voltage was greater than the slave strain gauge voltage, which advanced the master hydraulic ram at a constant velocity. The joystick was used to fully retract the master hydraulic ram and then it was released so that it could advance at a constant velocity. The ram had one-half inch to obtain its

constant velocity, and a stop watch was used to time the ram to travel one inch. This was repeated five times for four different master strain gauge amplifier gain control settings: 2.0, 4.0, 6.0, and 8.0. See Appendix B for data obtained. The hydraulic ram velocity was calculated by:

$$\dot{x}(\text{velocity}) = \frac{x(\text{distance})}{\text{time}} = \frac{1 \text{ in}}{\text{time}} \quad (4)$$

for all five repetitions at each of the four gain control settings. At each gain control setting, the five velocities were averaged, and the master servo gain is calculated using:

$$K = \frac{\dot{x}(\text{average velocity})}{(v_1 + v_2)} \quad (5)$$

where  $v_1$  is the master strain gauge voltage, and  $v_2$  is the slave strain gauge voltage. In Figure 9, each master servo valve gain is plotted against the four strain gauge amplifier gain control settings, and it shows an approximately linear relationship between them. The coefficient of multiple determination is very close to one which represents an accurate representation.

#### c. Master Potentiometer Gain ( $K_4$ )

Figure 10 is the block diagram relationship for  $K_4$ . The gain was obtained by measuring the potentiometer output voltage for various positions of the master hydraulic ram. A jumper wire was used to connect the master potentiometer terminals on the servo amplifier to the voltmeter. A ruler was set up to measure a total distance of 2.0 inches in nine increments of .25 inches. The master potentiometer voltage was recorded for each displacement value. See Appendix C for data obtained.

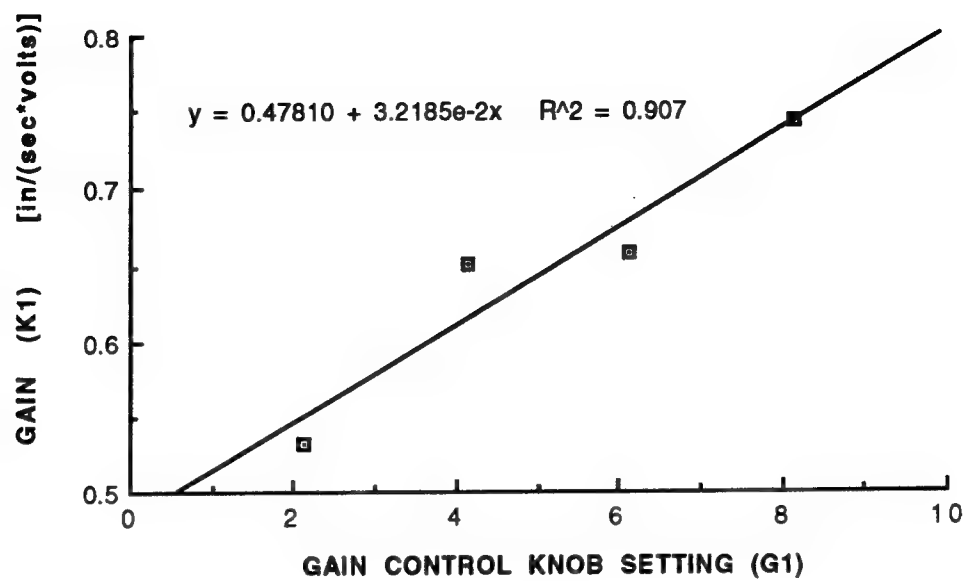


Figure 9. Master servo gain ( $K_1$ ) for various gain control knob settings ( $G_1$ ).

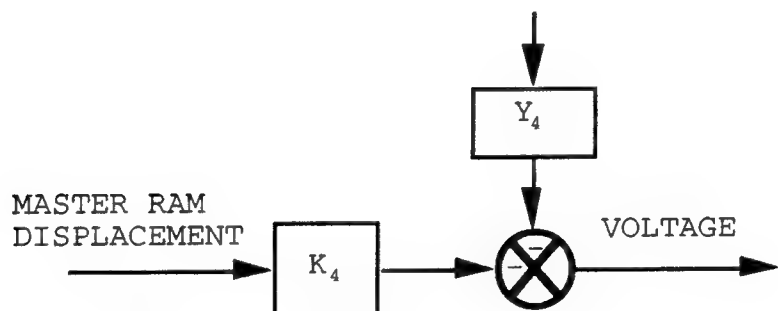


Figure 10. Master potentiometer gain ( $K_4$ ) block diagram.

From the data obtained, only the region after the slave ram contacts the obstruction is of interest. All data was plotted and the curve fit equation:

$$v = K_4 x + Y \text{ [volts]} \quad (6)$$

was obtained where  $K_4$  is -7.0207 and  $Y$  is 10.582. The equation needs to be shifted for the starting position to be at initial contact with the obstruction. For the master potentiometer voltage,  $v(x_m=0)=-1.256$  volts, a point-slope method for generating an equation:

$$m = K_4 = \frac{v(x) - v(x_0)}{x - x_0} \quad (7)$$

$$v(x) = K_4 + v(x_0) \quad (8)$$

was used to shift the graph to the desired region. Figure 11 shows the relationship between the master ram displacement distance and potentiometer voltage where the initial position is when the slave contacts the obstruction. The slope of this linear relationship (voltage divided by distance) was obtained by using a least squares curve fit, and it is the gain for the master potentiometer gain. The curve fit equation is in the form:

$$\text{POTENTIOMETER VOLTAGE} = (\text{Y-intercept}) + (\text{GAIN})x (\text{DISTANCE}) \quad (9)$$

The Y-intercept ( $Y_4$ ) for the curve fit represents a constant value that must be added when converting from input displacement position to output potentiometer voltage. For

the master ram, a larger displacement corresponds to a voltage that is greater in magnitude but is negative.

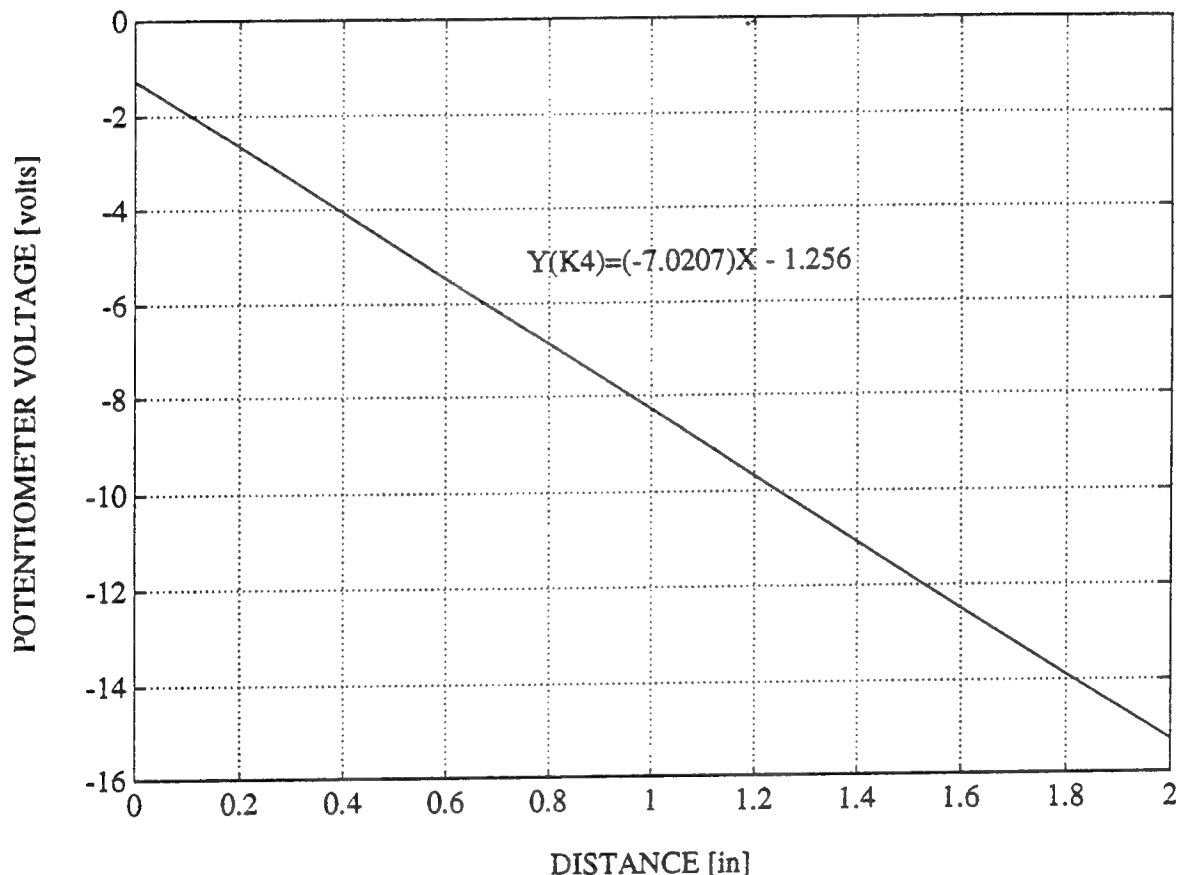


Figure 11. Master potentiometer gain ( $K_1$ ) relationship between master ram displacement distance and potentiometer voltage.

**d. Slave Servo Valve Gain ( $K_2$ )**

Figure 12 is the block diagram relationship for  $K_2$ .

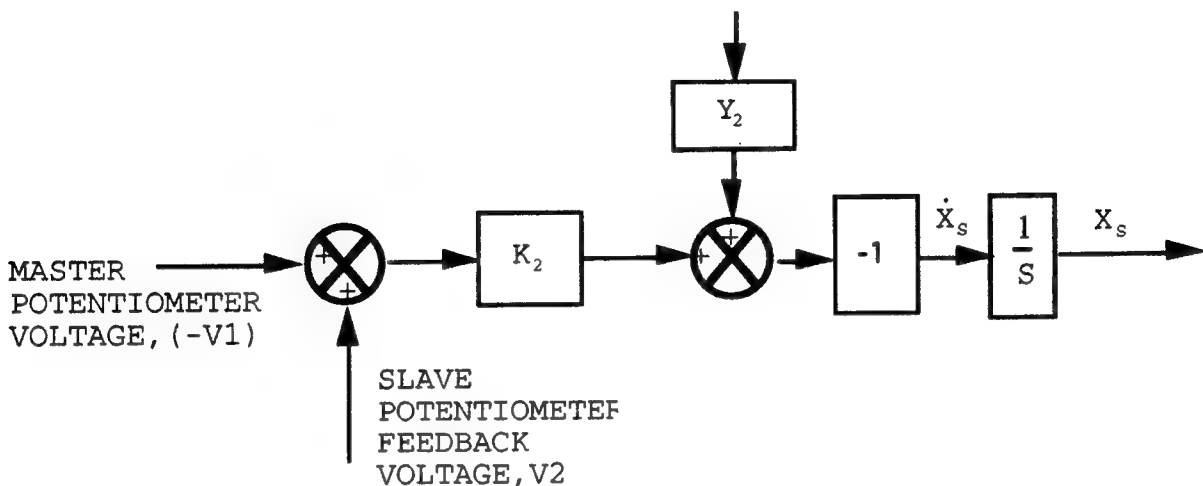


Figure 12. Slave servo valve gain ( $K_2$ ) block diagram.

It was desirable to disconnect the slave potentiometer feedback and only measure the voltage input from the master potentiometer. It was very difficult to control the system when the feedback voltage (V2) was disconnected. Larger than normal voltages would drive the slave servo valve when the feedback was disconnected because no feedback voltage would offset the master potentiometer voltage that increases in magnitude with increased master ram displacement. To maintain control of the system, very small voltages from the master potentiometer were used. The master ram was positioned such that its potentiometer voltage (V1) was zero so there was no driving voltage sent to the slave servo. By using the master strain gauge offset gain control, a very small positive displacement was created by the master ram. Its position was held constant, and the master potentiometer delivered a constant but negative input voltage to the slave servo valve, extending the slave hydraulic ram at a constant velocity.

The slave servo gain was calculated similarly to the master servo gain. No contact was made between the slave hydraulic ram and the obstruction while approximating the slave servo gain. The master and slave strain gauge amplifier gain control settings, G1 and G2 respectively, were independent of this calculation. A ruler was set up to measure one inch of travel distance by the slave hydraulic ram. The distance measurement began approximately one-half inch from the fully retracted position so that the ram would obtain a constant velocity before this position. A stop watch was used to time the ram to travel the measured inch. This was repeated eight times using various master potentiometer input voltages. See Appendix D for data obtained. Velocity of the hydraulic ram for each data point was calculated using Equation 4 from the master servo gain calculation. Figure 13 shows the relationship between input voltage and slave ram velocity. Since a negative voltage creates a negative slave ram velocity and then integrated to a negative displacement, the minus one block is used in the block diagram to give a positive displacement which is used in calculations for the slave potentiometer gain and slave strain gauge and spring gain.

The slope of this linear relationship (velocity divided by voltage) was obtained by using a least squares curve fit, and it is the gain for the slave servo valve. The curve fit equation for the line is in the form:

$$\text{VELOCITY} = (\text{Y-intercept}) + [(\text{GAIN}) \times (\text{VOLTAGE})] \quad (10)$$

The Y-intercept ( $Y_2$ ) for the curve fit represents a constant value that must be added when converting from negative input voltage output positive velocity. The coefficient of multiple determination is only 82.5% which represents a moderately accurate representation.

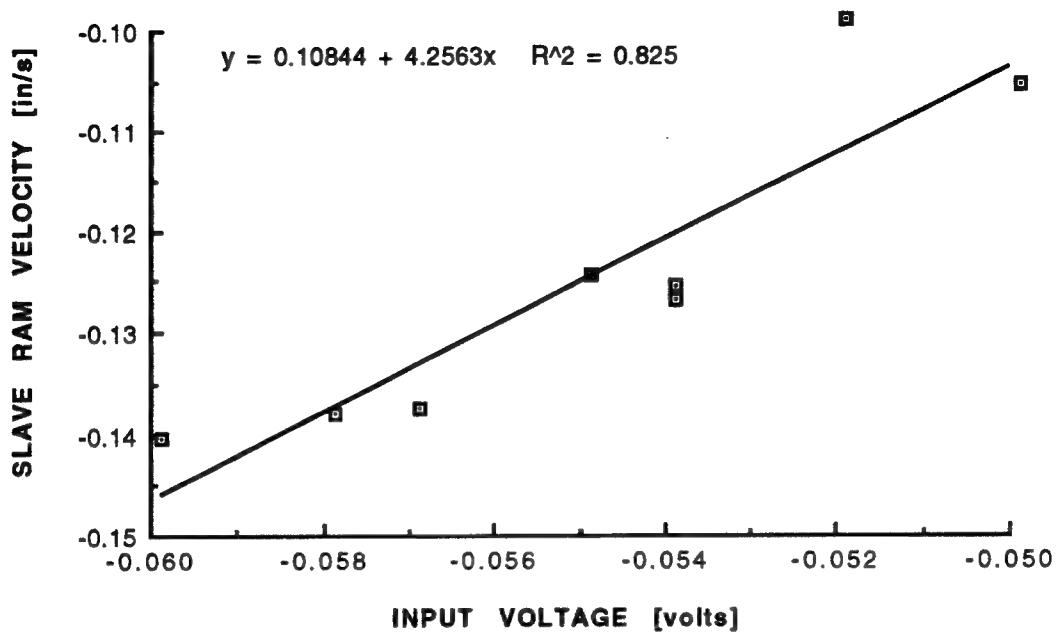


Figure 13. Slave servo valve gain ( $K_2$ ) relationship between input servo voltage and slave ram velocity.

#### e. Slave Potentiometer Gain ( $K_3$ )

Figure 14 is the block diagram relationship for  $K_3$ .

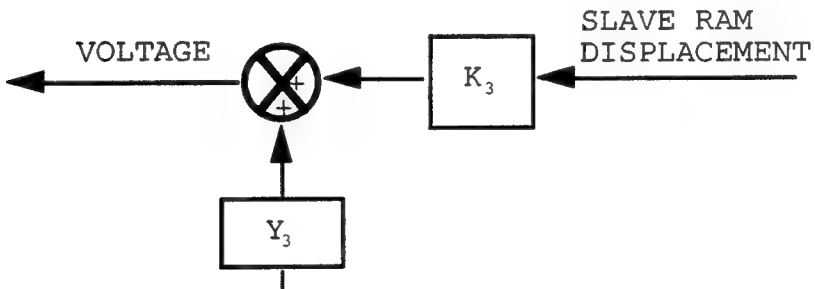


Figure 14. Slave potentiometer gain ( $K_3$ ) block diagram.

The slave potentiometer gain was calculated similarly to the master potentiometer gain. The gain was obtained by measuring the potentiometer output voltage for

various positions of the slave hydraulic ram. A jumper wire was used to connect the slave potentiometer terminals on the servo amplifier to the voltmeter. A ruler was set up to measure a total distance of 3.375 inches in 14 increments of .25 inches. Since the slave ram is longer than the master ram, there were more data points taken for the slave ram. The slave potentiometer voltage was recorded for each displacement value. See Appendix E for data obtained.

From the data obtained, only the region after the slave ram contacts the obstruction is of interest. All data was plotted and the curve fit equation:

$$v = K_3 x + Y \text{ [volts]} \quad (11)$$

was obtained where  $K_3$  is 3.6816 and  $Y$  is -9.8699. The equation needs to be shifted for the starting position to be at initial contact with the obstruction. For the master potentiometer voltage,  $v(x_s=0)=1.214$  volts, a point-slope method for generating an equation:

$$m = K_3 = \frac{v(x) - v(x_0)}{x - x_0} \quad (12)$$

$$v(x) = K_3 + v(x_0) \quad (13)$$

was used to shift the graph to the desired region. Figure 15 shows the relationship between the slave ram displacement distance and potentiometer voltage. The slope of this linear relationship (voltage divided by distance) was obtained by using a least squares curve fit, and it is the gain for the master potentiometer gain. Equation 6 was used again for the curve fit equation. The Y-intercept ( $Y_3$ ) for the curve fit represents a constant value that must be added when

converting from input displacement position to output potentiometer voltage. For the slave ram, a larger displacement corresponds to a voltage that is greater in magnitude but is positive.

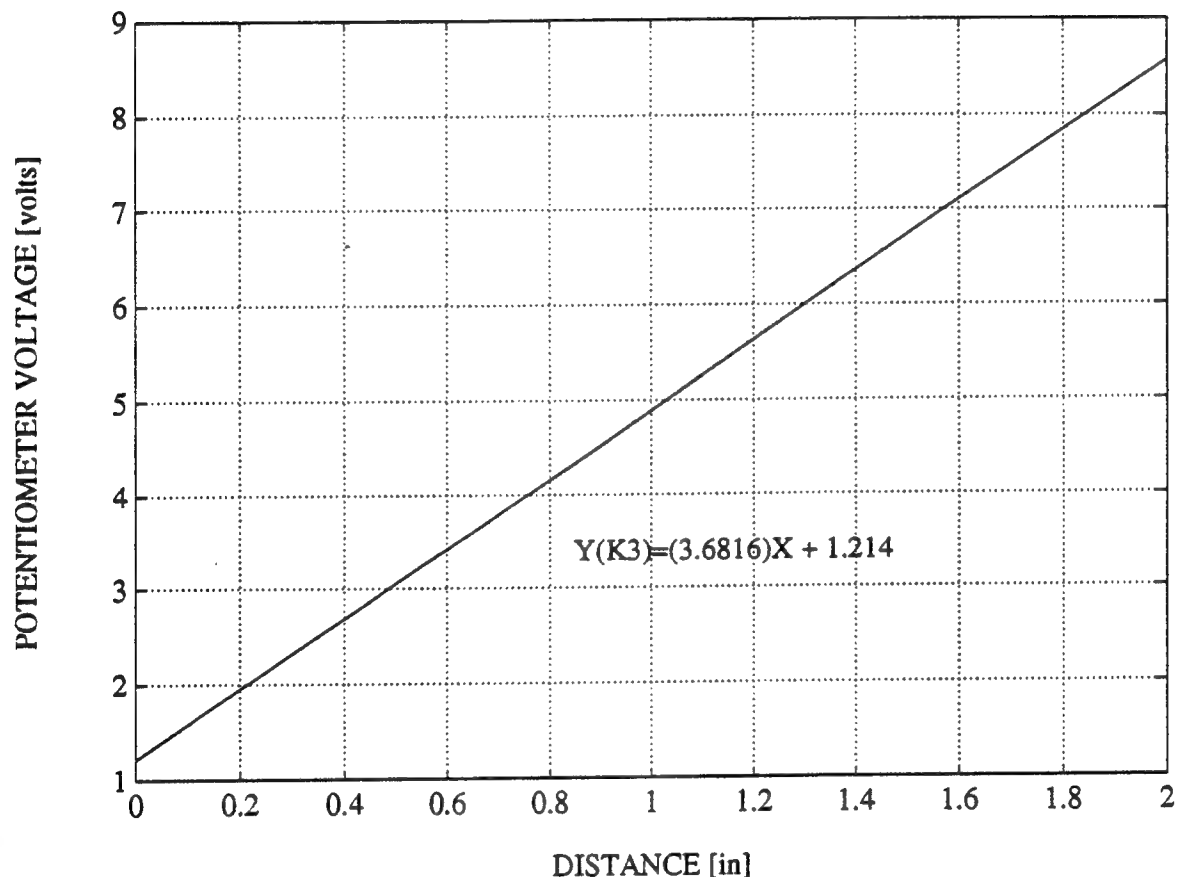


Figure 15. Slave potentiometer gain ( $K_3$ ) relationship between slave ram displacement distance and potentiometer voltage.

Figure 16 shows the displacement and voltage relationship for the master and slave potentiometer gains. The master potentiometer gain has an increasing negative voltage with increased displacement, and the slave potentiometer gain has an increasing positive voltage with increased displacement. Therefore they offset each other in the servo amplifier summation to obtain equilibrium in position control mode.

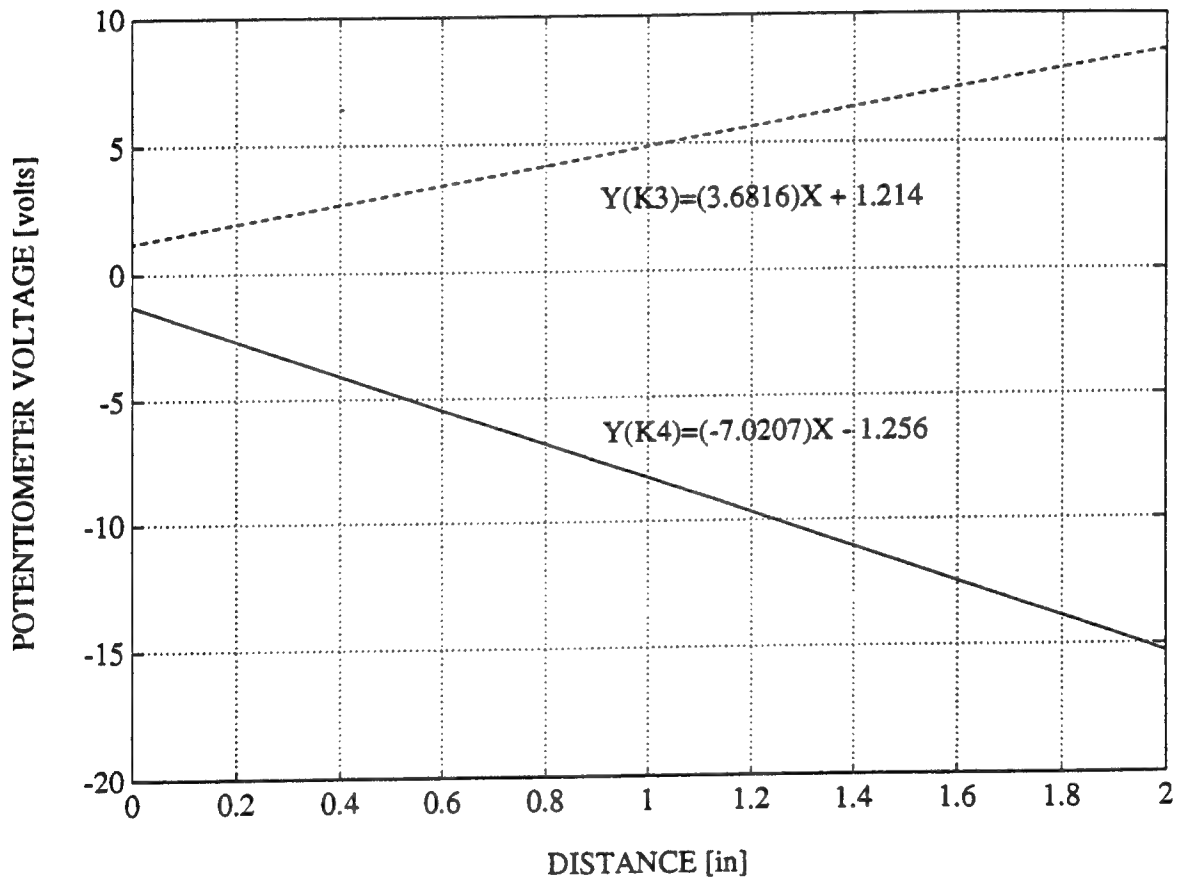


Figure 16. Master and slave potentiometer gain relationship ( $K_4$  and  $K_3$ , respectively).

**f. Slave Strain Gauge Gain ( $K_{os}$ ) and  
Obstruction Spring Gain ( $K_{sp}$ )**

Figure 17 is the block diagram relationship for  $K_{os}K_{sp}$ .

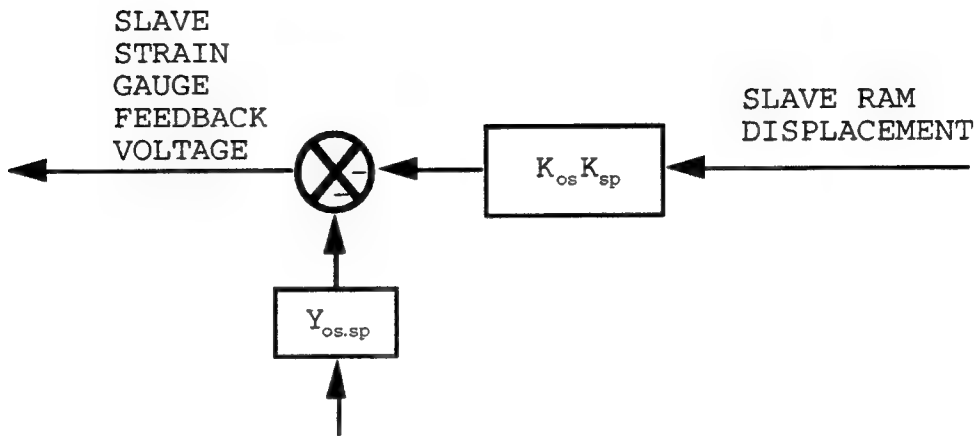


Figure 17. Slave strain gauge gain ( $K_{os}$ ) and obstruction spring gain ( $K_{sp}$ ) block diagram.

The master unit joystick was moved to positionally place the slave unit into contact with the obstruction. Once contact was first made, with no resistive force voltage reading on the voltmeter, the zero inch position for the slave ram was marked. A ruler was set up to measure a total distance of one inch in nine increments of .125 inches. Nine strain gauge voltages were recorded for each of four different slave strain gauge amplifier gain control settings: 2.0, 4.0, 6.0 and 8.0. The master strain gauge amplifier gain control setting remained constant at 1.0 for all data points, but it is independent of our calculations. See Appendix F for data obtained. Figure 18 shows the relationship between the input slave ram position and the output slave strain gauge feedback voltage for the four different gain control settings (G2). The slope of these linear relationships (voltage divided by position) was obtained by using a least squares curve fit, and it is the

gain for the master strain gauge. The curve fit equation for the lines are in the form:

$$\text{VOLTAGE} = (\text{Y-intercept}) + [(\text{GAIN}) \times (\text{POSITION})] \quad (14)$$

The Y-intercept ( $Y_{os,sp}$ ) for each curve fit represents a constant value that must be added when converting from input position to output voltage.

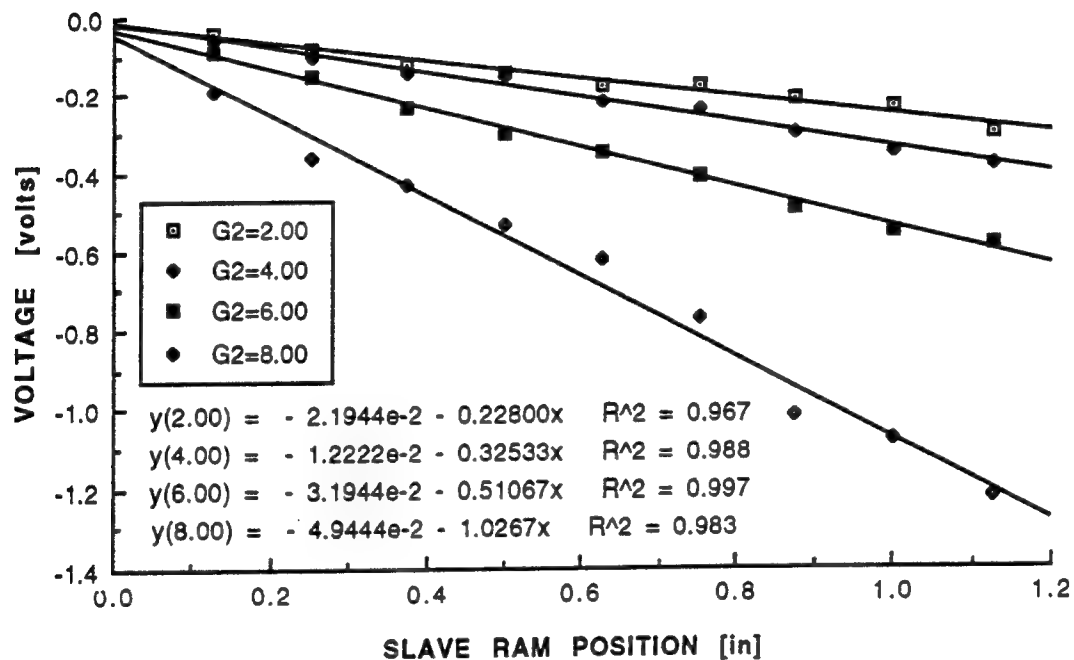


Figure 18. Spring and slave strain gauge gain ( $K_{os}K_{sp}$ ) relationship between slave ram position and output voltage.

Since the value of  $K_{os}K_{sp}$  varies with gain control setting, Figure 19 displays the relationship between  $K_{os}K_{sp}$  and G2. This shows how the gain amplification increases in magnitude for a constant increase in strain gauge amplifier gain control setting. The coefficient of multiple determination ranges from 96.7% to 99.7% which represents an accurate representation. The output voltage is negative for a positive slave ram displacement to offset the applied force voltage so a negative summing junction is used in the block diagram to create this negative output voltage.

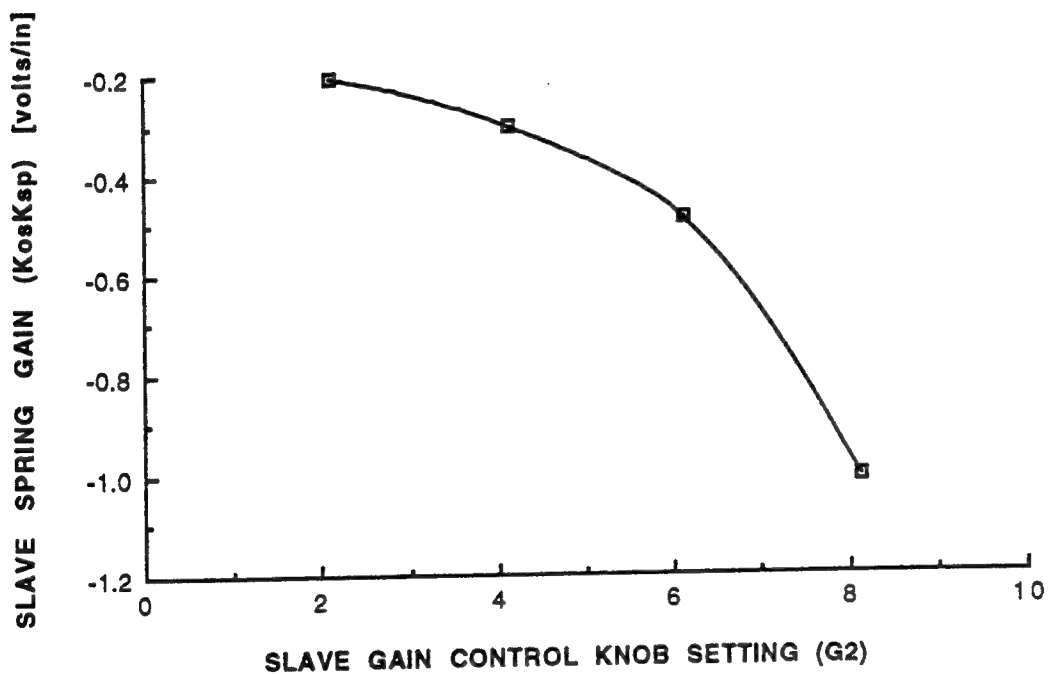


Figure 19. Spring and slave strain gauge gain ( $K_{os}K_{sp}$ ) for various strain gauge amplifier gain control settings (G2).

## D. THEORETICAL ANALYSIS

### 1. Gain Values for Theoretical Analysis

It is desirable to model the single degree of freedom force feedback system to predict the actual response and stability with various gain control settings. The gain values used were obtained from the gain approximation calculations.

The input force of 45.4 grams was the weight of an object that was used in the experimental analysis to create the step input.

The resistive force from the obstruction was felt easier by the operator when the strain gauge amplifier gain control knob was set higher for the slave unit (G2) than for the master unit (G1). Therefore, the magnitude of the feedback voltage was larger than the applied force voltage, causing the voltage difference to decrease at a faster rate. The hydraulic power assist was decreased at a much faster rate. For G1 set to four,  $K_{om}$  is .0092 and  $Y_{om}$  is .0099. For G2 set to six,  $K_{os}K_{sp}$  is .5107 and  $Y_{os.sp}$  is .0319.

The master and slave potentiometer gains ( $K_4$  and  $K_3$ , respectively) are fixed from our experimental calculations.  $K_4$  is 7.0207,  $Y_4$  is 1.256,  $K_3$  is 3.6816, and  $Y_3$  is 1.214.

The master servo valve gain ( $K_1$ ) is dependant on G1, and for G1 set to four,  $K_1$  is fixed at .6441 from the average velocity calculations.

The slave servo valve gain ( $K_2$ ) was calculated independently of G1 and G2, and it only depended on the input voltage from the master potentiometer.  $K_2$  and  $Y_2$  are fixed at 4.2563 and .108, respectively.

### 2. Manual Analysis

To develop an equation for the time response of the slave displacement as a function of six inputs, the principle

of superposition is used. One input is taken at a time while setting all other inputs to zero and developing a transfer function relationship between slave displacement output and the single input. This is repeated for all six inputs, and the slave displacement for all inputs is the sum of all the displacement equations for the individual inputs. Figures 20 thru 25 are the individual block diagram arrangements used for the single input superposition principle. The individual transfer function relationships for their respective single input block diagram are:

$$\frac{X_s}{F} = \frac{K_1 K_2 K_4 K_{OM}}{s^2 + K_2 K_3 s + K_1 K_2 K_4 K_{os} K_{sp}} \quad (15)$$

$$\frac{X_s}{Y_{om}} = \frac{K_1 K_2 K_4}{s^2 + K_2 K_3 s + K_1 K_2 K_4 K_{os} K_{sp}} \quad (16)$$

$$\frac{X_s}{Y_4} = \frac{K_2 s}{s^2 + K_2 K_3 s + K_1 K_2 K_4 K_{os} K_{sp}} \quad (17)$$

$$\frac{X_s}{Y_2} = \frac{-s}{s^2 + K_2 K_3 s + K_1 K_2 K_4 K_{os} K_{sp}} \quad (18)$$

$$\frac{X_s}{Y_3} = \frac{-K_2 s}{s^2 + K_2 K_3 s + K_1 K_2 K_4 K_{os} K_{sp}} \quad (19)$$

$$\frac{X_s}{Y_{os,sp}} = \frac{-K_1 K_2 K_4}{s^2 + K_2 K_3 s + K_1 K_2 K_4 K_{os} K_{sp}} \quad (20)$$

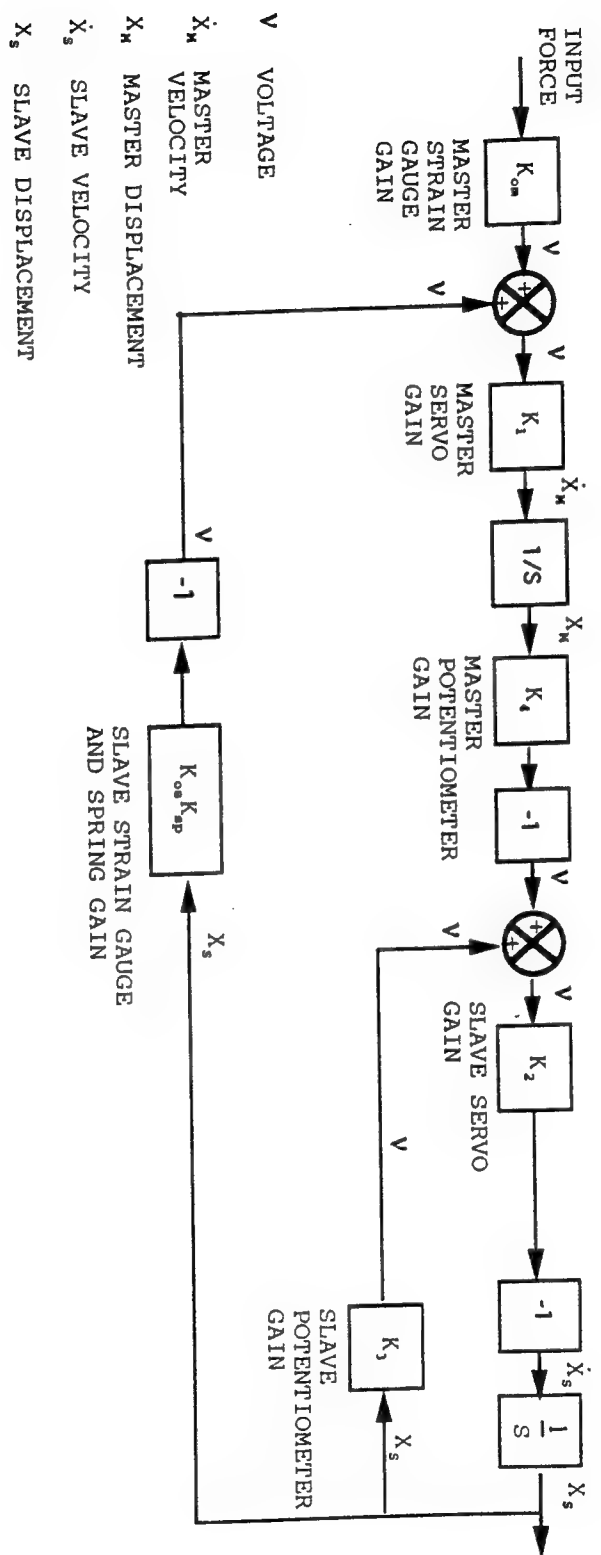


Figure 20. Single input block diagram for external step force.

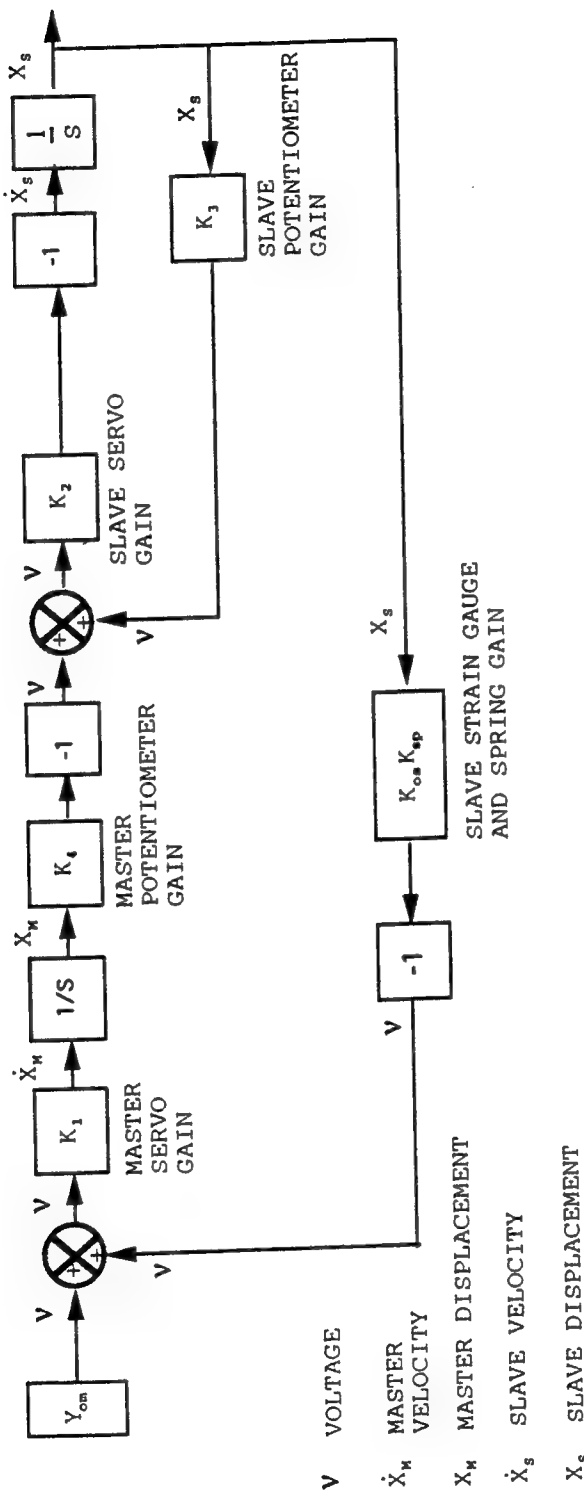


Figure 21. Single input block diagram for Kom's constant Y-intercept (Y<sub>om</sub>).

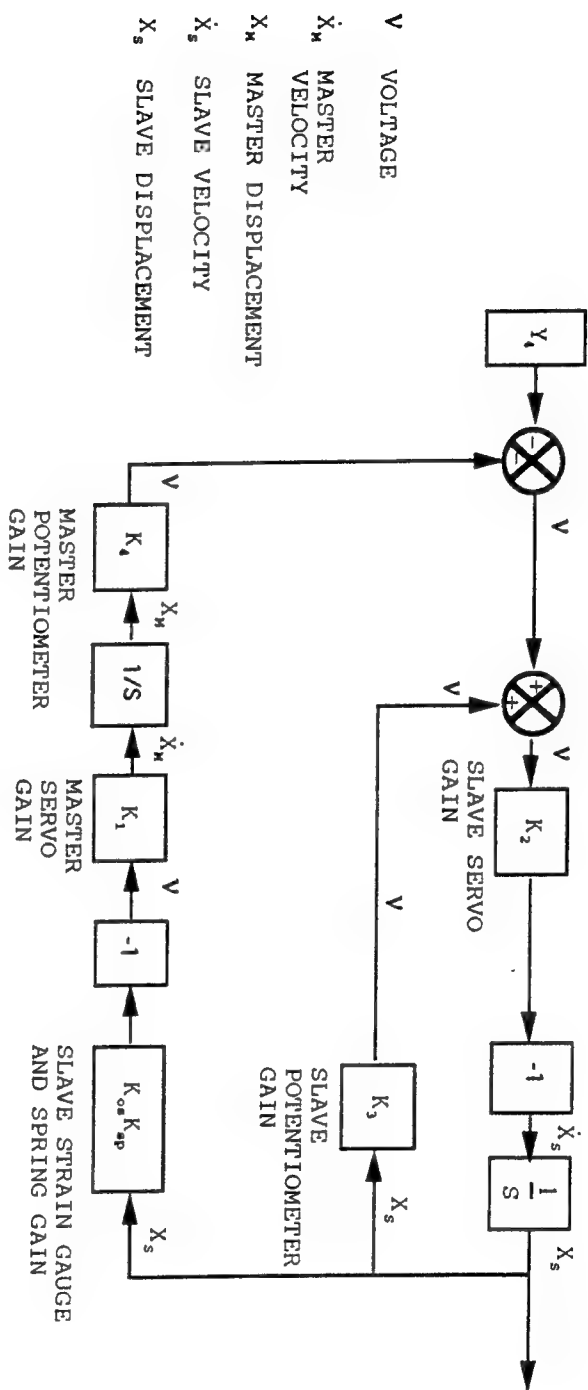


Figure 22. Single input block diagram for K4's constant Y-intercept (Y4).

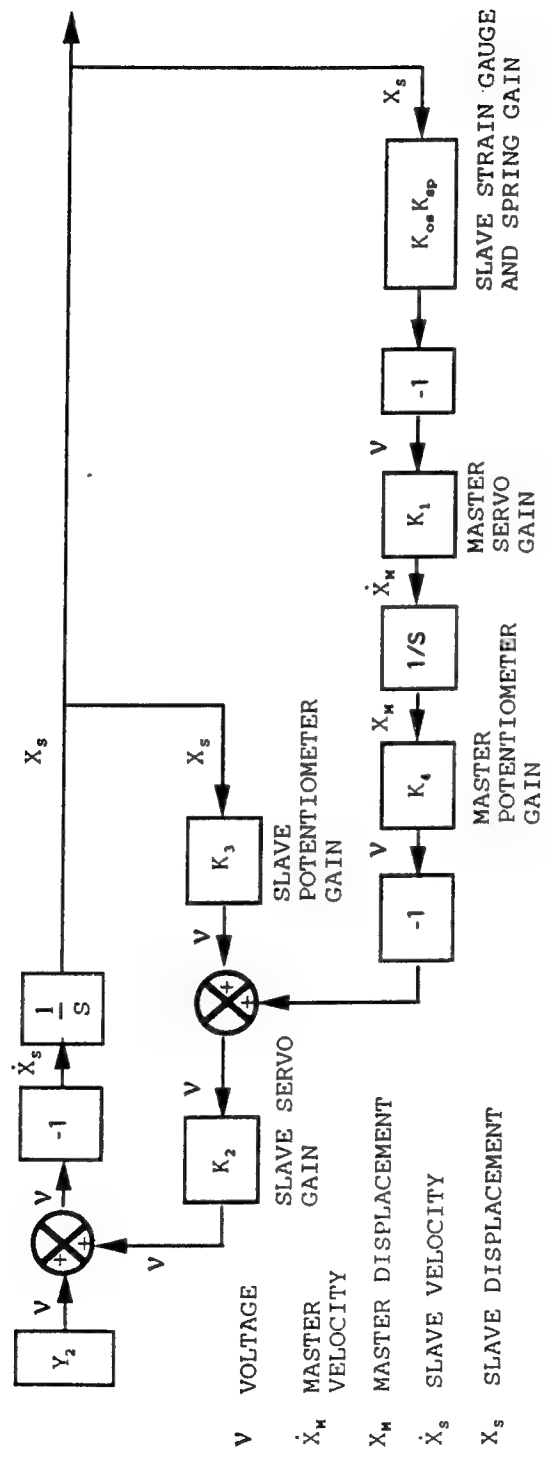


Figure 23. Single input block diagram for  $K_2$ 's constant Y-intercept ( $Y_2$ ).

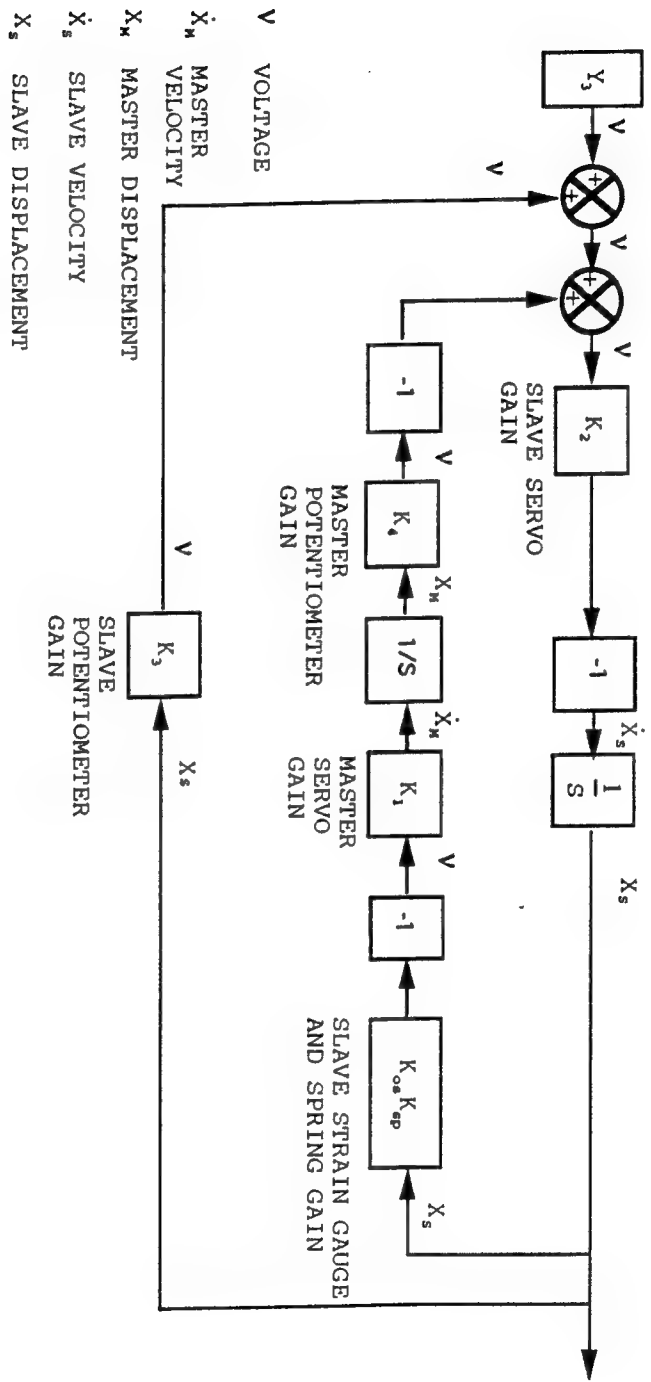


Figure 24. Single input block diagram for  $K_3$ 's constant  $Y$ -intercept ( $Y_3$ ).

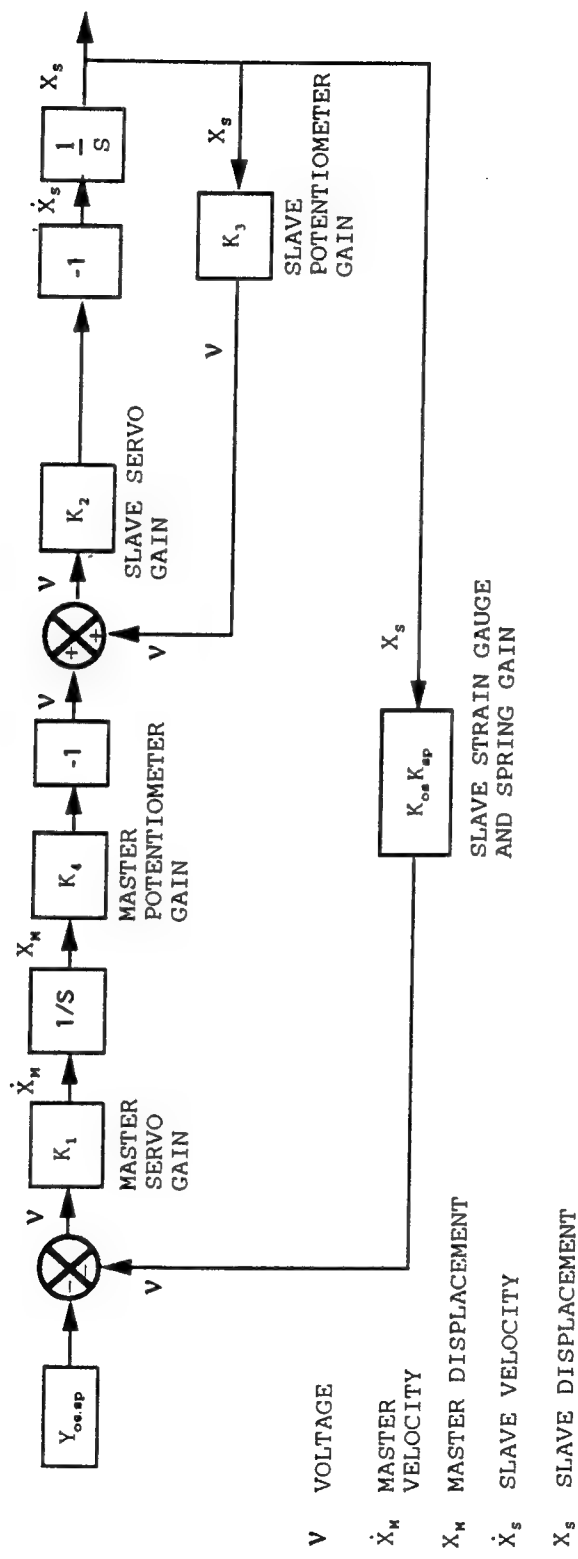


Figure 25. Single input block diagram for Kosksp's constant Y-intercept (Yos.sp).

By adding equations 8-13 in terms of slave ram position ( $X_s$ ), the combined equation is:

$$X_s = \frac{(F_1 K_1 K_2 K_4 K_{OM}) + (Y_{om} K_1 K_2 K_4) + (Y_4 K_2 s) - (Y_2 s) - (Y_3 K_2 s) - (Y_{os.sp} K_1 K_2 K_4)}{s^2 + K_2 K_3 s + K_1 K_2 K_4 K_{os} K_{sp}} \quad (21)$$

By collecting similar terms, the slave ram position equation can be written as:

$$X_s = \frac{s(Y_4 K_2 - Y_2 - Y_3 K_2) + (F_1 K_1 K_2 K_4 K_{OM} + Y_{om} K_1 K_2 K_4 - Y_{os.sp} K_1 K_2 K_4)}{s^2 + K_2 K_3 s + K_1 K_2 K_4 K_{os} K_{sp}} \quad (22)$$

The same characteristic equation appears in the denominator of the transfer function for all six individual inputs, and it is in the form:

$$s^2 + 2\zeta\omega_n s + \omega_n^2 = 0 \quad (23)$$

where:

$$2\zeta\omega_n = K_2 K_3 \quad (24)$$

$$\omega_n^2 = K_1 K_2 K_4 K_{os} K_{sp} \quad (25)$$

The damping ratio,  $\zeta$ , for the experimentally obtained gains for our system is:

$$\zeta = \frac{K_2 K_3}{2(K_1 K_2 K_4 K_{os} K_{sp})^{\frac{1}{2}}} = 2.50 \quad (26)$$

The natural frequency,  $\omega_n$ , for our system is:

$$\omega_n = (K_1 K_2 K_4 K_{os} K_{sp})^{\frac{1}{2}} = 3.14 \text{ [rad/sec]} \quad (27)$$

Since the damping ratio is greater than unity, the characteristic response for all six inputs is overdamped. The controls tool box in MATLAB [Ref.3] is used to plot the time response for a typical unit step transfer function for the single degree of freedom system using:

$$\frac{x_s}{\text{input}} = \frac{(\omega_n)^2}{s^2 + 2\zeta\omega_n s + \omega_n^2} \quad (28)$$

where  $x_s$  is the slave ram position output and the input is a unit step. Figure 26 is the time response plot, and the MATLAB computer code is presented in Appendix G.

The overdamped response demonstrates that the linear model for the system with six inputs should have a similar response since the characteristic equation is the same. The slave ram position response should be overdamped and reach 67% of its steady state value in approximately 1.7 seconds.

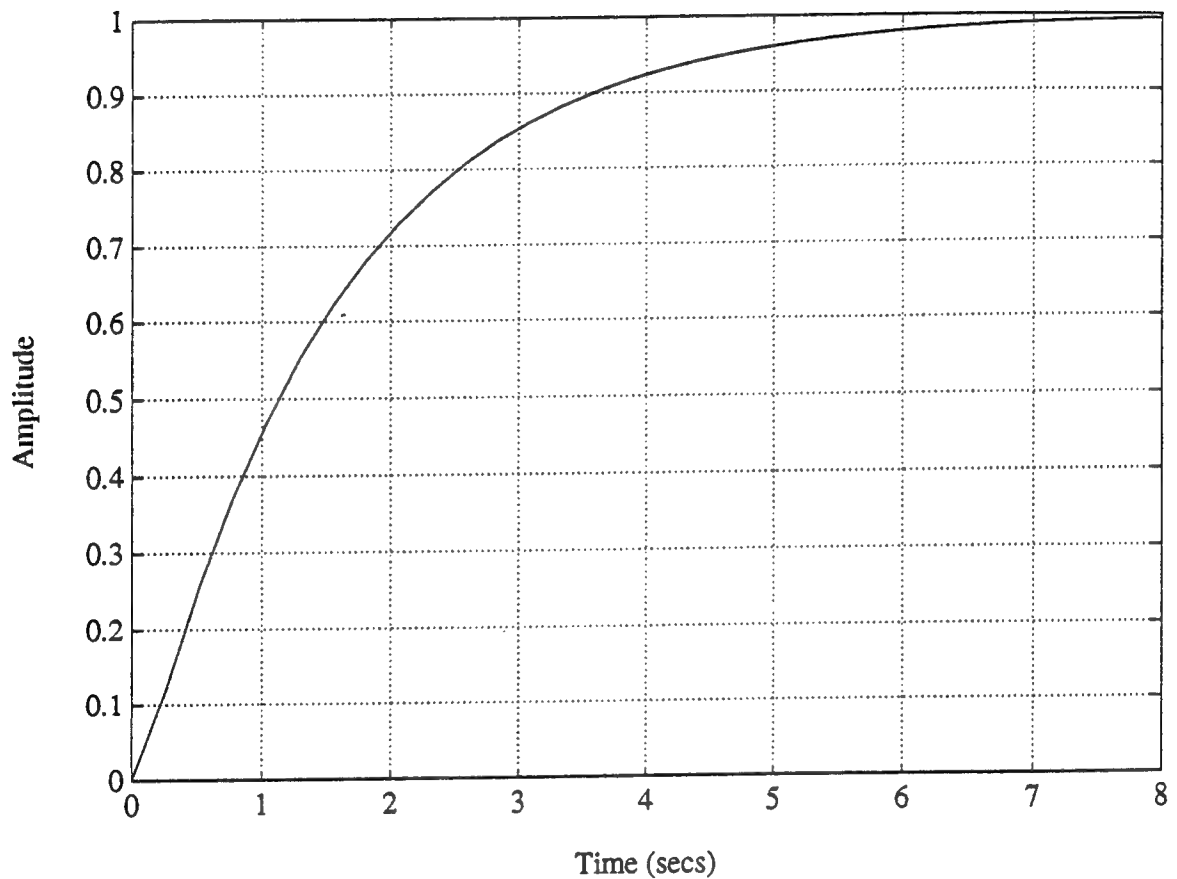


Figure 26. Typical single degree of freedom time response.

### **3. SIMULAB Analysis**

The manual approach to building an analytical model of a more complex system can be very time consuming. SIMULAB, [Ref.4], is a software program for simulating dynamic systems. The system to be simulated is built in block diagram format on a computer and the values for all gains and inputs are entered into their respective blocks. See Figure 27. The convenience in this software is that an oscilloscope can be tapped anywhere in the system onto a block junction line. A simulation command will construct a real time display of the system's particular variable at this tapped location of the oscilloscope. Another feature of this software is that discrete data can be taken anywhere along the system by tapping a block junction line similarly to the oscilloscope operation. It will be sent to a MATLAB data file in array format to plot the variable verse time.

SIMULAB's accuracy in modeling a linear system will be verified by comparing its results with the characteristic MATLAB response. For the single degree of freedom system, oscilloscopes were hooked up to view the master servo valve input voltage in the master unit, the obstruction resistive force voltage, and the slave ram position. The SIMULAB time response for the force driving voltage in the master unit is plotted in Figure 28. It is an exponentially decaying response which has an initial value equal to the voltage generated by the input force voltage minus initial obstruction force voltage, and it has a final value of zero as the resistive force voltage offsets the applied force voltage.

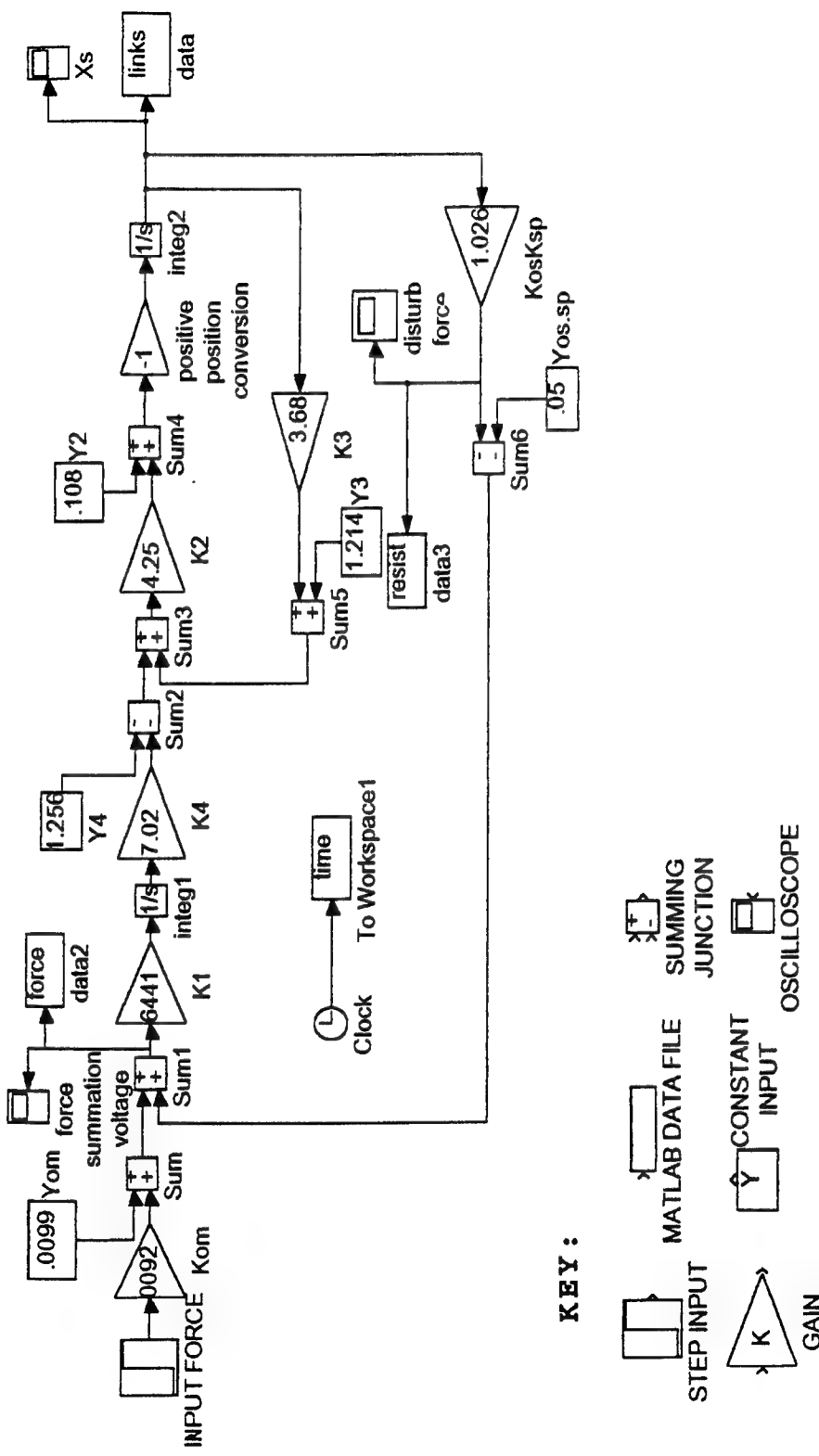


Figure 27. SIMULAB block diagram for single degree of freedom system.

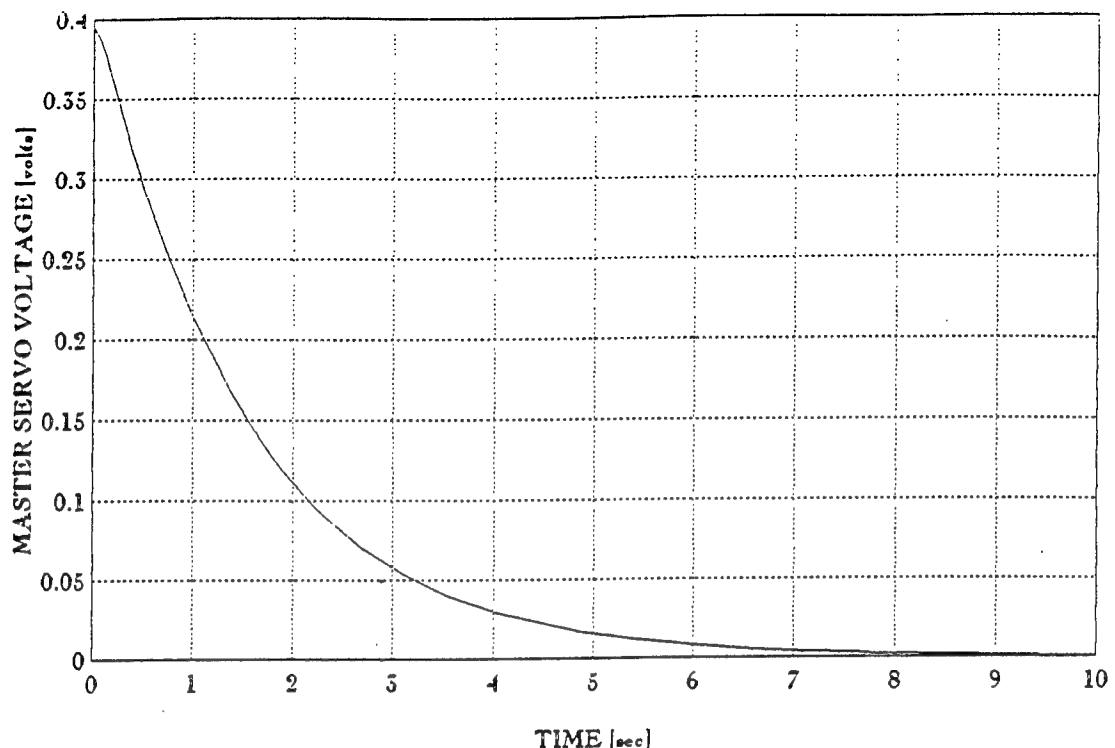


Figure 28. SIMULAB time response for the master servo input voltage.

The SIMULAB time response for the resistive force voltage in the slave unit is plotted in Figure 29. It is an overdamped response which has an initial value of zero and increases as the force resistance increases directly with ram displacement. Steady state occurs when the resistive force voltage offsets the applied force voltage.

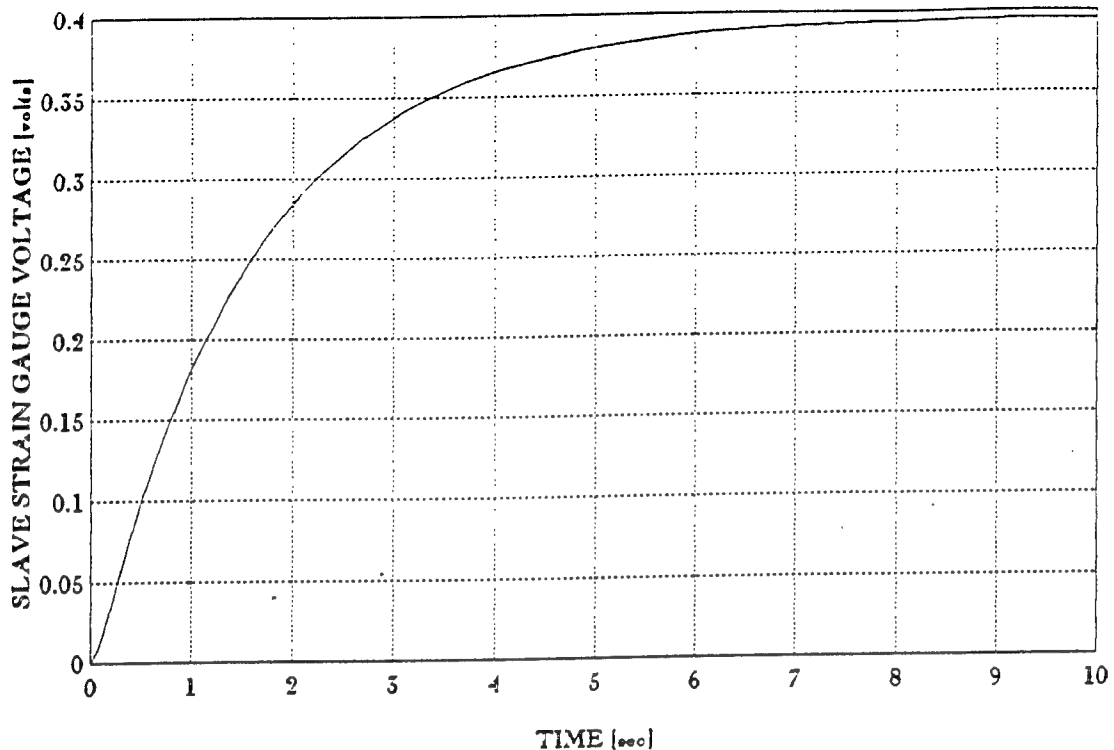


Figure 29. SIMULAB time response for the obstruction's resistive force voltage.

The time response for the slave ram displacement is plotted in Figure 30, and it looks similar to the MATLAB prediction. It is an overdamped system and is stable for the gain values selected. The slave ram position obtains 67% of its steady state value in approximately 1.7 seconds.

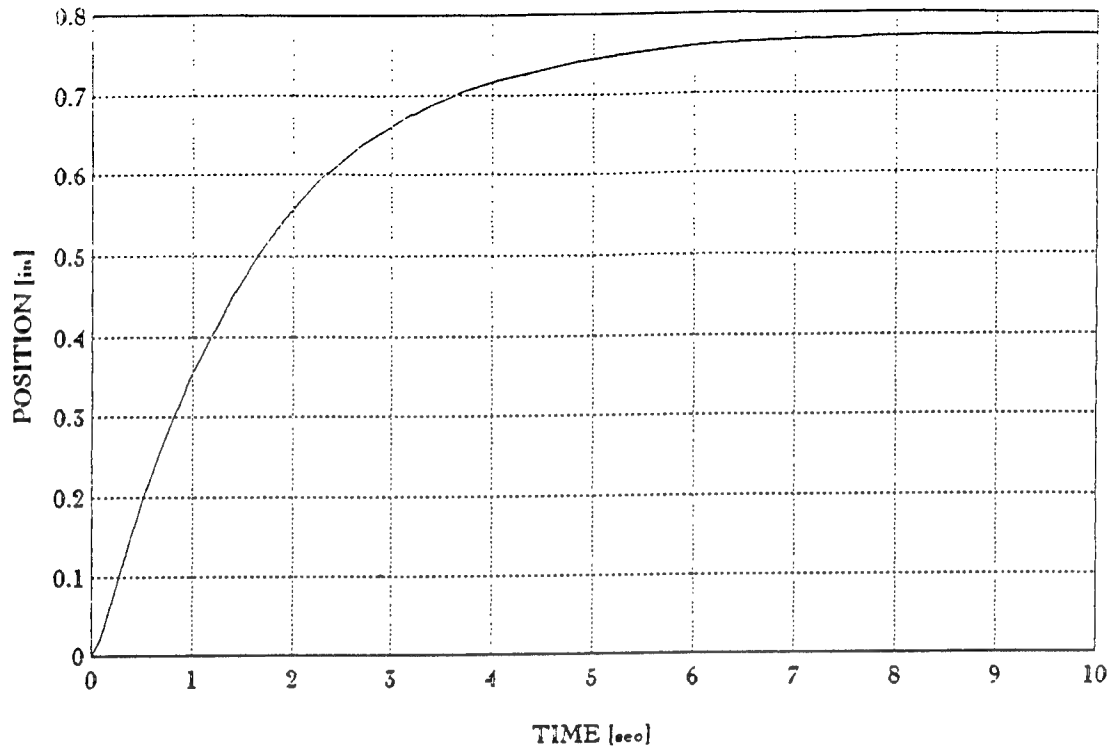


Figure 30. SIMULAB time response for the slave ram after contact with the obstruction.

A constant input force drives the master ram at a constant extension velocity, and the master unit positionally drives the slave unit to extend in a proportion manner. But since the initial position of the slave ram is in contact with the obstruction, it will deliver a voltage proportional to the resistive force to the master servo valve that will offset the force driving voltage. Since the constant, master force voltage is initially greater than the slave resistive

voltage, the slave ram will extend. As the resistive force voltage increases with slave ram displacement and the input force voltage remains constant, their difference continually decreases, causing a smaller driving voltage to the master servo valve. The reduced driving voltage will decrease the master ram velocity which will cause the slave ram velocity to also decrease. The decreasing slope of the time response function for the slave ram displacement represents the decreasing velocity of the slave ram. The resistive force increases proportionally to the increased slave ram displacement until the resistive voltage equals the constant force voltage. The summation of these two voltages cancel each other, and there is no longer a force voltage driving the master ram. A new equilibrium position is obtained as long as the input force is not removed.

These results verify that SIMULAB is an effective tool in modeling a linear system with multiple inputs since it compares to the characteristic response obtained from MATLAB, and it will be used to model a more complex, two degree of freedom force feedback system. SIMULAB's accuracy in predicting the actual single degree of freedom system response will be verified by experimentation.

## **E. EXPERIMENTATION**

### **1. Sensing Force Feedback**

When the operator applied a force input to the joystick, the system behaved in a position control mode before the slave ram contacted an obstruction. As a force was applied to the left, the master ram moved to the left, and the slave ram immediately followed to the left. When the force was applied to the right, the master ram moved to the right, and the slave ram immediately followed to the right. When the force was applied to the left so that the slave ram came into

contact with the obstruction, the operator felt the hydraulic resistance in the joystick increase as the resistive voltage offset the force voltage. A greater force needed to be applied to the joystick to keep the master ram moving. This demonstrated that the resistive force feedback can be felt by the operator.

## 2. Dynamic Response

It is desirable to verify the accuracy of the theoretical model by measuring the time response of the step input force and the slave ram displacement. A strip chart recorder was connected to the master strain gauge and the slave ram potentiometer, and it was set to a speed of 5mm/sec. The joystick was rotated 90 degrees so that the strain gauge would experience a bending stress, and a weight of 45.4 grams was dropped to apply a step input force. Figures 31-34 are the strip chart recordings of the time response for the force input and slave ram displacement for four observations. The amplitude for two-thirds of the slave's steady state ram position is marked with a tick mark. The plot on the left is the force response with the center line as the zero force reference, and a positive step input force registers to the left of the reference. The plot on the right is the slave ram position response with the center line as the initial position of the ram in contact with the obstruction, and a positive ram displacement registers to the right of the reference. For the four runs, the times to reach two-thirds of its steady state value are 1.8, 1.6, 1.6, and 1.4 seconds, respectively, with an average of 1.6 seconds. The force input recording demonstrates the accuracy of creating a step input by dropping a light weight. Oscillations at the beginning of the step response were avoided by minimizing the distance the weight was dropped.

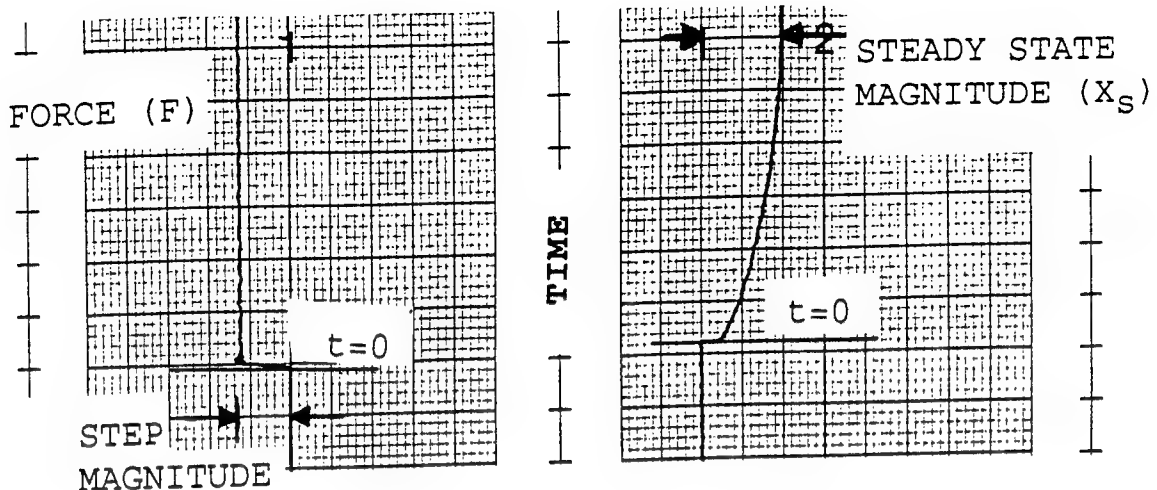


Figure 31. Strip chart recording for the force input and slave ram displacement, run #1.

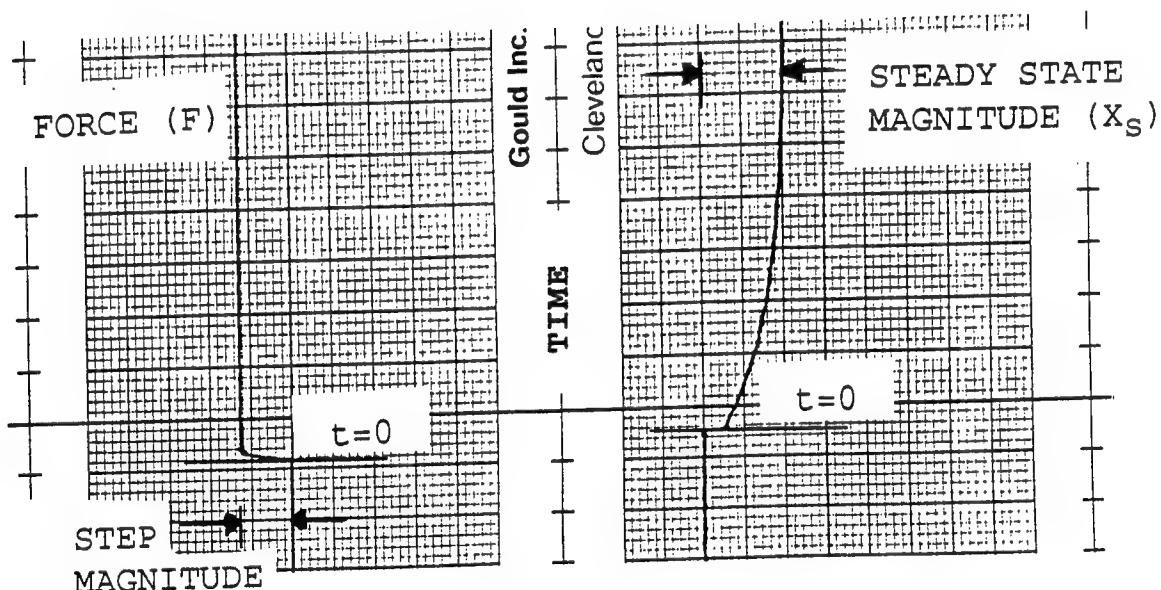


Figure 32. Strip chart recording for the force input and slave ram displacement, run #2.

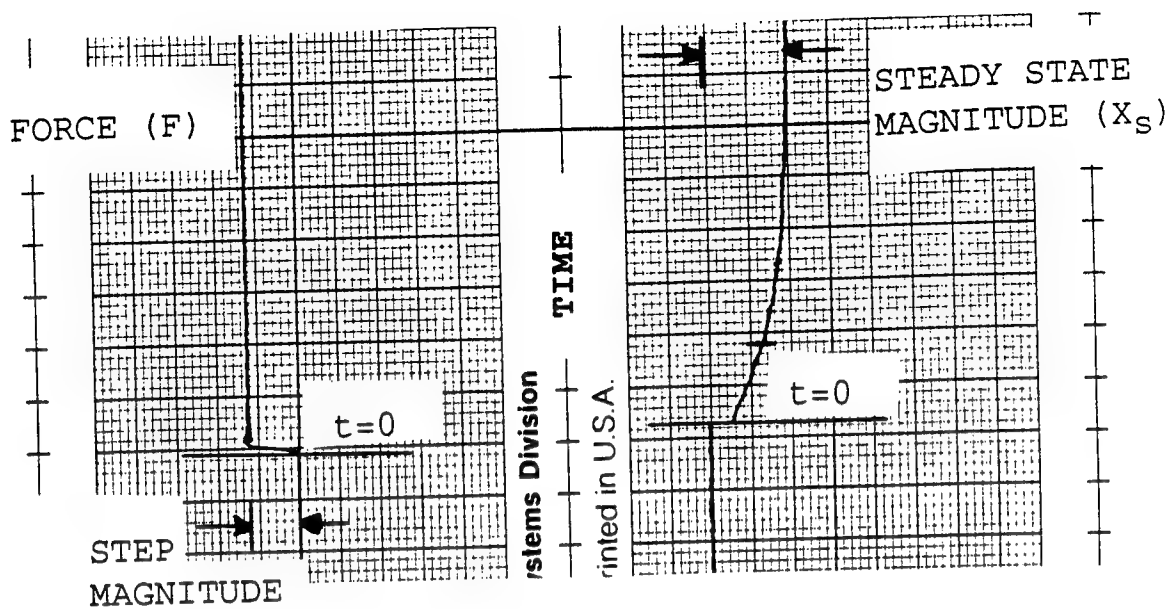


Figure 33. Strip chart recording for the force input and slave ram displacement, run #3.

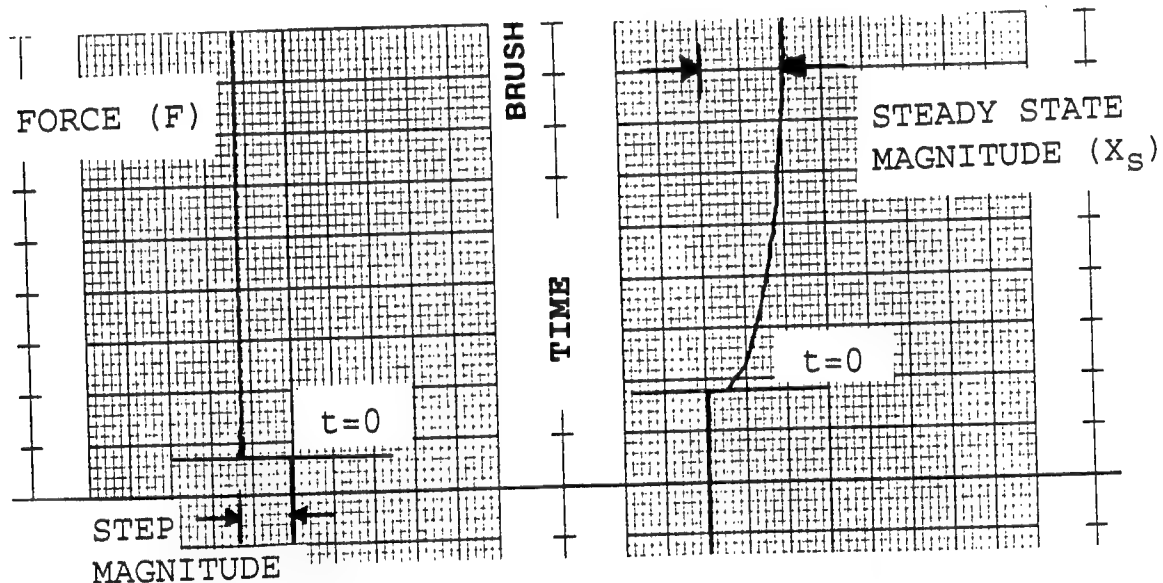


Figure 34. Strip chart recording for the force input and slave ram displacement, run #4.



### **III. TWO DEGREES OF FREEDOM FORCE FEEDBACK**

#### **A. OBJECTIVE**

The primary objective in designing, building, and testing a two degree of freedom force feedback system is to verify that an operator who physically inputs a force to a master hydraulic system, will feel a resistive force proportional to the obstruction force encountered by the slave hydraulic system. This will be accomplished by designing a master unit that will positionally drive an identical slave unit, and the obstruction's resistive force will act as a force feedback to offset the applied force, reducing the hydraulic power assist to the operator. It is desirable to have the system's displacement be rotational to compare the effects with the linear one degree of freedom system. It will be designed with two independent rotational links to resemble human arm motion in a horizontal plane. A theoretical analysis will be conducted to ensure system stability before construction, and then the stability will be verified by an experimental comparison after construction.

#### **B. THEORETICAL ANALYSIS USING SYSTEM PARAMETERS FROM SINGLE DEGREE OF FREEDOM MODEL**

##### **1. System Overview**

Figure 35 is a top view of the entire system that operates in the horizontal plane. A fixed rotary hydraulic actuator controls the rotational motion of link #1. A linear hydraulic actuator is fixed to links #1 and #2, and it is designed to control the rotation of link #2 about link #1. An input force is applied to the master unit which positionally drives the slave unit. Once the slave unit meets the obstruction, the resistive force becomes the feedback signal to the master unit.

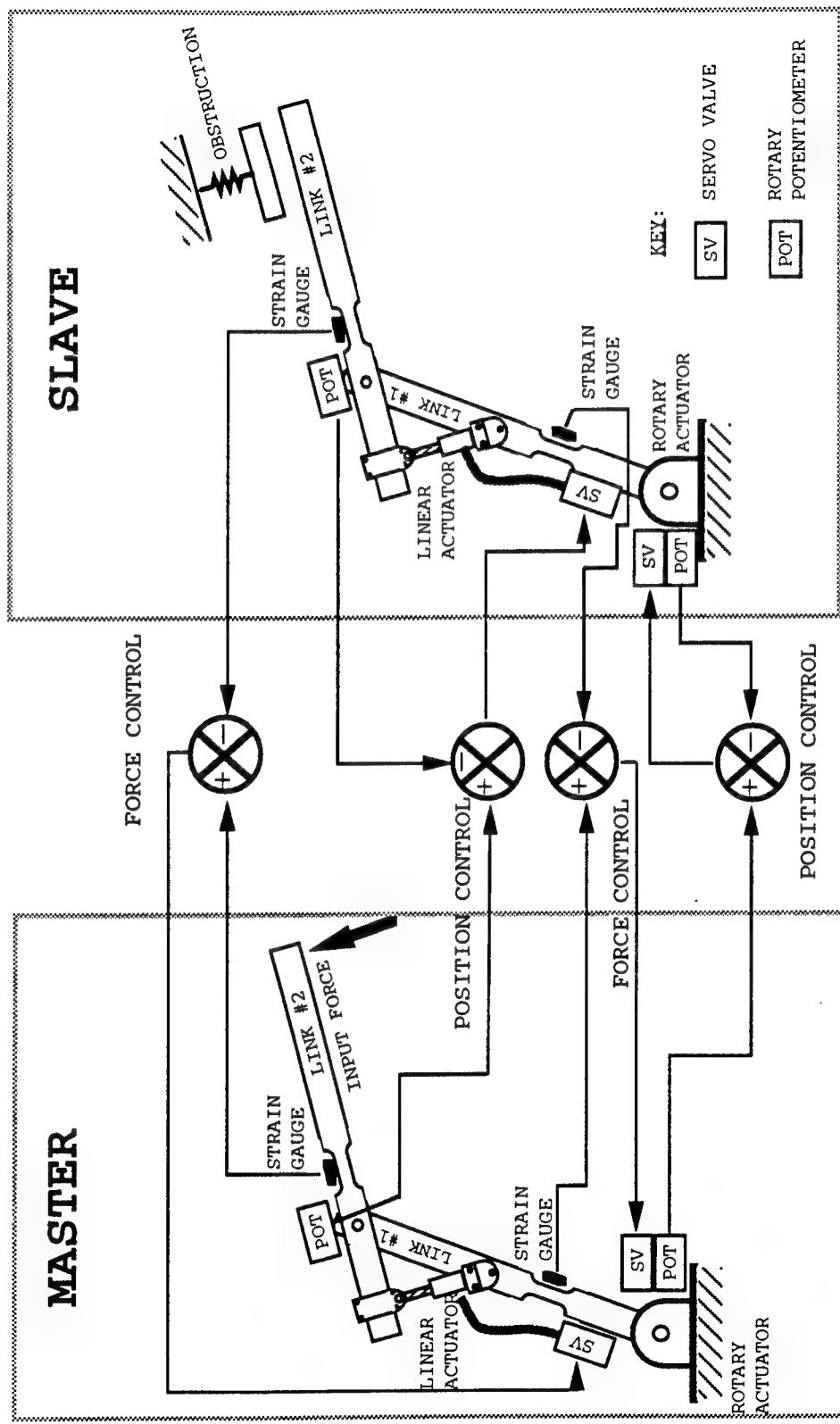


Figure 35. Top view of two degrees of freedom force feedback system.

Figure 36 presents the block diagram for the two degree of freedom force feedback system. The performance of the system is assumed to be linear for simplicity, and the servo control valve gains are assumed to be constant since the system frequency is lower than the natural frequency of the servo valve.

For a given input force to the master unit or for the obstruction resistive force on the slave unit, only the force component that is tangent to link #2 and link #1 will have a significant effect on the stress at either of the strain gauge webs. Axial stresses are neglected since they are much smaller than bending stresses in the beam. Also, for a given applied force, the tangential components to links #1 and #2 do not have to be equal. Therefore, the performance of link #1 is treated independently from link #2 since they may have different input force magnitudes.

## 2. SIMULAB Analysis Using Expected Gains

### a. *Expected Gains*

The single degree of freedom system was used to approximate the expected gains for the two degrees of freedom system. The major differences between the two are that one is linearly translated and the other is rotationally translated, the two degrees of freedom system is larger in size, and rotary potentiometers are used vice linear potentiometers. Some similarities exist to simplify the approximation. The system operates at a low pressure (approximately 450 psi), and the servo amplifiers provide a voltage range of -15 to +15 volts to the servo valves. Since summation junctions are used for the position and force control, the amount of amplification of the combined

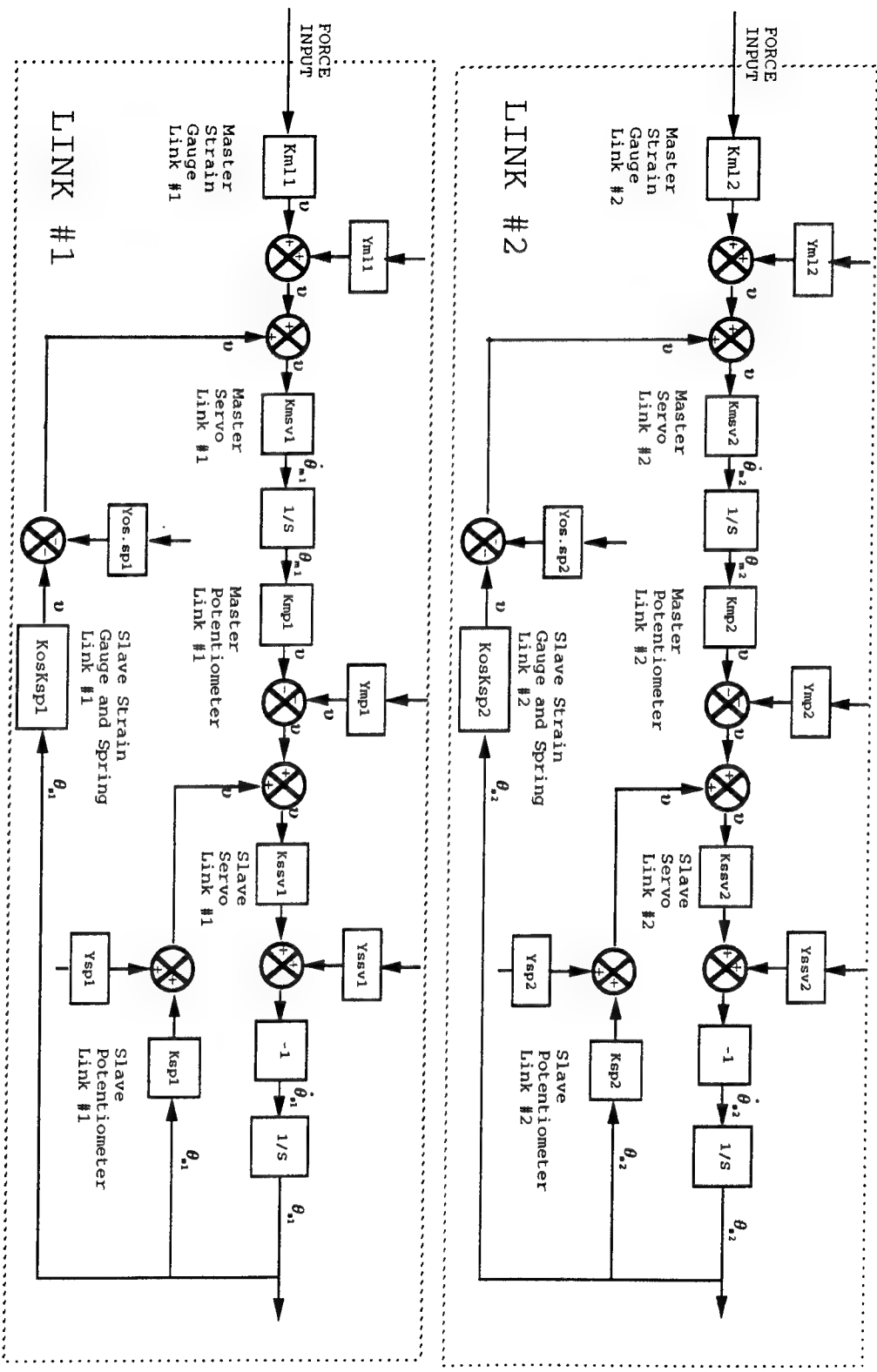


Figure 36. Two degrees of freedom block diagram.

potentiometer voltages and strain gauge voltages is relatively consistent between the two systems.

The master and slave units are identicle in dimensions and equipment except for a couple of minor variations: the two rotary actuators are different in size which requires links #1 for the master and slave to be mounted differently with unequal lengths, creating different bending stresses in the links. Therefore, the master and slave units will be assumed to have the same gain values since their variations are small, and system stability will be verified for a variation of each gain. The actual input force applied to the system will have various effects on links #1 and #2 since only the tangential component to the respective link will create a significant bending stress on the strain gauge. Therefore, the same force will be used for both links to simplify the analysis, and the input force of 70 grams (equivalent to five lbf) is used since this is an estimate of the force levels used to create bending stresses in the relatively rigid links. The master strain gauge gains ( $K_{m11}$  and  $K_{m12}$ ) are assigned the same value as the single degree of freedom system equal to .0092. The Y-intercept cannot be deleted in our assumption since its magnitude is approximately equal to the magnitude of the gain, so it is set equal to .0099 as obtained in the single degree of freedom system. All other Y-intercepts for the two degrees of freedom system are assumed to be zero since they are much smaller than the gain values obtained in the single degree of freedom system. The master servo gains ( $K_{msv1}$  and  $K_{msv2}$ ) are set equal to .6441, the same value as the single degree of freedom system. The master and slave potentiometers ( $K_{mp1}$ ,  $K_{mp2}$ ,  $K_{sp1}$ , and  $K_{sp2}$ ) are set equal to five since they are similar in design, and the single degree of freedom potentiometer gains were close to this value. The slave strain gauge and obstruction gains ( $K_{osKsp1}$  and  $K_{osKsp2}$ ) are

set equal to .5107, the same value as the single degree of freedom system since the two degrees of freedom system will also have a soft compliance to prevent oscillations.

### b. Analysis

It was shown in Chapter II that a system with multiple inputs will have the same characteristic equation when each input is taken separately while all other inputs are set equal to zero. A transfer function relationship between the externally applied input force (F) and the rotational output position of the slave link ( $\theta_s$ ) is derived to be:

$$\frac{F}{\theta_s} = \frac{K_{msv} K_{mp} K_{ssv} K_{m1}}{s^2 + s(K_{ssv} K_{sp}) + K_{msv} K_{mp} K_{ssv} K_{os} K_{sp}} \quad (29)$$

where the characteristic equation in the denominator of the transfer function is in the form:

$$s^2 + 2\zeta\omega_n s + \omega_n^2 = 0 \quad (30)$$

where:

$$2\zeta\omega_n = K_{sv} K_{sp} \quad (31)$$

$$\omega_n^2 = K_{msv} K_{mp} K_{ssv} K_{os} K_{sp} \quad (32)$$

The damping ratio ( $\zeta$ ) and natural frequency ( $\omega_n$ ) for the approximated gains for the system is 4.36 and 2.87, respectively. Since the damping ratio is greater than unity, the characteristic response of the two degrees of freedom system should be overdamped.

The manual approach of developing individual transfer functions and plotting the system's time response using the controls toolbox from MATLAB [Ref.3] can be very time consuming for a two degrees of freedom force feedback system. SIMULAB [Ref.4] was proven in section II.D.3 to be an accurate and effective computer tool in modeling and observing the time response of a linear, dynamic system.

Figure 37 is the SIMULAB block diagram relationship, and it displays the gain value approximations used for the initial position of the slave in contact with the obstruction. Oscilloscopes are connected throughout the system at various points of interest to view a real time response of selected variables.

Figure 38 is the time response for the slave rotational displacement. This is the same for link #1 and link #2 since they are modeled with the same gains. It is an overdamped response that takes approximately 3.5 seconds to obtain two-thirds of its steady state value.

## C. DESIGN AND CONSTRUCTION

### 1. Operation

#### a. Master and Slave Unit

The master unit was designed so that an external force applied tangentially to the free end of link #2 creates a bending stress at the master strain gauge web, resulting in a force driven voltage to the servo valve for the master linear actuator. The linear actuator will cause link #2 to pivot about link #1 in response to the applied force. The link #2 master potentiometer will positionally rotate the slave's link #2, at a proportional angle by sending the master potentiometer voltage to the servo valve for the slave linear actuator. The master unit will positionally drive the

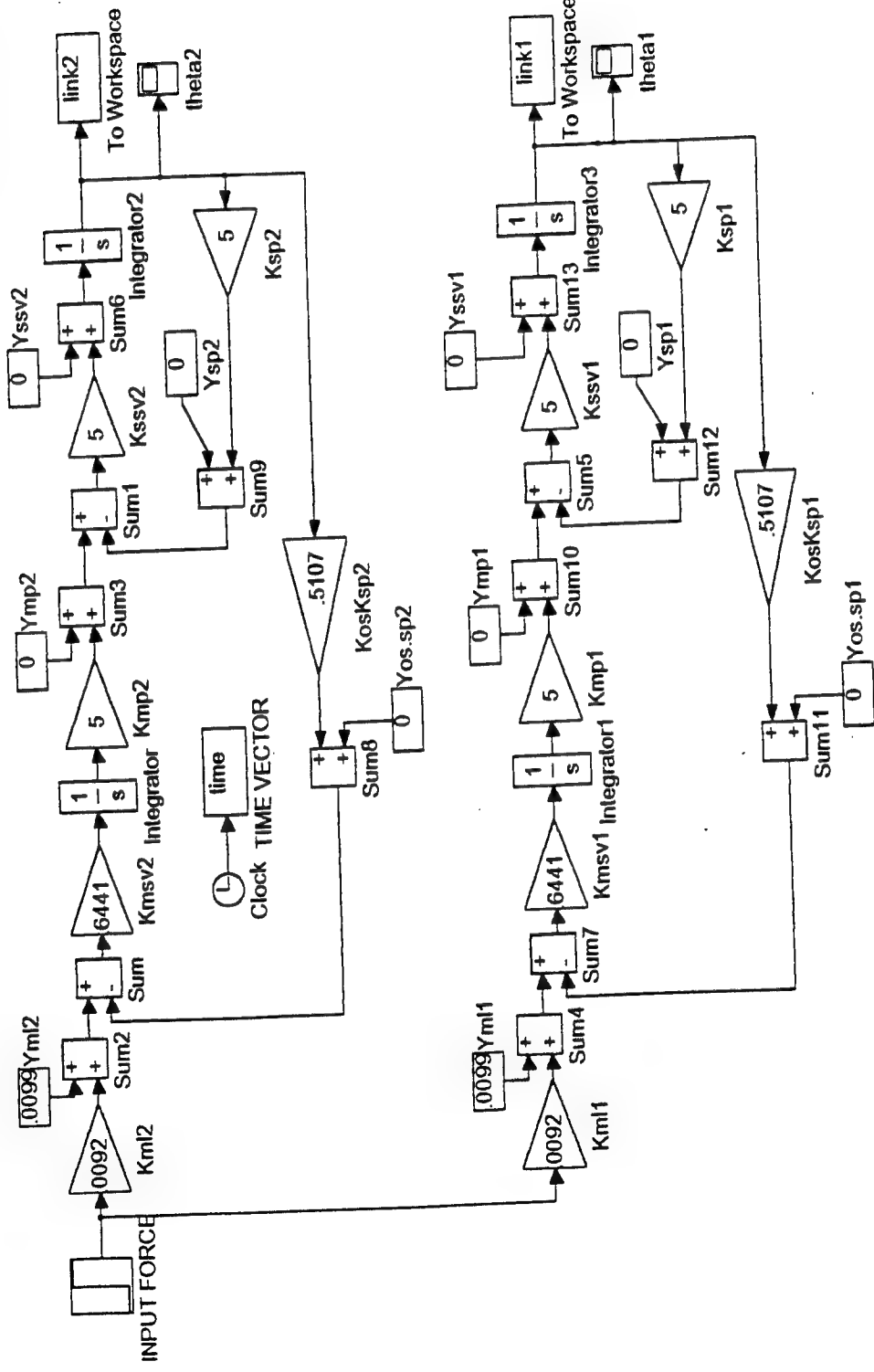


Figure 37. SIMULAB two degree of freedom block diagram.

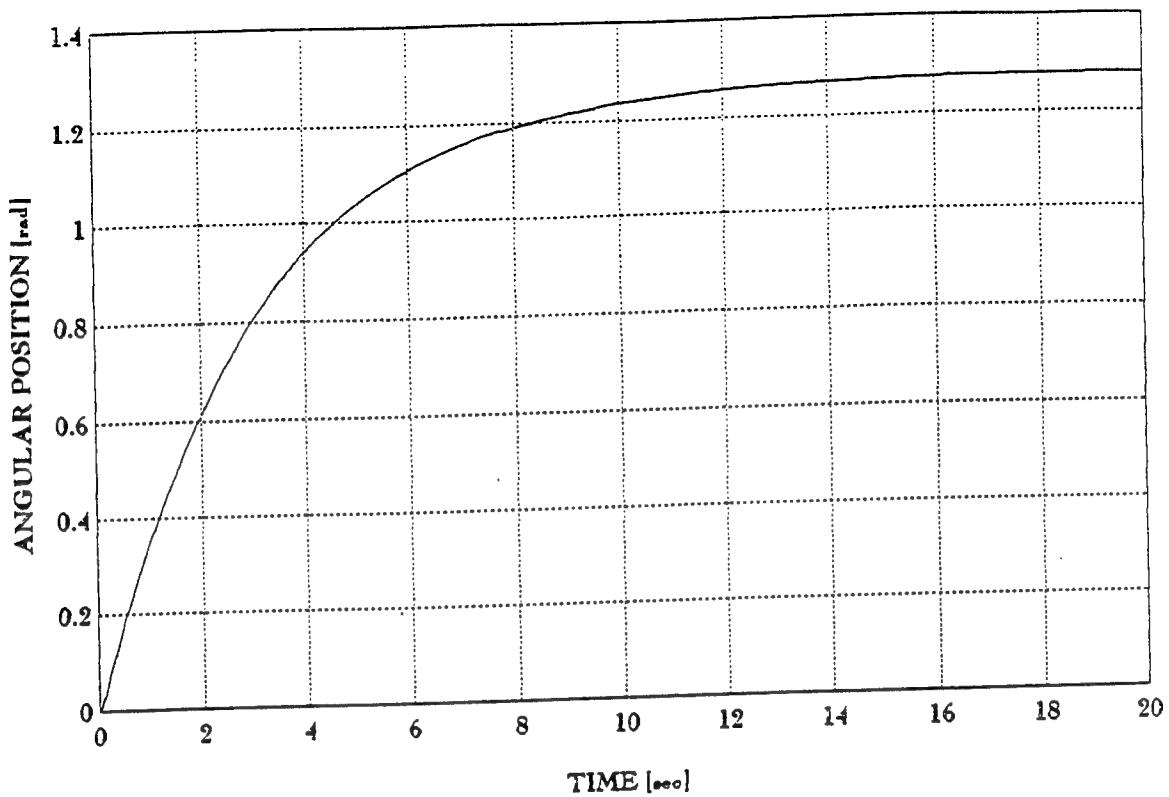


Figure 38. SIMULAB two degree of freedom dynamic response.

slave unit until the slave meets the obstruction in which a bending stress is created from the tangential force component at the slave's strain gauge web, on link #2. The obstruction strain voltage is used in a feedback to offset the input force voltage to the master linear servo valve, creating a loss in the hydraulic power assist to the master unit. The same procedure and effects will be experienced for link #1 on the master and slave units.

**b. Wiring Diagram and Electrical Components**

Figure 39 is the wiring diagram for the two degrees of freedom force feedback system. Link #1 and link #2 are wired identically but operate independently of each other. The slave and master strain gauges are passed through the gain controller before being split to the voltmeter and the force amplifier. The force amplifier sums the master and slave voltages and amplifies it before sending it to drive the master servo valve. The slave and master potentiometer voltages are passed to the servo amplifier for summation and amplification before sending it to drive the slave servo valve.

**2. Design Considerations and Constraints**

**a. Link Geometry**

The link geometry was selected to meet various operating requirements. The size of operating area is limited so the length of each link is limited to provide full range of motion for the slave and master units and to provide adequate space for the operator to safely move the master links without being in the path of any moving link. For the master unit, links #1 and #2 are both 23 inches long. For the slave unit, links #1 and #2 are 28 and 23 inches long, respectively. The reason for the difference in length of link #1 for the master and slave units is because they are mounted differently to their respective rotary actuator so that their rotation is about the center of rotation of the rotary actuators.

To minimize torsional effects on joints and strain gauges, weight is minimized whenever possible so aluminum, square tubing is used. Its cross sectional dimensions are two inches for the outside width and .125 inches thick.

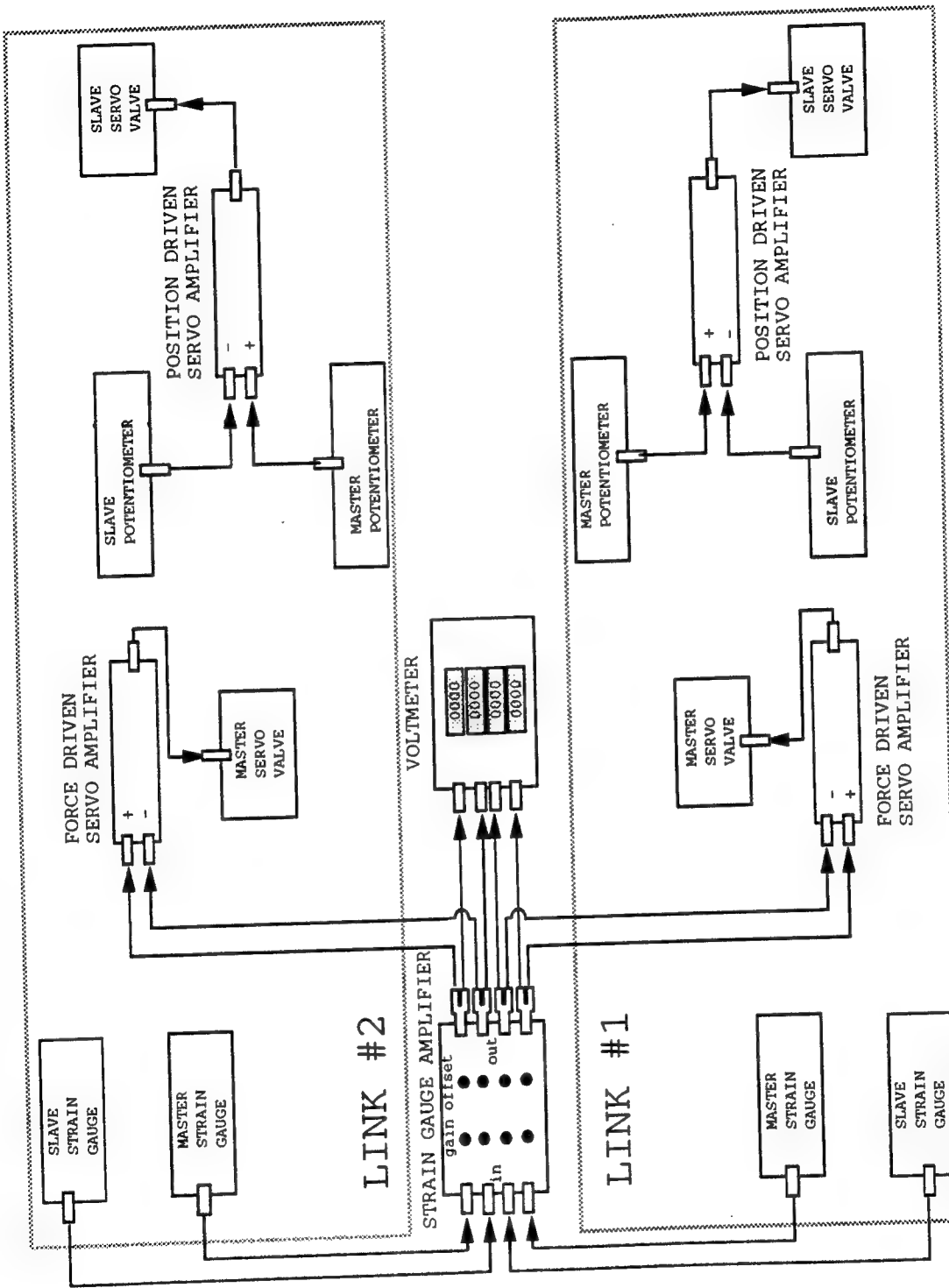


Figure 39. Wiring diagram for two degrees of freedom system.

**b. Variable Position Link Joint**

At the joint where link #2 pivots about link #1, the linear actuator has a bracket on both ends that can slide along links #1 and #2 to vary the range of motion and operating position of link #2. See Appendix H for the AUTOCAD drawing of the joint design and dimensions. The body of the linear actuator is bolted to a triangular plate that is mounted to a sleeve attached to link #1. The plate will be free to pivot about the sleeve, and the sleeve can be moved along the length of link #1 and secured at any desired position. The ram end is screwed into a brass cylinder that is used as a pivoter in another sleeve that can be moved along the overhanging length of link #2.

**c. Linear Actuator Placement**

A linear actuator is used to rotate link #2 about link #1, and it is desirable to place the actuator such that the motion linearity in the angular direction is obtained and the range of motion in the angular direction is maximized.

To determine the maximum range of motion, the placement of the linear hydraulic actuator needs to be determined. Figure 40 shows the position of link #2 when the linear actuator is fully retracted and fully extended. Link #1 is fixed, and the length (b) of link #2 between the pivot and where the linear actuator is connected is held constant at five inches. For the fully retracted position,  $\theta_1$  is the maximum angle above the tangent line to link #1, but it varies with the actuator position length (L) of link #1 between the pivot and where the linear actuator is connected. The maximum actuator position length (L) is 16 inches which is the sum of the fully retracted actuator length (a), 11 inches, and the five inch fixed length (b). This occurs when  $\theta_1$  is 90 degrees (i.e. link #2 is parallel with link #1), and binding effects are disregarded at the joints for the

analysis. For the fully extended position,  $\theta_2$  is the maximum angle below the tangent line to link #1, but it also varies with the actuator position length (L) of link #1 between the pivot and where the linear actuator is connected. The minimum actuator position length is ten inches which is the difference between the fully extended actuator length (a), 15 inches, and the five inch fixed length. This occurs when  $\theta_2$  is 90 degrees (i.e. link #2 is parallel with link #1), and

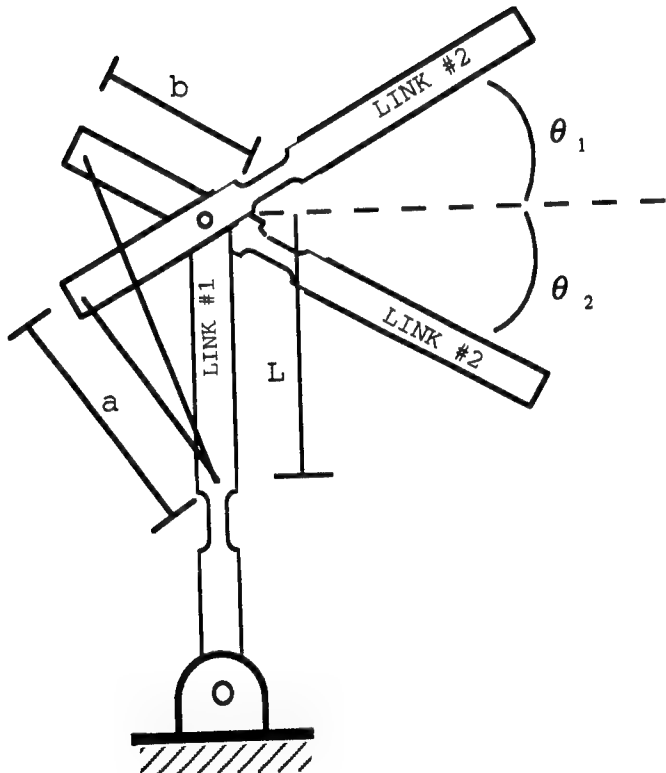


Figure 40. Fully retracted and extended ranges for link #2.

again binding effects are disregarded at the joints for the analysis. The angles  $\theta_1$  and  $\theta_2$  are calculated using the law of cosines:

$$a^2 = b^2 + l^2 + 2bl\cos(90 - \theta_1) \quad (33)$$

$$a^2 = b^2 + l^2 + 2bl\cos(90 + \theta_2) \quad (34)$$

The angular rotations,  $\theta_1$  and  $\theta_2$ , verses actuator position ( $L$ ) are plotted individually in Figure 41, using a MATLAB program, Appendix I. For the actuator fully retracted, it can be seen that as the distance of the base of the linear actuator on link #1 increases from the pivot point, the angle ( $\theta_1$ ) above the tangent line to link #1 increases. It can also be seen that as the distance of the base of the linear actuator on link #1 increases from the pivot point, the angle ( $\theta_2$ ) below the tangent line to link #1 decreases. The summation of these two angles ( $\theta_1 + \theta_2$ ) is also plotted to give the total range of motion for a given actuator position length. The maximum range of motion occurs when the actuator is fully extended or fully retracted, but it is not desirable to operate at these extremes because the links will bind since the linear actuator is parallel to link #1. It is desirable to operate in between these extremes.

As the linear hydraulic actuator ram extends and retracts in a linear direction, it is important to have the resulting rotation be linear to satisfy our linearity assumption of our system model. A MATLAB program, Appendix J, was used in Figure 42 to plot the linear actuator ram displacement with an 11 to 15 inch range, verse the angular position of link #2 with respect to a line tangent to link

#1. This is repeated for seven actuator positions (L) along link #1, ranging from 10 to 16 inches for the rotational extremes.

By looking at the slope of the lines, a constant slope throughout the entire range of motion for the linear actuator represents a linear relationship between linear and rotational displacement. It can be seen that rotation is approximately linear except when the actuator placement is located at its extremes along link #1, ten and 16 inches, respectively. The best linearity occurs when the actuator position is 12, 13, or 14 inches. Figures 41 and 42 can be used to determine the optimum placement of the linear actuator to obtain maximum range of rotation and linearity. The system was initially set up with the actuator length equal to 11 inches which allows for maximum angular rotation (60 degrees) while preserving linearity throughout its full range of motion.

#### *d. Strain Gauge Web*

When a force is applied tangentially to a link, the bending stress will be measured by a strain gauge at a point of interest. To increase the bending stress at this point while maintaining sufficient rigidity along the rest of the link, a web is installed along the length to reduce the cross-sectional area, Figure 43. A two arm bridge, or half bridge, Figure 44, is used to compensate for temperature, axial, and torsional effects [Ref.5].

The web is installed by cutting the link, inserting the ends of the web inside the square tubing, and bolting the web to the link. The orientation of the web is such that it will bend from a horizontally applied force to the link. A strain gauge web is installed in each of the four links of the system.

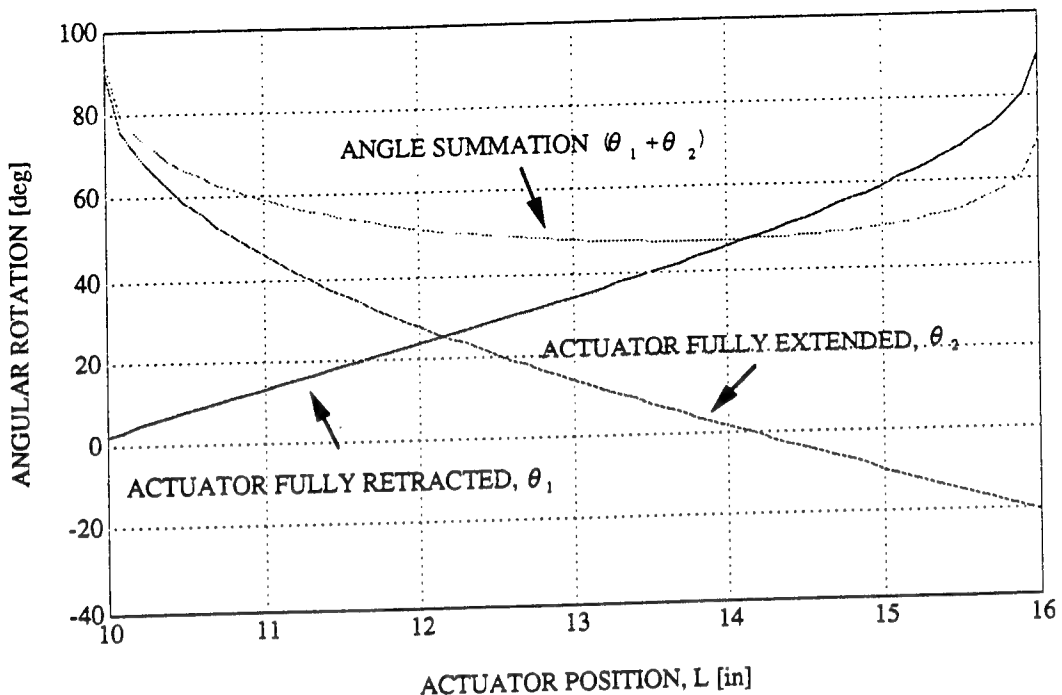


Figure 41. Angular rotations of link #2 verses actuator position along link #1.

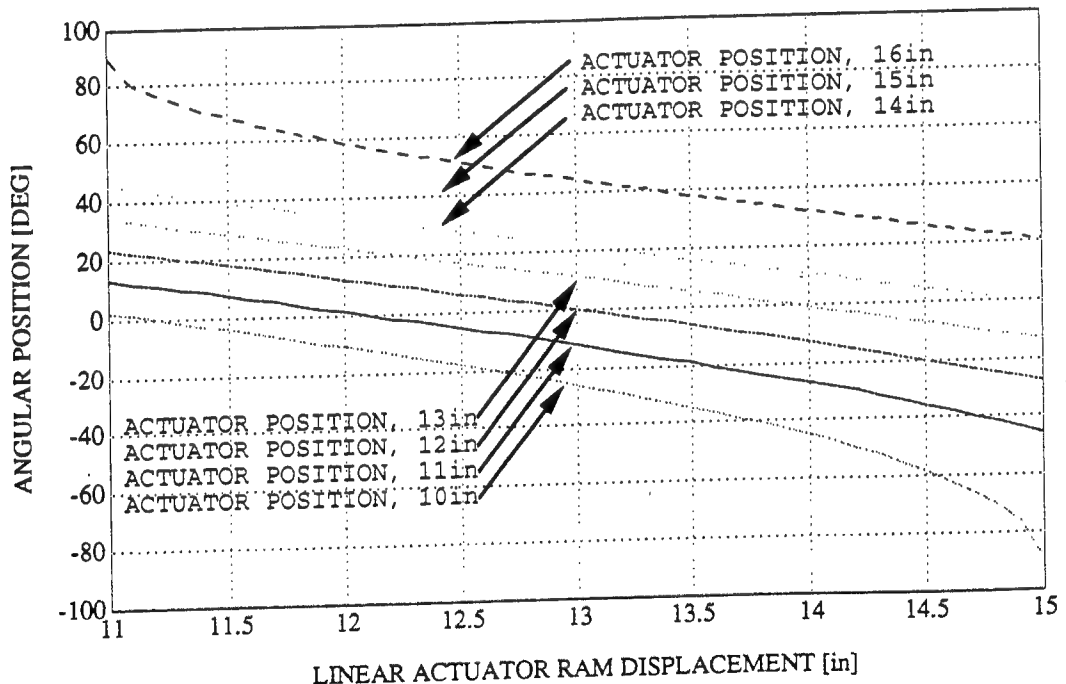


Figure 42. Angular position of link #2 verses linear actuator ram displacement for various actuator positions along link #1.

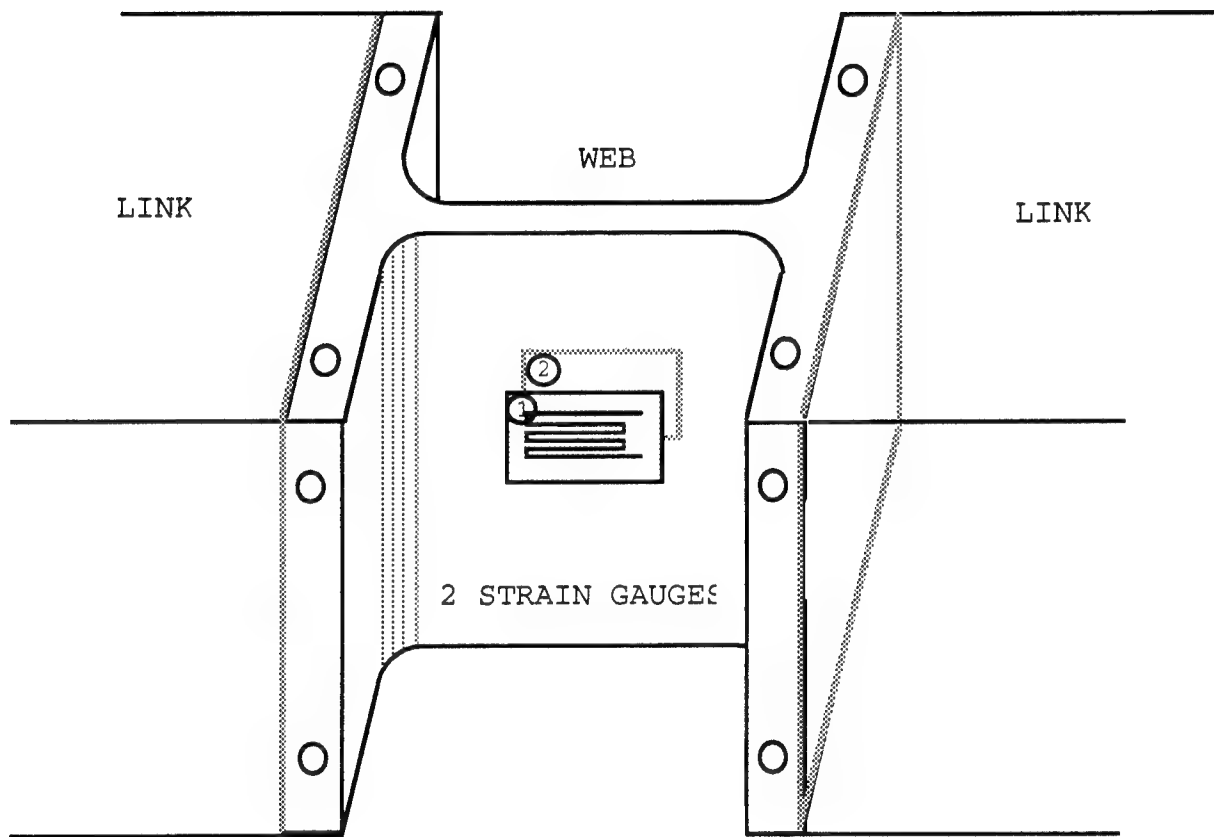


Figure 43. Strain gauge web.

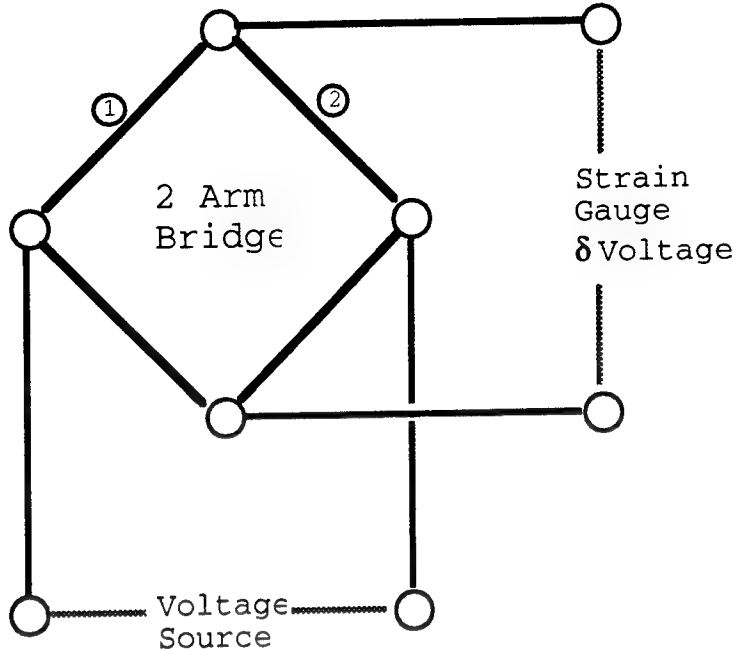


Figure 44. Two arm strain gauge bridge.

The thickness of the web is critical in order to accurately measure bending stresses. If the strain gauge only experiences small microstrain levels, then the voltage drop across the bridge is small, more amplification of the signal is required, and noise greatly interferes with the strain gauge voltage when amplified. To minimize noise interference, it is desirable to have at least 500  $\mu$ -strain at the strain gauge. A static approach is taken to estimate the desired web thickness for link #1. The bending moment at the strain gauge is calculated from the load, shear, and bending moment curves, Figure 45. Bending stress is calculated using:

$$\sigma = \frac{MC}{I} = \frac{(16F)\left(\frac{t}{2}\right)}{\left(\frac{1}{12}\right)(b)(t)^3} = \frac{54.68F}{t^2} \quad (35)$$

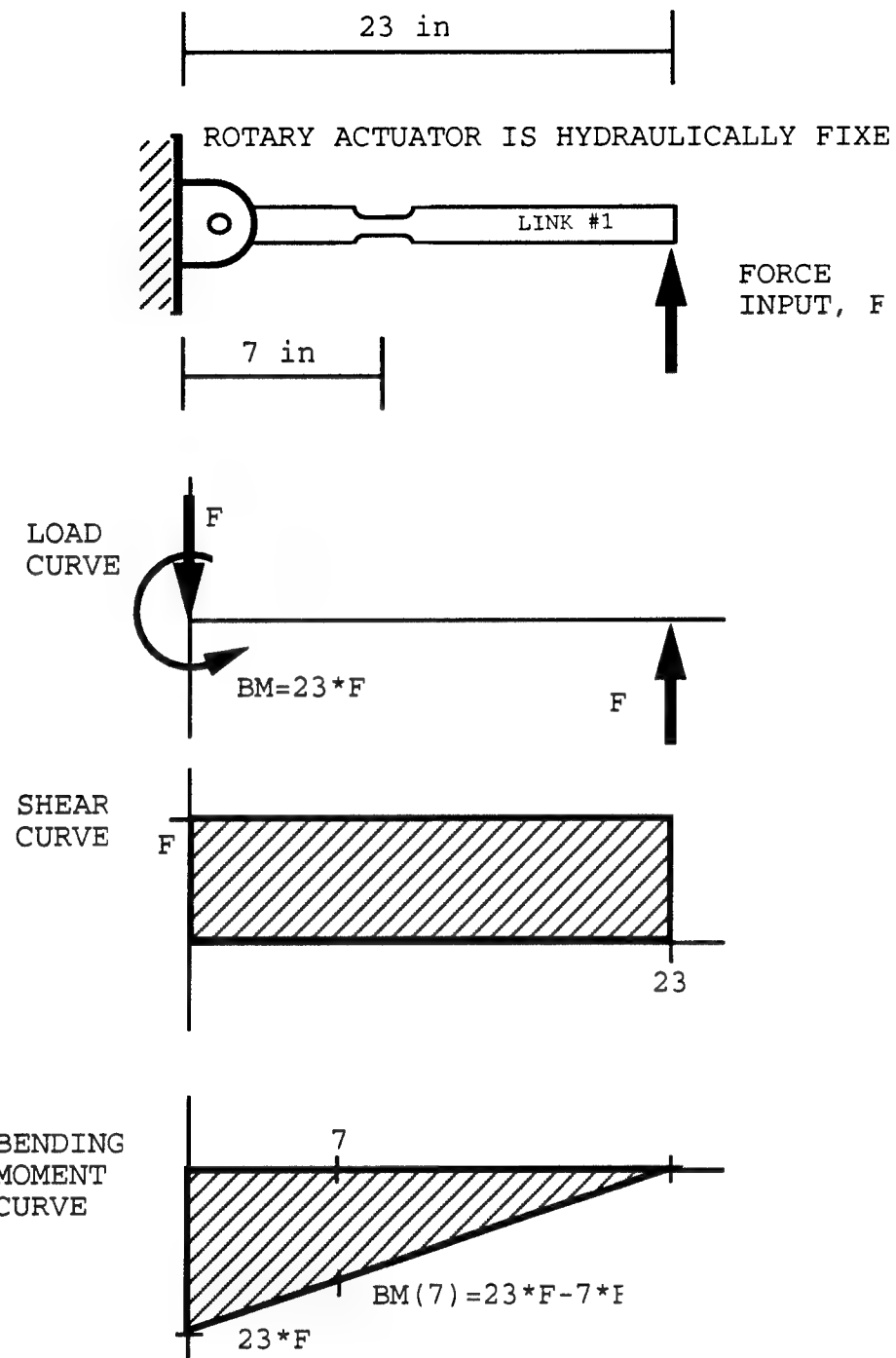


Figure 45. Loading, shear, and bending moment curves.

where  $\sigma$  is the bending stress,  $M$  is the bending moment,  $C$  is the distance from the neutral axis for maximum bending stress,  $I$  is the mass moment of inertia,  $b$  is the width of the web,  $t$  is the web thickness, and  $F$  is the applied force. Strain is calculated using:

$$\epsilon = \frac{\sigma}{E} = \frac{54.68F}{(t)^2(10^7)} = 500 \text{ } \mu\text{strain} \quad (36)$$

where  $\epsilon$  is the strain and  $E$  is the Young's modulus of the material. The web thickness is calculated from:

$$t = \left( \frac{54.86F}{(10^7)(500 \text{ } \mu\text{strain})} \right)^{\frac{1}{2}} \quad (37)$$

for an input force ( $F$ ) of five lbf and 500  $\mu$ -strain. A MATLAB program, Appendix K, is used to plot the web thickness versus applied force, Figure 46, to obtain a bending strain of 500  $\mu$ -strain.

#### e. Joint Friction

It is important to minimize friction in all pivoting joints throughout the system. To minimize cost, a low cost bushing is used with relatively low frictional resistance that the hydraulic system can easily overcome. The applied and resistive forces are the predominant factors driving the system since they are much greater in magnitude than the frictional forces.

The pivoting point between the two links is an area with potentially high friction between the flat surfaces of the links. Delrin plastic discs were used for friction reduction by separating the aluminum surfaces. A bolt goes

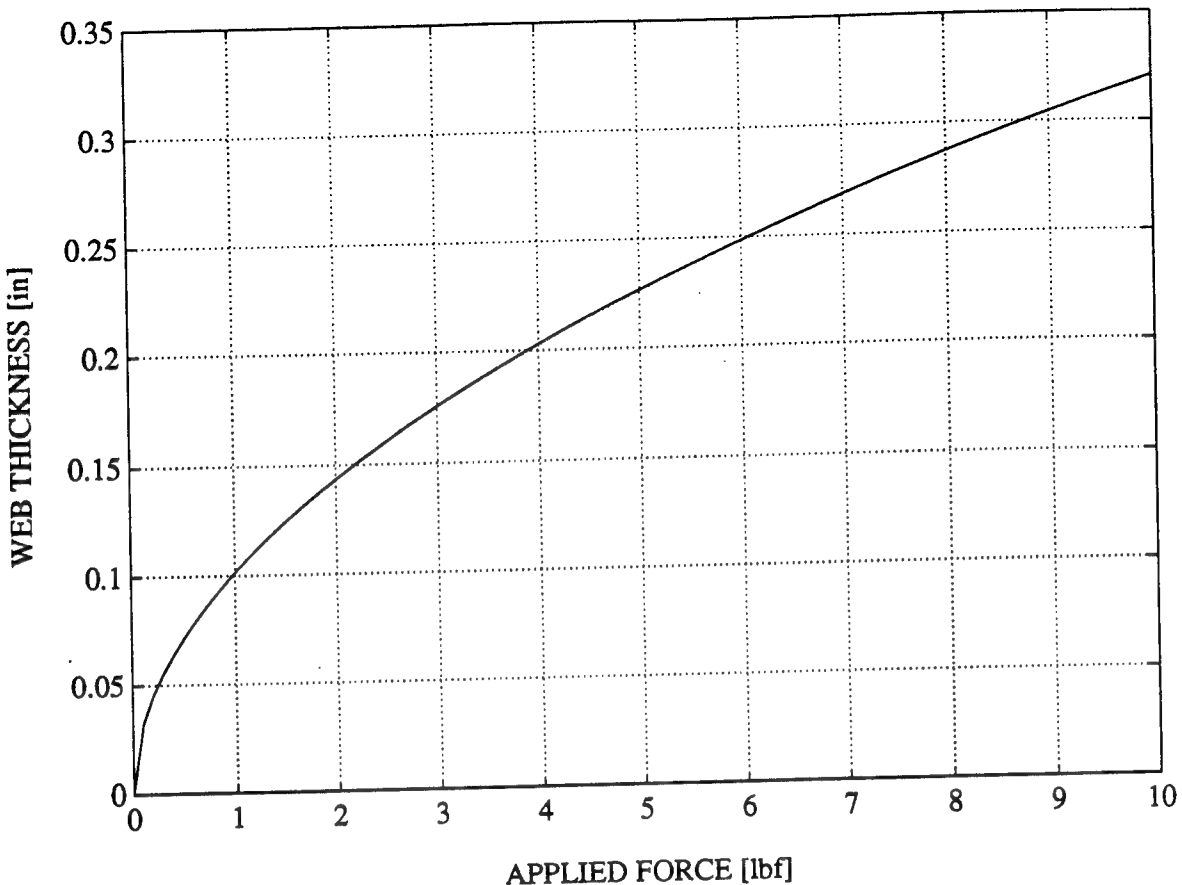


Figure 46. Web thickness verse applied force.

through both links with the plastic bushings between the bolt head and link #2 and between the two links.

#### **f. Link #1 and Rotary Actuator Interface**

Since the master and slave rotary hydraulic actuators are different in size and configuration, link #1 is mounted differently on each one.

The master rotary hydraulic actuator has a shaft on its center line which allows the actuator to be mounted to the work bench with the shaft oriented directly upward. Figure 47. Link #1 is mounted to a round mounting pad which is attached to the actuator shaft. The mounting pad has an

eight hole array so that the master links can be rotated to operate in eight possible positions without shifting the actuator assembly and supporting hydraulic components. See Appendix L for the AUTOCAD drawing of the master rotary actuator mounting bracket and mounting pad. A similar mounting pad with an eight hole array was designed for the slave rotary actuator; this allows flexibility in the operating position of the slave unit; see Appendix M for the AUTOCAD drawing.

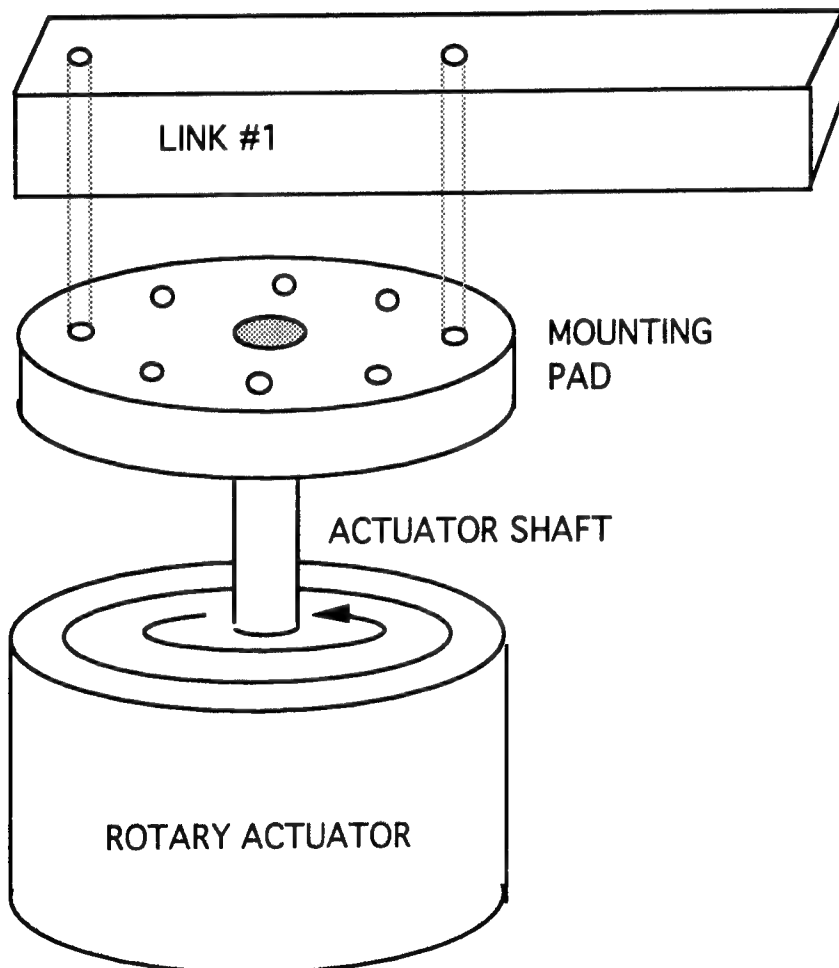


Figure 47. Mounting pad for master link #1.

The slave rotary hydraulic actuator is much larger and does not have a shaft on its center line to mount link #1. A flat plate is permanently fixed at a constant radius off the center line and rotates about the actuator, Figure 48. If link #1 were mounted parallel to the flat plate, it would not rotate about the center of the rotary actuator like the master unit. In order to avoid this rotational offset, a bracket is made to mount link #1 perpendicular to the plate, so that the link will always be radially aligned with the center of rotation.

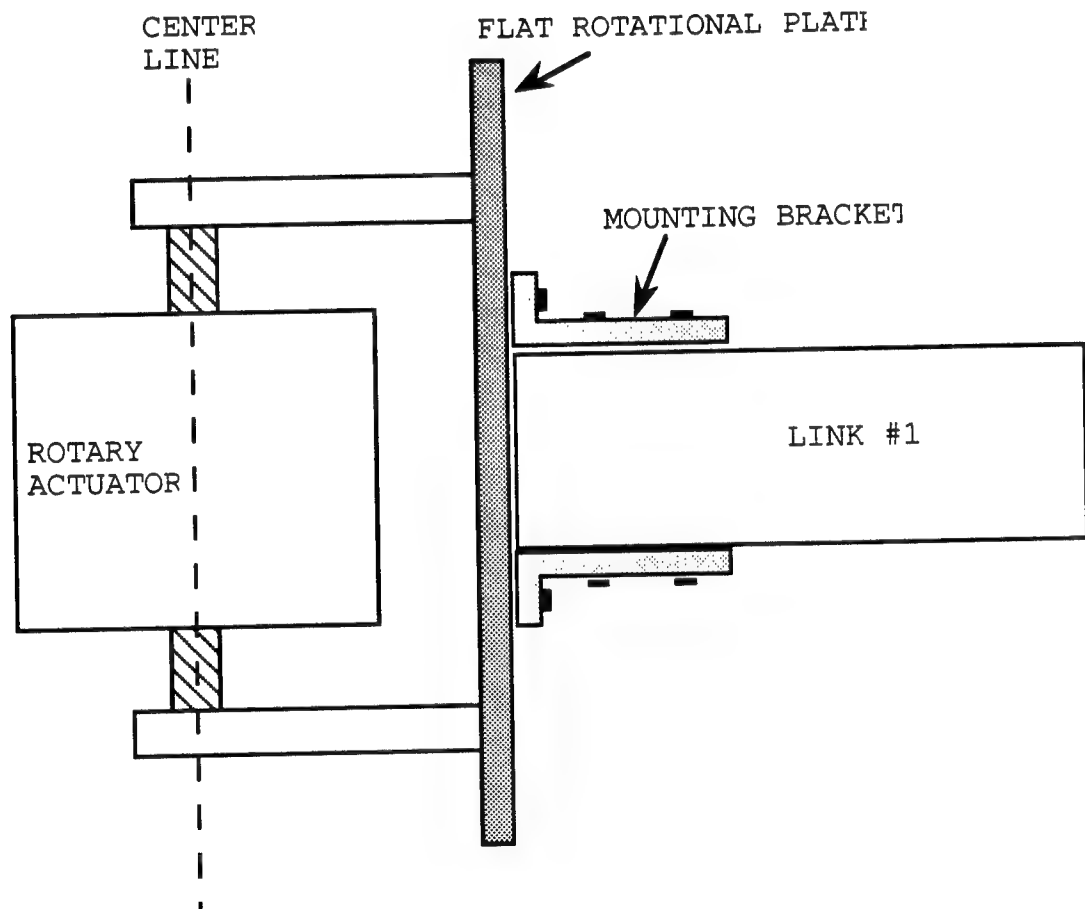


Figure 48. Mounting bracket for slave link #1.

### **g.      Rotary Potentiometers**

For the position control mode of our system, rotary potentiometers are used to generate a voltage proportional to rotational displacement. Potentiometers are mounted in different ways to accommodate dissimilar rotary hydraulic actuators and to provide for a relative rotational position between links #1 and #2 when a linear hydraulic actuator is used.

The master rotary hydraulic actuator has a rotary potentiometer mounted to the actuator housing. The rotating component of the potentiometer has a pin that is pressure fitted into a hole that is bored into the end of the rotating actuator shaft. The slave rotary hydraulic actuator has a rotary potentiometer built in, and no modifications were required.

The relative position between the two links for the master and slave units is obtained by mounting a rotary potentiometer so that its housing is fixed to link #2 by a mounting bracket, and the rotational component of the potentiometer is mounted to link #1. Figure 49 shows how the potentiometer's rotational component underneath its housing is attached to the head of the bolt connecting the two links. The bolt pivots freely through link #2, but the end of the bolt is flattened on two sides and is fixed to link #1 with a shaft locking plate. A securing nut is attached to the bolt after it passes through the locking plate.

The four rotary potentiometers have different resistances and range of motion. The master link #1 potentiometer has a  $2.5\text{ k}\Omega$  resistance and 360 degree range. The master link #2 potentiometer has a  $50\text{ k}\Omega$  resistance and 360 degree range. The slave link #1 potentiometer has a  $5\text{ k}\Omega$  resistance, and the range cannot be determined because the potentiometer housing is sealed but it has at least 180 degrees for the slave rotary actuator range of motion.

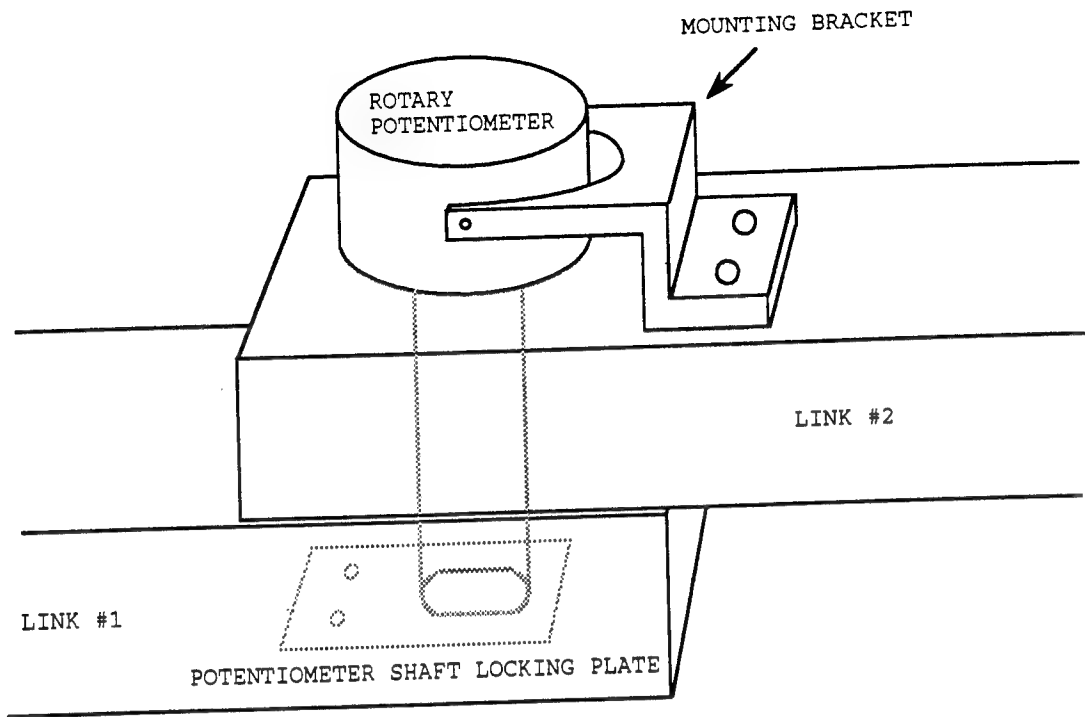


Figure 49. Rotary potentiometer mounting configuration.

The slave link #2 potentiometer has a  $20\text{ k}\Omega$  resistance and a 360 degree range.

#### *b. Servo Valve Locations*

The electro-hydraulic servo valves for the master and slave rotary hydraulic actuators are mounted on their respective housing mounts. The servo valve for the master linear hydraulic actuator is mounted on the end of link #1 near the rotary actuator. This arrangement will allow the servo valve to rotate with the link and to prevent the hydraulic lines from inhibiting the link's rotational motion. The servo valve for the slave linear hydraulic actuator is mounted to the housing of the rotary actuator because there

are existing hydraulic ports internal to the rotating bracket that is used to mount link #1. Hydraulic lines are tapped into the link mounting bracket and connected to the linear actuator. These hydraulic lines also rotate with the link to prevent them from inhibiting the link's rotational motion, and the hydraulic port holes internal to the rotating bracket do not have any hoses to inhibit motion.

All hydraulic lines for the linear actuator are long enough to allow the actuator to be placed in various positions along the length of the link.

#### D. EXPERIMENTATION

##### 1. System Equilibrium

The system was placed in equilibrium by selecting a reference direction on the master unit and ensuring that the slave unit potentiometers and strain gauge voltages were either positive or negative to offset the corresponding master unit voltages.

For the strain gauges, the master strain gauge amplifier leads were arranged so that a clockwise applied force created a positive strain gauge voltage, and the slave strain gauge amplifier leads were arranged so that a clockwise applied force also created a positive strain gauge voltage. When the slave unit meets an obstruction, the resistive force will oppose the applied force direction (counterclockwise in this case), which creates a negative strain gauge voltage to offset the master strain gauge voltage.

For the potentiometers, the zero voltage position was adjusted so that it would occur half way through maximum link rotational range. The master potentiometer amplifier leads were arranged so that a clockwise rotation from the zero volt position created a positive voltage. The slave potentiometer amplifier leads were arranged so that a clockwise rotation

from the zero volt position created a negative voltage to offset the master potentiometer voltage.

For the servo valves, the master servo amplifier leads were arranged so that a clockwise applied force to the link created a positive voltage, and it moved the master rotary actuator in the clockwise direction. The slave servo amplifier leads were arranged so that an increasing positive servo voltage occurred in the clockwise direction to match the master potentiometer voltage (opposite from the slave potentiometer voltage).

## **2. Sensing Force Feedback**

When the operator applied a tangential force input to one link at a time on the master unit, the system behaves in a position control mode before the slave link contacts an obstruction. As a force was applied in a counterclockwise direction, the master strain gauge created a voltage that rotated the master rotary actuator in the clockwise direction. When the force was reversed to the counterclockwise direction, the master rotary actuator rotated in the counterclockwise direction, and thus the slave followed in both cases. When the force was applied in a counterclockwise direction and another person placed his hand in the path of the rotating slave link to resist motion, very large resistive forces were felt by the operator on the master unit. A greater force needed to be applied to the master link to keep the master rotary actuator in motion. The same procedure was conducted for the second link, and the same effect was experienced. This demonstrated that the resistive force feedback can be felt by the operator.

## **3. Dynamic Response**

The dynamic response of the slave link rotational position did not correspond to the theoretical prediction.

The system was initially run in position control mode with the obstruction force feedback to the master servo amplifier disconnected, Figure 50. When a force was placed on the master unit, the slave unit would respond with a similar motion. Low frequency oscillations occurred in the slave when the input force was removed and the master actuator was stopped. The expected response of the open loop control mode is overdamped with no overshoot by the slave, but overshoot did occur.

A step input force was applied by the operator and was measured on a strip chart for accuracy. The step input was removed and Figure 51 shows the strip chart recording for the dynamic response of slave link #1. The linear portion of the plot is the slave response to the step input. The oscillations occurred immediately after the force is removed and lasts for approximately four cycles with a period of approximately one second. Figure 52 shows the strip chart recording for the dynamic response of slave link #2. The linear portion of the plot is the slave response to the step input. The continuous oscillation occurs immediately after the force is removed and does not stop until the master link moves to a new position. It has a period of approximately three seconds.

#### 4. System Reversibility

System reversibility was verified (i.e. applying an input force to the slave unit to drive the master unit by force control). A force was applied tangentially to the slave link, but the slave rotary actuator had a delay before it would go in motion. It was very difficult to control the system with this delay. The delay occurs because a force is applied to the slave link, causing a bending stress in the web. The voltage from the strain gauge will first go to the master rotary actuator, and since there is no strain on the

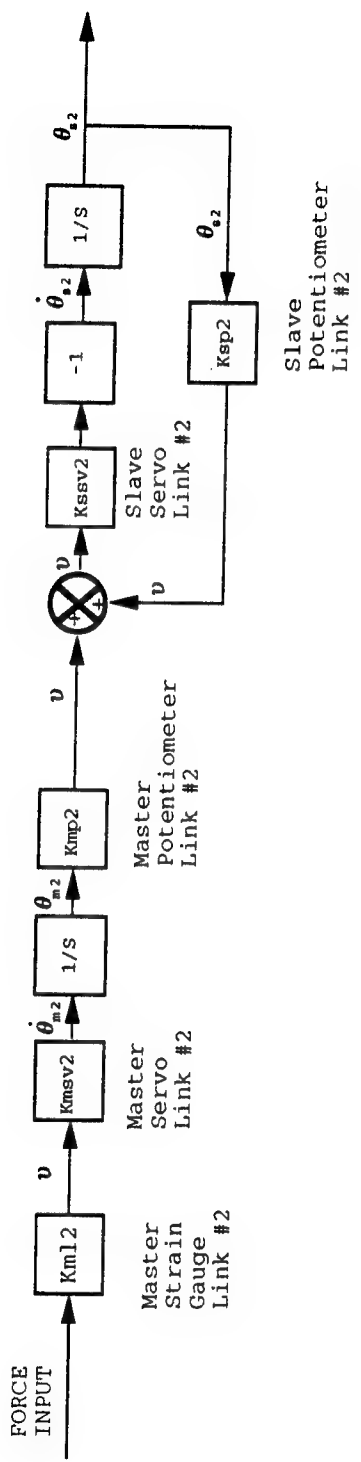


Figure 50. Open loop feedback block diagram.

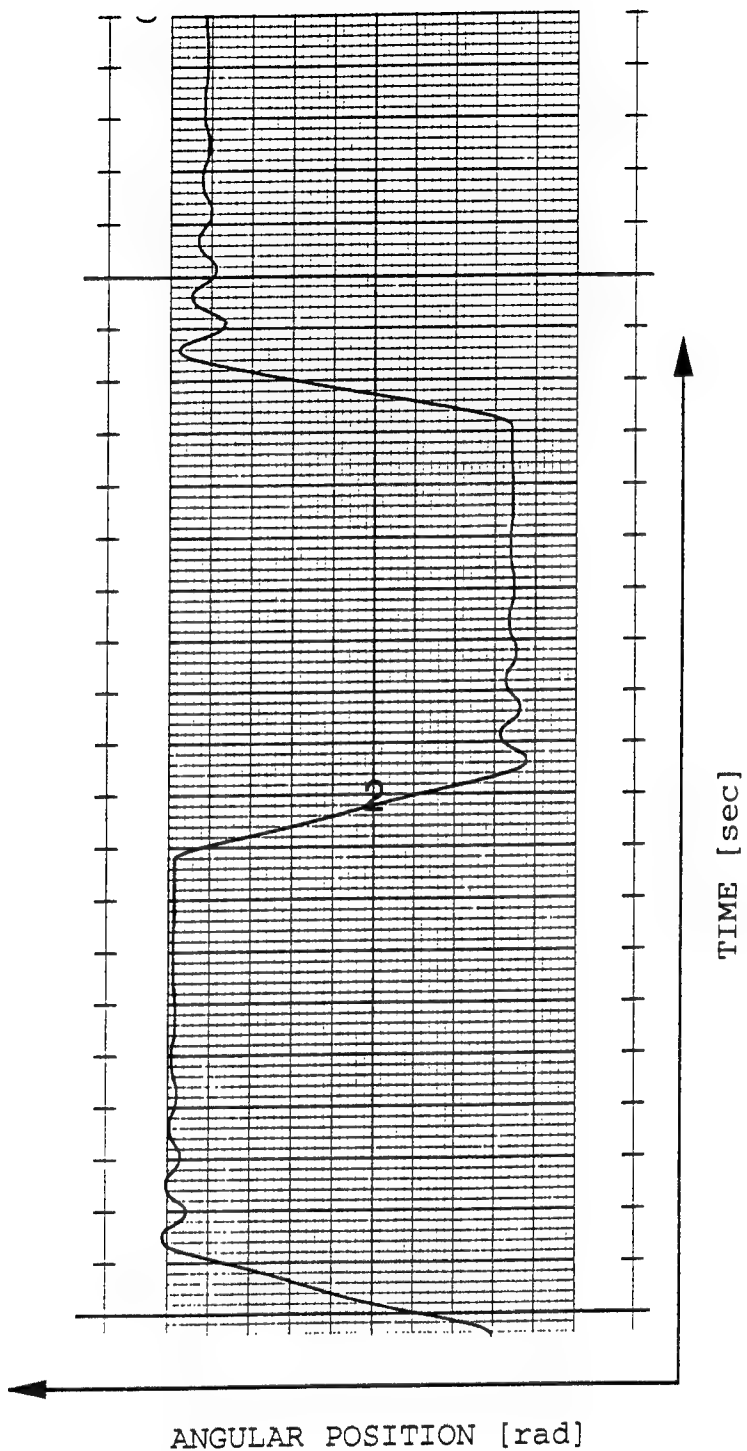


Figure 51. Dynamic response for slave link #1 after step input was removed.

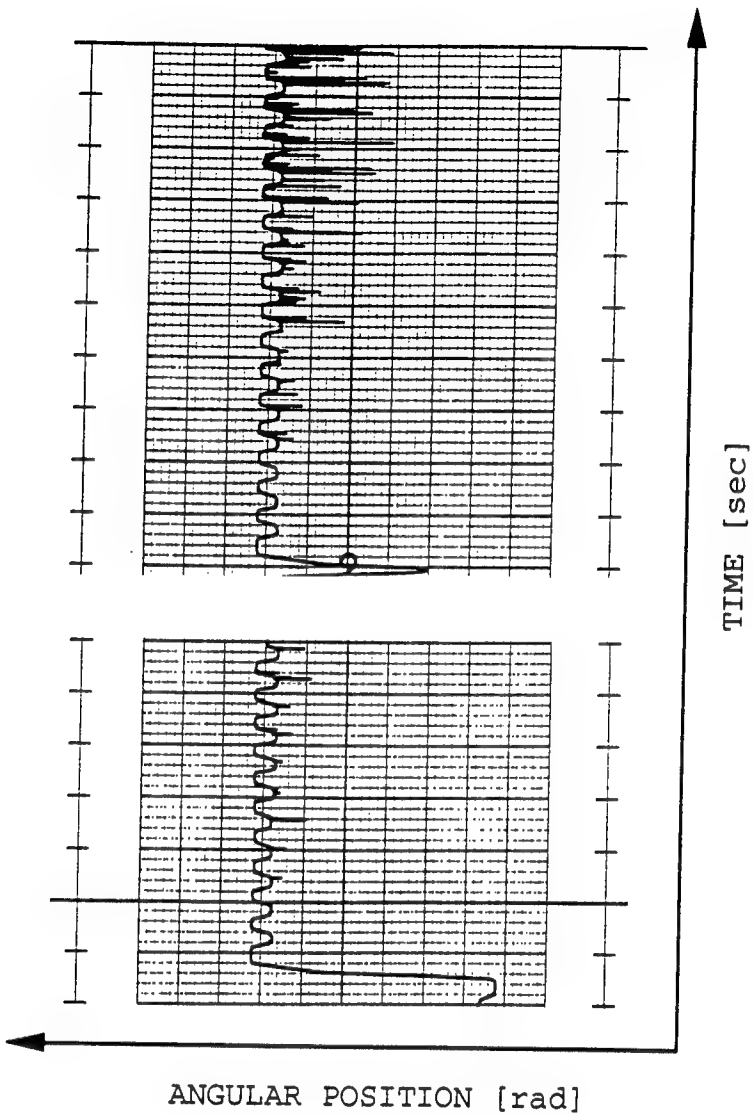


Figure 52. Dynamic response for slave link #2 after step input was removed.

master link, the master servo valve will directly respond to the slave strain voltage. The master rotary actuator is placed in motion by the strain voltage, and it is not until now that the master potentiometer voltage changes to drive the slave rotary actuator. If the operator is not perfect in applying a constant force, the slave link will start to bend back and forth with a delayed reaction by the slave servo valve.

##### **5. Bending Stress Fluctuations in Links**

It was observed that the internal bending stress on links #1 for both the master and slave units fluctuated as the angular position of links #2 varied. The strain gauge amplifier offset was used to vary the voltage of the master strain gauge link #1 to bring the system into equilibrium; this was for the initial position of link #2. But when the master link #2 was moved to another position, its linear actuator would change position to produce the angular rotation. Because the linear actuator is free to pivot at both ends, the stiff, hydraulic supply and drain hoses would create a bending stress in link #1 that would vary with position of the actuator. Therefore the system would not be in equilibrium for a new link #2 position until the master strain gauge amplifier offset was adjusted again.

## IV. DISCUSSION

### A. ONE DEGREE OF FREEDOM SYSTEM

#### 1. Results

As initially expected after a theoretical analysis of the single degree of freedom system, the bilateral force feedback system can be successfully constructed and operated so that a resistive force encountered by a slave hydraulic unit will oppose the direction of an externally applied force by the master unit operator. The force resistance is accomplished by decreasing the hydraulic power assist to the master unit. By altering various gains throughout the system, the sensitivity of the resistive force could be increased to drastically oppose the input force, or it could be decreased to only provide a slight resistance to the operator.

A theoretical analysis predicted an overdamped system that reaches two-thirds of its steady state ram displacement of .77 inches in approximately 1.7 seconds when using gain values obtained from system experimentation. The single degree of freedom dynamic response was recorded for the same step input force and amplifier gain values used in the theoretical analysis, and it is an overdamped system that reaches two-thirds of its steady state value in approximately 1.6 seconds (the average time for four responses). The theoretical analysis accurately predicted the system's actual dynamic response.

#### 2. Assumption Errors

The initial assumption that the system could be modeled by a series of linear gain relationships for all components throughout the system seems to be an accurate assumption based on the accuracy of the theoretical and experimental

comparison. The small difference between the dynamic responses can be contribute to several inaccuracies in the gain approximations. The master servo valve gain ( $K_1$ ) was based on the average of five trials for each amplifier gain setting. The time for the ram to travel one inch had a large variation from .20 to .35 seconds for each set of calculations. The slave servo valve ( $K_2$ ) was difficult to obtain since the feedback from the slave potentiometer was disconnected. There were variations in the collected data as evident in the coefficient of multiple determination of  $r^2=.825$  in the curve fit equation. This does not provide very high confidence in its linearity relationship between its input voltage and output ram displacement. The slave strain gauge and obstruction spring gain ( $K_{os}K_{sp}$ ) was difficult to calculate for small and large amplifier gain settings ( $G_2$ ). As the ram displacement became larger and the obstruction spring more compressed, the system would oscillate while attempting to hold the system steady with the joystick and to take data recordings.

For the experimental dynamic response recording, it was difficult to induce a perfect step input force. It was accomplished by hanging a weight from the master joystick. The weight was dropped a short distance to provide the instant force input, but it was difficult to not induce bouncing oscillations of the weight. The frequency of the oscillations are larger than the system's hydraulic natural frequency and probably had little effect on the dynamic response of the slave ram position.

The slave and master servo valve gains were modeled as constants, but they are not. The servo valve as mentioned in the gain calculations and block diagram actually represents the response of the electro-hydraulic servo valve mechanism and the hydraulic dynamics of the ram assembly. The electro-hydraulic servo valve component of this combination can be

modeled as a second order response with a large frequency bandwidth that is much higher than the hydraulic frequency of the system; therefore this portion of the gain can be considered constant. The hydraulic dynamics of the hydraulic ram can also be modeled as a second order response whose natural frequency is unknown and difficult to predict. This is where some inaccuracies may exist in the linearity assumption as evident by small nonlinearities in our experimentally obtained gain values.

SIMULAB was used to find the initial steady state position of the slave ram before an external force was applied. The gain approximations were used with the assumption that the slave ram initial position was in contact with an obstruction. The step input force in SIMULAB was defined to have an initial value of zero, and at a delayed step time,  $t_0 = 30$  seconds, the step value would change to 45.4 grams. Figure 53 shows that by using the gain approximations, the system was not initially in equilibrium before the external force was applied. There were some residual gains in the system model that had the ram equilibrium position before the slave ram comes into contact with the obstruction.

### **3. Obstruction Stiffness**

An analysis was conducted to observe the dynamic response of the slave ram when the stiffness of the obstruction becomes large. Figure 54 shows that when  $K_{os}K_{sp}$  is set equal to 100, very large oscillations initially develop, and then they diminish but do not disappear. This occurs because the master ram initially has a positive displacement from the externally applied force, and its potentiometer voltage will be greater than the slave potentiometer voltage causing the slave ram to have an initial extending displacement. Since the hydraulic ram can

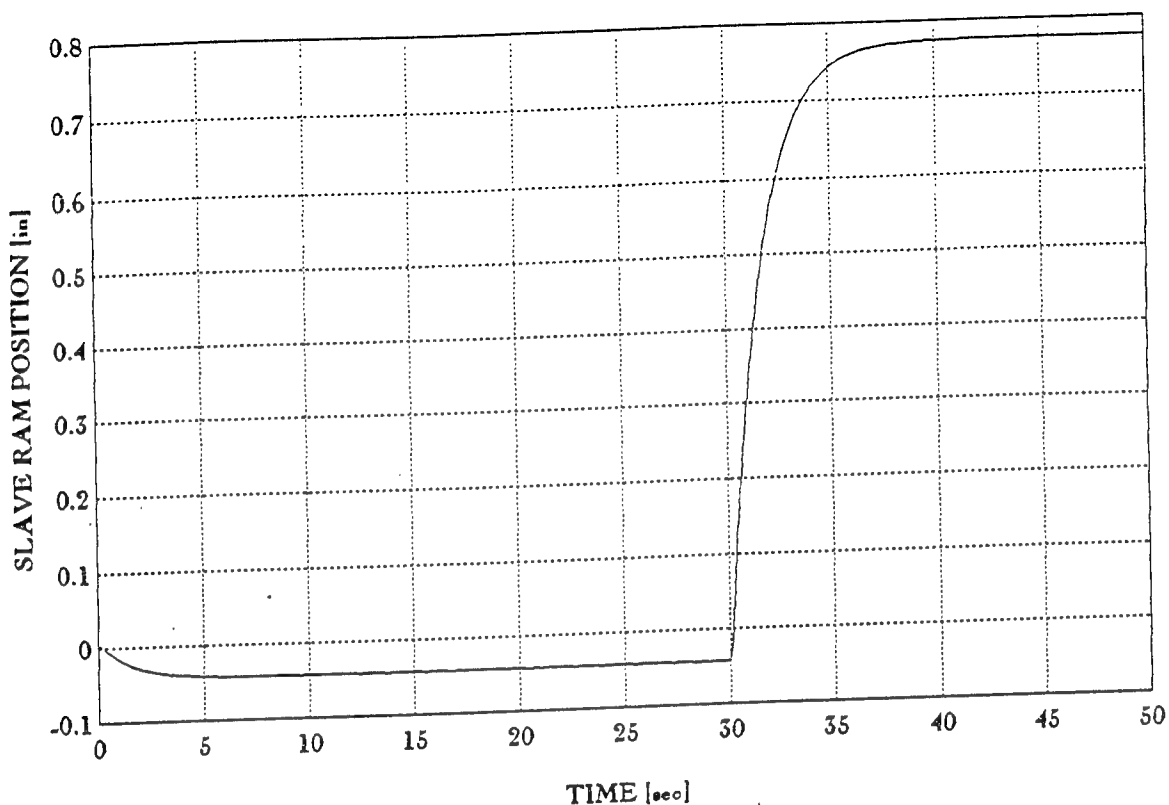


Figure 53. Initial equilibrium for single degree of freedom system before step input is applied at  $t=30$  seconds.

overcome large forces and since the obstruction is not very compliant, the plate on the end of the ram develops very large bending stresses. The slave strain gauge now produces a much larger voltage than the applied force voltage, causing the master ram to retract, and thus the slave follows. The slave ram retracts to unload the obstruction induced bending stress until the bending strain voltage becomes less than the constant applied force voltage. Now the master strain gauge voltage is larger and causes the master ram to extend, and this cycle continues.

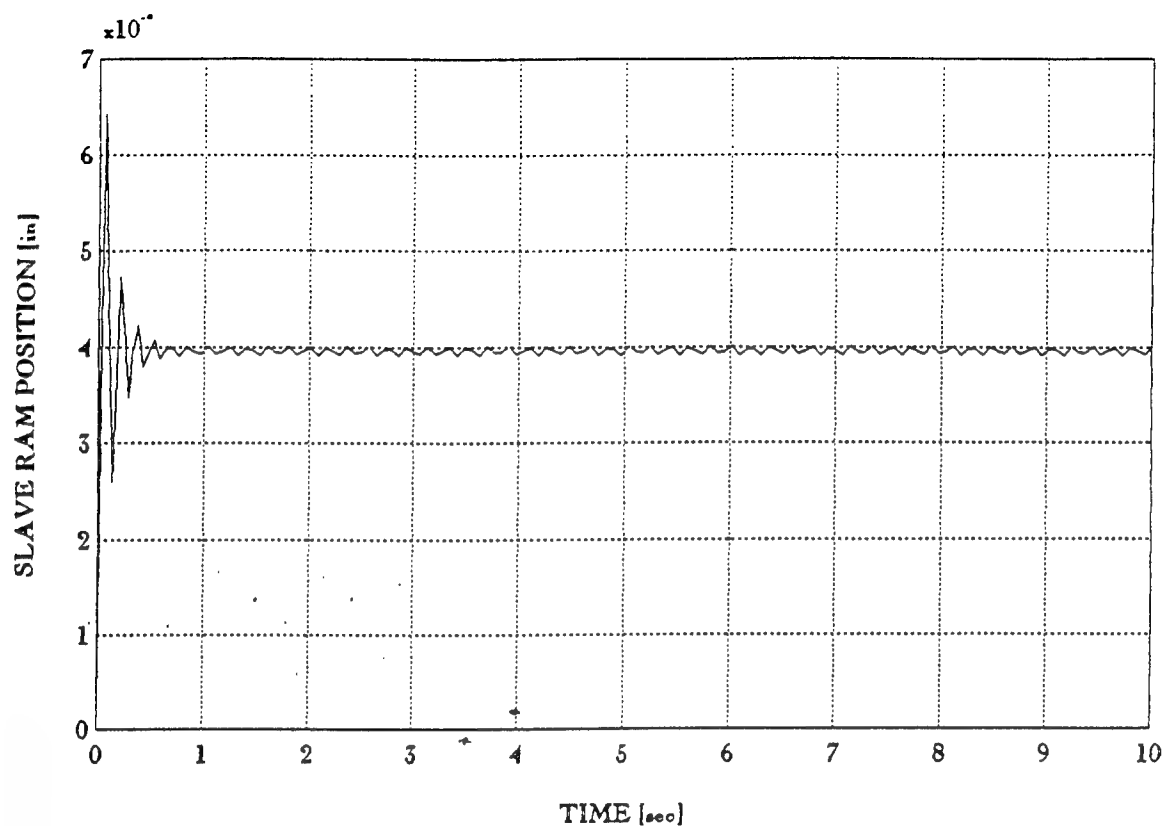


Figure 54. Dynamic response when obstruction stiffness is large.

#### B. TWO DEGREES OF FREEDOM SYSTEM

##### 1. Results

###### a. Bilateral Force Feedback

As initially expected after a theoretical and experimental analysis of a single degree of freedom system and a theoretical analysis of a two degrees of freedom

system, the bilateral force feedback system can be successfully constructed and operated so that a resistive force encountered by a slave hydraulic unit will oppose the direction of an externally applied force to the master unit in two dimensions. The force resistance is again accomplished by decreasing the hydraulic power assist to the master unit.

**b. Dynamic Response**

A theoretical model was constructed using gain values obtained from the single degree of freedom system. The dynamic response for both links was overdamped with no signs of instability. The two degrees of freedom system was expected to perform similar to the single degree of freedom system. But the more complex, rotary, two dimensional system actually did not have the dynamic response as expected.

The slave links would continue to oscillate at a low frequency of approximately one hertz after the input force to the master unit was removed and the master rotary actuator came to a complete stop (i.e., constant master potentiometer voltage). This occurred for both the linear and rotary hydraulic actuators. It was initially assumed that inertia effects from the links in motion caused unexpected, oscillating bending stresses to the strain gauge webs. An oscilloscope was used to verify that the strain voltage in the webs actually oscillated. Three modes of vibration were noticeable, but the lowest mode frequency was still much higher than the frequency of link oscillation, so the feedback effect to the master strain gauge amplifier was not significant enough to cause the master servo valve to oscillate. Therefore, the master potentiometer voltage did not change during this oscillatory period, and it did not contribute to the slave servo valve fluctuations.

The oscillations occurred when the force feedback was considered open; therefore, there were only a few gain values to analyze for causing the system to oscillate. All amplifier gains were initially set at their maximum value when the oscillations were discovered. The slave servo gain ( $K_{SSV}$ ) was reduced a little at a time, and the number of oscillations began to decrease.  $K_{SSV}$  was reduced until the oscillations were eliminated, but the slave actuator moved very sluggishly. The oscillations were eliminated by preventing the link to overshoot its commanded position, but this is not a desirable speed to complete simple system tasks. This was also done to the slave servo valve gains for the other link. Oscillations were eliminated, but the slave link was very sluggish.

$K_{SSV}$  was set back to its maximum value to maintain good reaction speed of the servo valve. The master and slave potentiometer voltage signal wires (input to servo amplifier) were hooked up one at a time to terminal three on the servo amplifier which has a voltage scale adjustment instead of their normal input terminal. The slave potentiometer was adjusted first. Since the master potentiometer voltage signal was held constant, the scale for the slave potentiometer was reduced so that the master potentiometer would have the greater effect in driving the slave actuator. The scale was reduced significantly, but the oscillations were only reduced and not eliminated. A problem with operating in this mode was that a small change in the master rotational displacement resulted in a large slave rotational displacement. That is because, for equilibrium to occur, the slave must have a greater displacement for its voltage, which is scaled down, to equal the master potentiometer voltage. This method does not satisfy system requirements since oscillations still occur, and the slave and master rotational displacements are no longer equal in magnitude. The same

adjustments were conducted by connecting the slave potentiometer to the non-adjustable amplifier terminal, and connecting the master potentiometer to the scaling terminal of the servo amplifier. The oscillations again were not eliminated, and it took 90 degrees of master displacement to rotate the slave 45 degrees.

SIMULAB was used to simulate oscillations. The force feedback was disconnected in the model, and the step input force was changed to an off switch (i.e., initial force of 70 grams, and at step time,  $t_0$ , the force was changed to zero grams). The gain values were varied, and oscillations could not be created in the system.

Therefore, the system is more complex than the initial assumption. There must be dynamic effects in the hydraulic actuators and in the hydraulic hoses that connect the servo valve to the actuators that prevent  $K_{SSV}$  from being assumed constant. The slave servo valve dynamics must be more closely analyzed. It is composed of the electro-hydraulic servo mechanism, the hydraulic actuators (linear or rotary), and the hoses that connect the servo valve to the actuators. The dynamics can be divided into two system with each having their own characteristics. Figure 55 represents the more accurate block diagram for an input voltage to a servo valve and the output actuator displacement [Ref.6, pgs 238,268]. The input voltage from the master potentiometer has an amplification from the servo amplifier with a value of  $K_o$ . The two port electro-hydraulic servo valve has a second order dynamic characteristic where  $\omega_o$  is the servo valve natural frequency,  $\zeta_o$  is the servo valve damping ratio, and  $\omega_1$  and  $\omega_2$  are lags (rad/sec) which stem from the inductive time constant ( $L/R$ ) of the torque motor armature and from the crossover frequency of the spool position loop [Ref.6, p.236]. The output of the electro-hydraulic servo valve ( $X_{SV}$ ) is the spool displacement that ports hydraulic fluid to

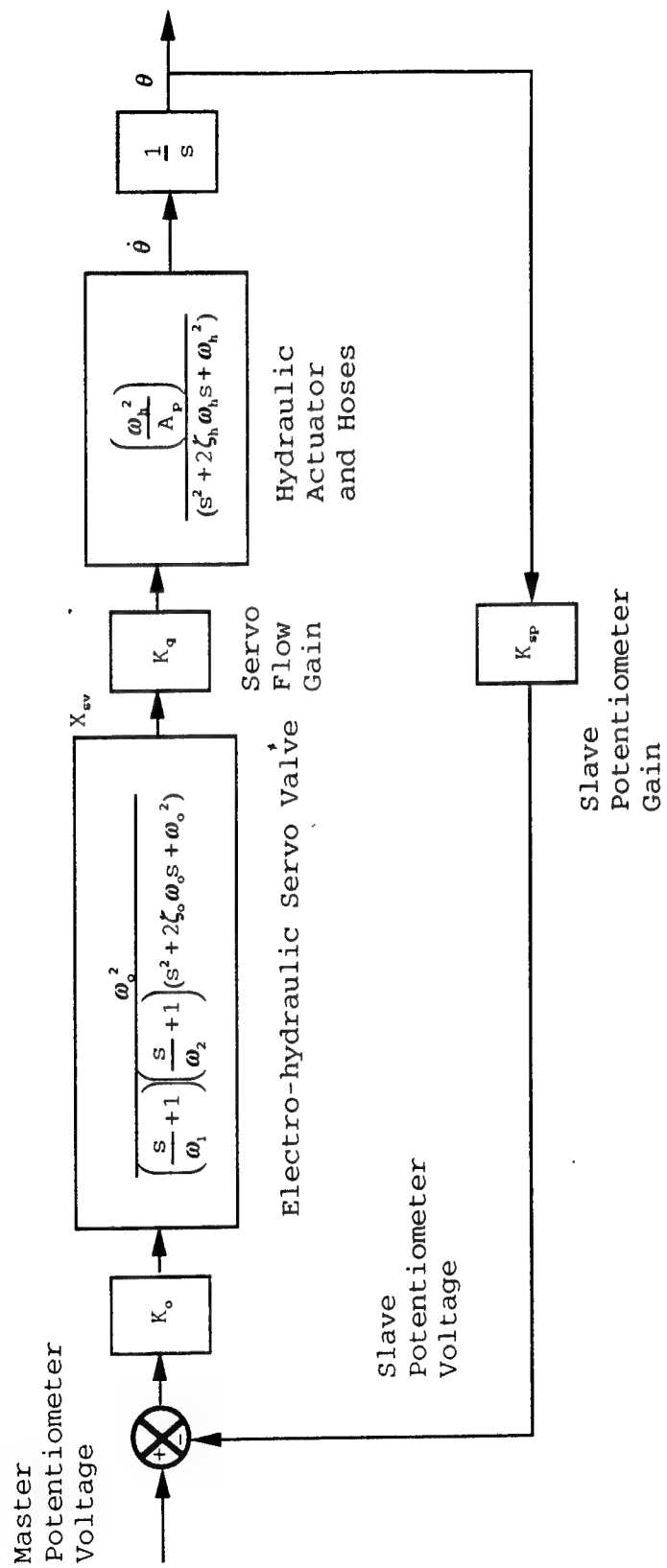


Figure 55. Servo valve, hydraulic actuator, and hose dynamic relationship.

the actuator.  $x_{sv}$  is converted into a volumetric flow rate ( $\text{in}^3/\text{s}$ ) by the servo flow gain ( $K_q$ ). The hydraulic hoses and actuator can be modeled with another second order characteristic polynomial where  $\omega_h$  is the hydraulic natural frequency,  $\zeta_h$  is the hydraulic damping ratio, and  $A_p$  is the cross sectional area of the actuator [Ref.6, p 268]. This is to represent the dynamics involved in the hydraulic flow through the hoses and the dynamics of the actuator that moves a large mass. The servo valve natural frequency,  $\omega_o$ , can still be assumed to be much higher than the overall system frequency, and therefore be represented as a constant. The hydraulic natural frequency of the actuator and hoses,  $\omega_h$ , can no longer be assumed to be high enough to represent a constant gain. SIMULAB was used to predict a dynamic response with this new relationship for the slave servo valve and actuator. The servo valve gain was set at .5, the hydraulic frequency was set at .5 Hz, the cross-sectional area was set to 1  $\text{in}^2$ , and the hydraulic damping ratio was set to .5. Figure 56 shows the possible effects of introducing hydraulic effects into the system. In this particular simulation, when the step force input is removed at time,  $t=10$  seconds, oscillations begin to grow without bound at a frequency of .5 Hz.

### **c. System Sensitivity**

The overall system was very sensitive to several external factors, and it was difficult to maintain the system in constant equilibrium. After each completed movement of a link and the applied force was removed, the master strain gauge offset would have to be adjusted to keep the master servo valve from rotating on its own. The amount of bending stress at the master and slave strain gauge webs would vary slightly as the position of link #1 would change. For each

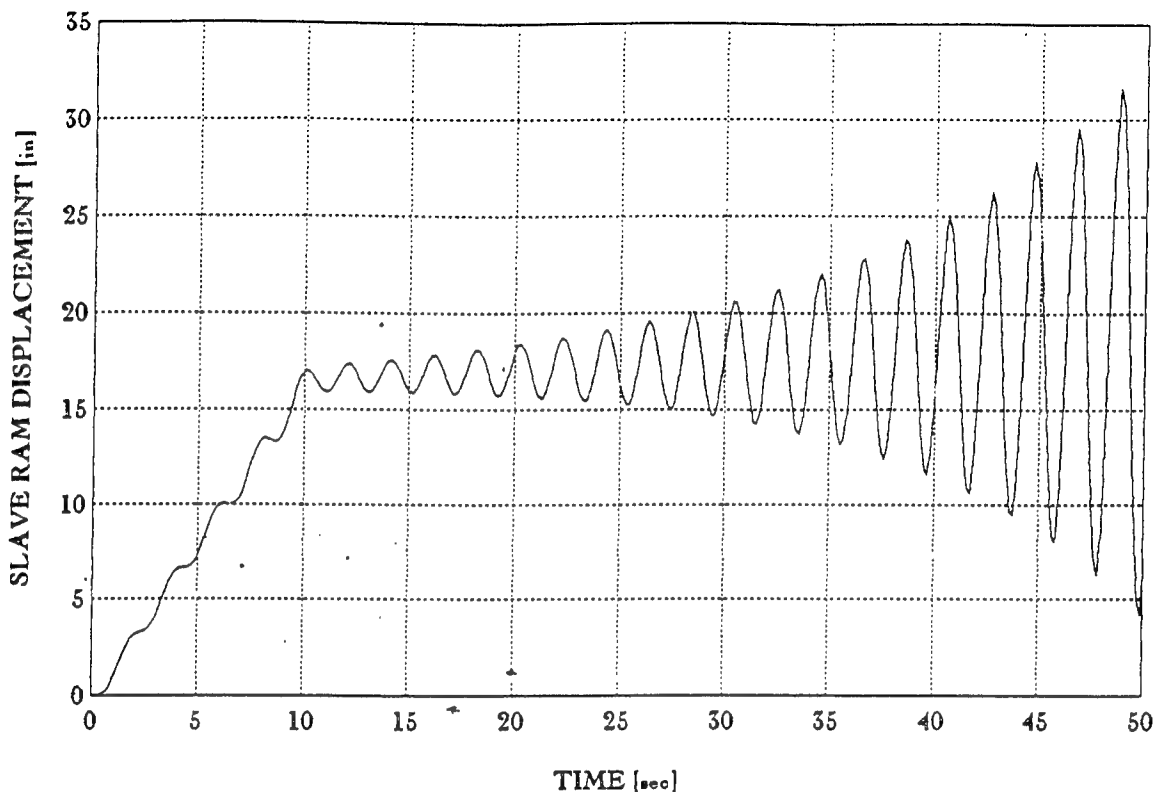


Figure 56. Dynamic response using a separate hydraulic characteristic.

new position, the hydraulic hoses leading to the linear actuator for link #2 would change angular position to the actuator and would cause a different bending stress on link #1. Since the web thickness was designed to measure small stresses, the strain voltage would change after each movement, causing the loss of equilibrium.

Very small forces needed to be applied to the master link to cause a large bending stress at the strain gauges. Therefore, small forces resulted in large motions. Because a half bridge was used, the strain on the web was doubled. It was also easy to cause oscillations in the system by resisting the motion of the slave link with too large of a force. Because of the strain gauge sensitivity, it was difficult for an individual to apply a small resistive force with his hand. The strain voltage was greatly amplified and fed back to the master servo amplifier. The large amplification had the same effect as the single degree of freedom model when the obstruction stiffness was increased to a large value; oscillations occurred.

## **V. CONCLUSIONS AND RECOMMENDATIONS**

### **A. CONCLUSIONS**

- The concept of a bilateral force feedback, hydraulically actuated system can be feasibly constructed and operated in various environments.
- A remotely located slave hydraulic unit that is positionally driven by a master hydraulic unit can encounter small resistive forces and convert the force into a voltage to be fed back to offset the hydraulic power assist to the master unit operator.
- The system tends to be very sensitive when using flexible material and strain gauges to measure bending stresses caused by externally applied forces.
- System equilibrium is difficult to maintain when changing system position.
- System hardware, such as stiff hydraulic hoses, can cause fluctuating bending stresses in the strain gauge webs that requires continuous strain gauge offset adjustments to maintain equilibrium.
- The dynamic effects of the hydraulic hoses, connectors, flow control ports, inertia of the large links, and actuators are believed to greatly effect the overall response of the force feedback system.

### **B. RECOMMENDATIONS**

The biggest concern for future success in the operation of the bilateral force feedback system using large hydraulic components and support hardware, is to determine what caused oscillations in the two degrees of freedom system. It is believed that the dynamic effects caused by the hydraulic hoses, connectors, flow control ports, inertia of the large

links, and actuators greatly effect the overall response of the force feedback system. It was assumed that a constant gain could be used to model the transfer function relationship between potentiometer summation input and actuator displacement, but this may be incorrect. The hydraulic natural frequency should be estimated for the system and compared to the frequency of oscillations to see if they are closely related. If the hydraulic effects are causing the oscillations, a method needs to be developed to increase the hydraulic damping.

The system sensitivity needs to be reduced. A thicker strain gauge web should be used to generate less than 500  $\mu$ -strain on the strain gauge. The bulky hydraulic hoses cause varying bending stresses with positional changes. This could be reduced by configuring the hose connections differently or by attaching fixed hydraulic ports to the links.

The theoretical analysis for the single degree of freedom system predicted the effect of the slave encountering an obstruction with a very large stiffness; large oscillations developed. The range of stiffness tolerance needs to be determined to maintain an overdamped system response. The system needs to be altered to be able to handle stiff obstructions without creating large oscillations at high frequencies that could damage equipment or injure personnel controlling the master unit.

**APPENDIX A. MASTER STRAIN GAUGE GAIN ( $K_{om}$ )**  
**EXPERIMENTAL DATA**

Kom(M.STRAIN GAUGE)		
Bolt	G1	Voltage
W=48.8grams	1.00	0.305
	2.00	0.343
	3.00	0.392
	4.00	0.459
	5.00	0.55
	6.00	0.687
	7.00	0.917
	8.00	1.376
Battery	G1	Voltage
W=108.4g	1.00	0.667
	2.00	0.75
	3.00	0.857
	4.00	1.001
	5.00	1.201
	6.00	1.499
	7.00	2.001
	8.00	3.002
Angle	G1	Voltage
W=128.8g	1.00	0.795
	2.00	0.895
	3.00	1.024
	4.00	1.195
	5.00	1.435
	6.00	1.792
	7.00	2.393
	8.00	3.58
Straight	G1	Voltage
W=164.7g	1.00	1.013
	2.00	1.139
	3.00	1.302
	4.00	1.522
	5.00	1.823
	6.00	2.276
	7.00	3.045
	8.00	4.552

**APPENDIX B. MASTER SERVO VALVE GAIN ( $K_1$ ) EXPERIMENTAL  
DATA**

<b>K1(MASTER SERVO)</b>	<b>G2=</b>	0.0 for all runs	
	<b>v1=</b>	0.515	
<b>G1=2.00</b>	<b>v2=</b>	-0.025	
	<b>(v1+v2) =</b>	0.49	
Xm [in]	time [sec]	velocity [in/s]	
	1	3.79 0.26385224	
	1	3.57 0.28011204	
	1	3.36 0.29761905	
	1	3.41 0.29325513	
	1	3.68 0.27173913	
<b>K1=[in/(sec*volts)]</b>	0.574113305		
	<b>G2=</b>	0.0 for all runs	
	<b>v1=</b>	0.685	
<b>G1=4.00</b>	<b>v2=</b>	-0.025	
	<b>(v1+v2) =</b>	0.66	
Xm [in]	time [sec]	velocity [in/s]	
	1	2.46 0.40650407	
	1	2.24 0.44642857	
	1	2.47 0.4048583	
	1	2.29 0.43668122	
	1	2.32 0.43103448	
<b>K1=[in/(sec*volts)]</b>	0.644092922		
	<b>G2=</b>	0.0 for all runs	
	<b>v1=</b>	0.505	
<b>G1=6.00</b>	<b>v2=</b>	-0.025	
	<b>(v1+v2) =</b>	0.48	
Xm [in]	time [sec]	velocity [in/s]	
	1	3.33 0.3003003	
	1	3.36 0.29761905	
	1	3.28 0.30487805	
	1	3.03 0.330033	
	1	3.03 0.330033	
<b>K1=[in/(sec*volts)]</b>	0.651193085		
	<b>G2=</b>	0.0 for all runs	
	<b>v1=</b>	0.515	
<b>G1=8.00</b>	<b>v2=</b>	-0.028	
	<b>(v1-v2) =</b>	0.487	
Xm [in]	time [sec]	velocity [in/s]	
	1	2.75 0.36363636	
	1	2.91 0.34364261	
	1	2.84 0.35211268	
	1	2.73 0.36630037	
	1	2.72 0.36764706	
<b>K1=[in/(sec*volts)]</b>	0.73648422		

**APPENDIX C. MASTER POTENTIOMETER GAIN ( $K_4$ )  
EXPERIMENTAL DATA**

<b>K4-MASTER POT</b>		
	DISTANCE [in]	VOLTAGE [volts]
	0.125	9.92
	0.375	8.17
	0.625	6.17
	0.875	4.10
	1.125	2.34
	1.375	0.78
	1.625	-0.78
	1.875	-2.30
	2.125	-4.25

**APPENDIX D. SLAVE SERVO VALVE GAIN ( $K_2$ ) EXPERIMENTAL  
DATA.**

<b>K2</b>				
<b>SLAVE SERVO</b>				
G1=	5.00			
G2=	5.00			
DISTANCE[in]	TIME [sec]	VOLTAGE [volts]	VELOCITY [in/s]	
1	9.4	0.05	0.106382979	
1	7.22	0.057	0.138504155	
1	7.19	0.058	0.139082058	
1	7.91	0.054	0.12642225	
1	7.82	0.054	0.127877238	
1	7.07	0.06	0.141442716	
1	7.97	0.055	0.125470514	
1	9.99	0.052	0.1001001	
<b>K2=</b>	<b>2.329062</b>	[in/(sec*volts)]		

**APPENDIX E. SLAVE POTENTIOMETER GAIN ( $K_3$ )  
EXPERIMENTAL DATA**

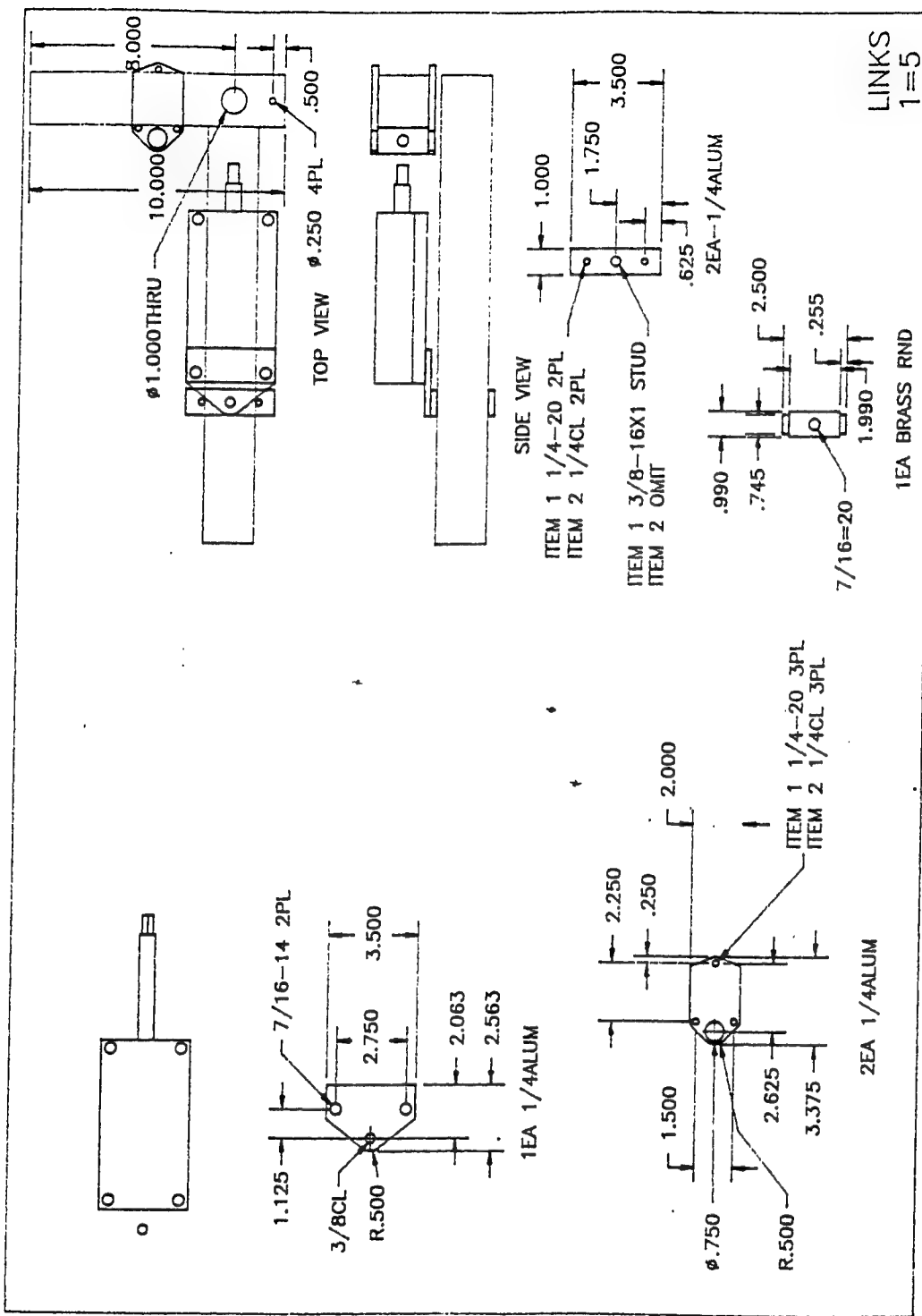
K3-SLAVE POT			
	DISTANCE [in]	VOLTAGE [volts]	
	0.125	-9.46	
	0.375	-8.50	
	0.625	-7.56	
	0.875	-6.62	
	1.125	-5.74	
	1.375	-4.78	
	1.625	-3.89	
	1.875	-2.92	
	2.125	-2.04	
	2.375	-1.12	
	2.625	-0.21	
	2.875	0.72	
	3.125	1.60	
	3.375	2.54	

**APPENDIX F. SLAVE STRAIN GAUGE GAIN ( $K_{OS}$ ) AND  
OBSTRUCTION SPRING GAIN ( $K_{sp}$ ) EXPERIMENTAL DATA.**

DISTANCE	G2=2.00	G2=4.00	G2=6.00	G2=8.00	KNOB SETTING	GAIN
1      0.125	-0.040	-0.060	-0.090	-0.190	2.00	0.22800
2      0.250	-0.080	-0.100	-0.150	-0.360	4.00	0.32533
3      0.375	-0.120	-0.140	-0.230	-0.430	6.00	0.51067
4      0.500	-0.140	-0.150	-0.300	-0.530	8.00	1.02670
5      0.625	-0.180	-0.220	-0.350	-0.620		
6      0.750	-0.180	-0.240	-0.410	-0.770		
7      0.875	-0.210	-0.300	-0.490	-1.020		
8      1.000	-0.230	-0.350	-0.550	-1.080		
9      1.125	-0.300	-0.380	-0.590	-1.220		

**APPENDIX G. MATLAB CODE FOR A TYPICAL UNIT STEP  
RESPONSE FOR SINGLE DEGREE OF FREEDOM MODEL**

```
% natural frequency
wn=3.14;
%
% damping ratio
zeta=2.5;
%
% transfer function
num=[wn^2];
den=[1 2*zeta*wn wn^2];
%
step(num,den)
```



Drawing provided by Tom McCord, Naval Postgraduate School.

**APPENDIX I. MATLAB CODE FOR ANGULAR ROTATIONS VS.  
ACTUATOR POSITION FOR TWO DEGREES OF FREEDOM SYSTEM**

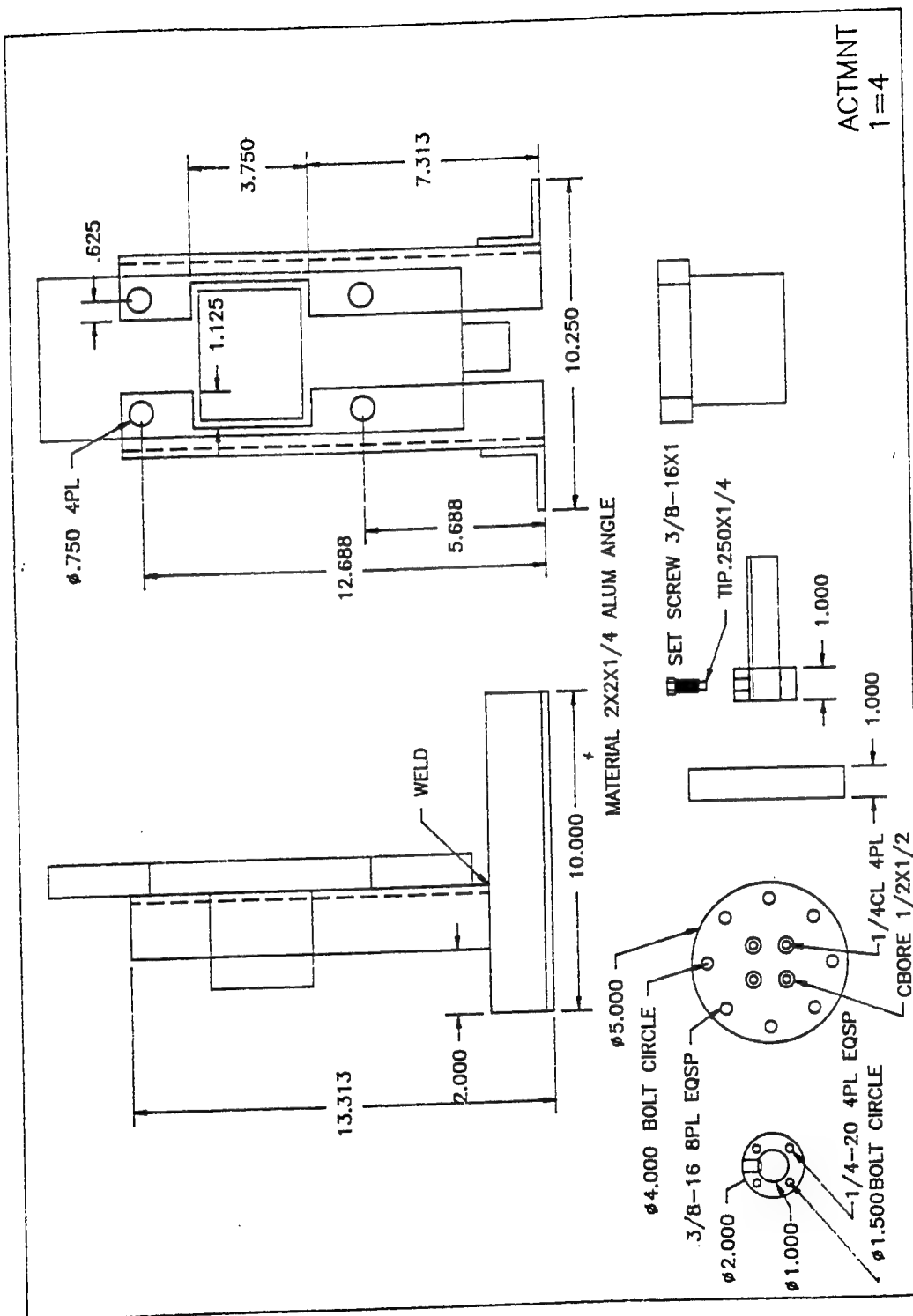
```
% ANGULAR ROTATIONS VS. ACTUATOR POSITION FOR 2DOF SYSTEM
%
% actuator position along link #1
l=10:0.1:16;
l=l';
%
% minimum actuator ram length
a1=11;
%
% maximum actuator ram length
a2=15;
%
% fixed length along link #2 where actuator ram is attached
b=5;
%
% angular position of link #2 when ram is fully retracted for varying actuator
% position along link #1
theta1=90-(acos((a1^2-b^2-(l.^2))./(-2*l*b)))*360/(2*pi);
%
% angular position of link #2 when ram is fully extended for varying actuator
% position along link #1
theta2=acos((a2^2-b^2-l.^2)./(-2*l*b))*360/(2*pi)-90;
%
% combined minimum and maximum angle to give full range of motion for a given
% actuator position
thetasum=theta1+theta2;
%
% plot three results: min angle, max angle, total range
plot(l,thetasum,l,theta1,l,theta2)
```

APPENDIX J. MATLAB CODE FOR LINEARITY OF LINK  
ROTATION VS. ACTUATOR RAM DISPLACEMENT

```
% LINEARITY OF LINK ROTATION VS. ACTUATOR RAM DISPLACEMENT
%
% range of motion for the actuator ram
a=(11.0:0.1:15.0);
%
% fixed length along link #2 where actuator ram is attached
b=5;
%
% l is the distance on link #1 from the pivot point where the actuator is
% attached.
% theta is the resulting angular position for a varying actuator ram
% displacement.
%
l=10;
theta1=90-(acos((a.^2-b^2-l.^2)./(-2*b*l)))*360/(2*pi);
%
l=11;
theta2=90-(acos((a.^2-b^2-l.^2)./(-2*b*l)))*360/(2*pi);
%
l=12;
theta3=90-(acos((a.^2-b^2-l.^2)./(-2*b*l)))*360/(2*pi);
%
l=13;
theta4=90-(acos((a.^2-b^2-l.^2)./(-2*b*l)))*360/(2*pi);
%
l=14;
theta5=90-(acos((a.^2-b^2-l.^2)./(-2*b*l)))*360/(2*pi);
%
l=15;
theta6=90-(acos((a.^2-b^2-l.^2)./(-2*b*l)))*360/(2*pi);
%
l=16;
theta7=90-(acos((a.^2-b^2-l.^2)./(-2*b*l)))*360/(2*pi);
%
% plot the results of ram displacement vs. angular position for eight
% positions along link #1
%
plot(a,theta1,a,theta2,a,theta3,a,theta4,a,theta5,a,theta6,a,theta7)
```

APPENDIX K. MATLAB CODE FOR WEB THICKNESS VS. APPLIED FORCE.

```
% WEB THICKNESS VS. APPLIED FORCE CALCULATION
%
% input force range
f=0:.1:10;
%
% web thickness for a various input force
t=(51.429*f/(1e7*500e-6)).^.5;
%
% plot web thickness for various input forces
plot(f,t)
```

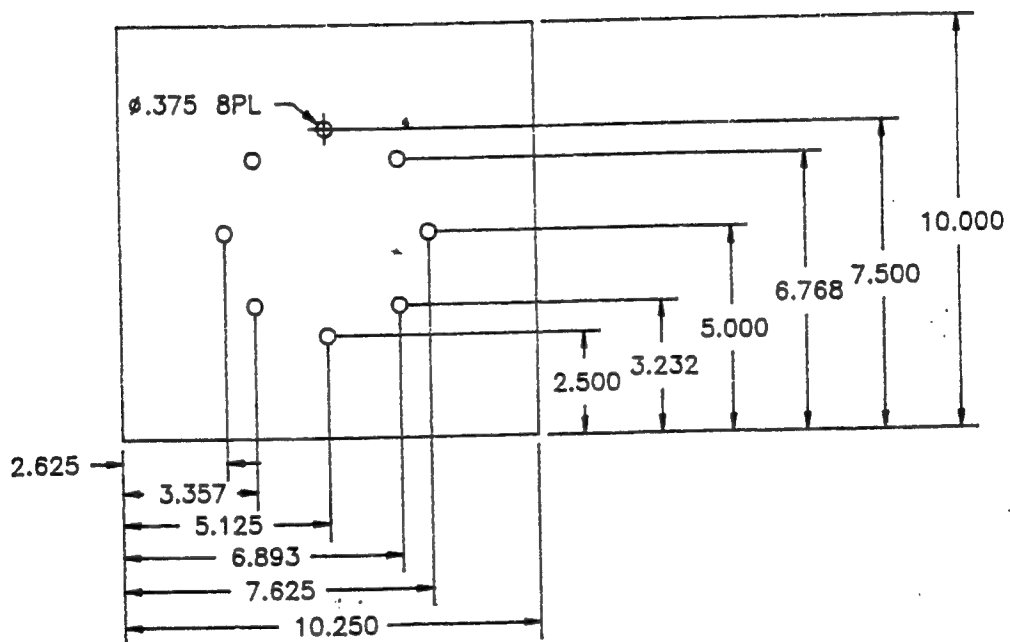


Drawing provided by Tom McCord, Naval Postgraduate School.

APPENDIX I. AUTOCAD DRAWING OF MASTER ACTUATOR MOUNTING BRACKET AND LINK MOUNTING PAD

**APPENDIX M. AUTOCAD DRAWING OF SLAVE ACTUATOR  
MOUNTING PAD**

Drawing provided by Tom McCord, Naval Postgraduate School.



MATERIAL 1/2ALUM

ACTMNT  
1=4



#### LIST OF REFERENCES

1. Sheridan, Thomas B., *Telerobotics, Automation, and Human Supervisory Control*, The MIT Press, 1992.
2. Walpole, Ronald E., Myers, Raymond H., *Probability and Statistics for Engineers and Scientists*, 5th ed, Macmillan Publishing Company, 1993.
3. MathWorks, Inc., The, *The Student Edition of MATLAB, Student User Guide*, Prentice-Hall, Inc., 1992.
4. MathWorks, Inc., The, *SIMULAB, A Program for Simulating Dynamic Systems*, Prentice-Hall, Inc., 1990.
5. Beckwith, Thomas G., Marangoni, Roy D., Lienhard, John H., *Mechanical Measurements*, 5th ed, Addison-Wesley Publishing Company, 1993.
6. Merritt, Herbert E., *Hydraulic Control Systems*, John Wiley & Sons, 1967.



**INITIAL DISTRIBUTION LIST**

1. Defense Technical Information Center.....2  
Cameron Station  
Alexandria, Virginia 22304-6145
2. Library, Code 52.....2  
Naval Postgraduate School  
Monterey, California 93943-5101
3. Department Chairman, Code ME.....1  
Department of Mechanical Engineering  
Naval Postgraduate School  
Monterey, California 93943-5002
4. Professor Morris R. Driels .....3  
Code ME/DR  
Department of Mechanical Engineering  
Naval Postgraduate School  
Monterey, California 93943-5002
5. Director, Training and Education.....1  
MCCDC, Code C46  
1019 Elliot Rd.  
Quantico, Virginia 22134-5027
6. Naval/Mechanical Engineering Curricular Office.....1  
Code 34  
Naval Postgraduate School  
Monterey, California 93943-5002
7. LT Gregory S. Johnson.....1  
712 Manchester Rd.  
Neenah, WI 54956